Hydrogeology and groundwater regime of the Stanford Aquifer, South Africa

Sören Östergaard Holm

**Dissertations in Geology at Lund University,
Master's thesis, no 291
(45 hp/ECTS credits)**

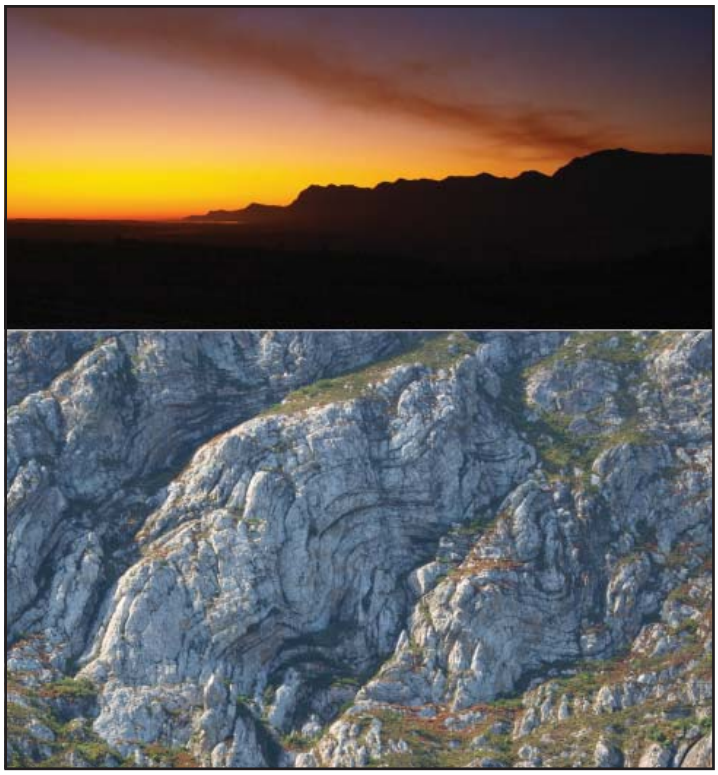

**Department of Earth- and Ecosystem Sciences
Division of Geology
Lund University**
2011

HYDROGEOLOGY AND GROUND-WATER REGIME OF THE STANFORD AQUIFER, SOUTH AFRICA

Master Thesis

SÖREN ÖSTERGAARD HOLM

Department of Geology
Lund University

2011

Table of Contents

Cover Picture: Top: Sunset over the Kleinriviersberge. Bottom: Folded section of the Table Mountain Group, part of the Cape Fold Belt.

Hydrogeology and Groundwater Regime of the Stanford Aquifer, South Africa

Sören Östergaard Holm

Holm, S.Ö., 2011: Hydrogeology and Goundwater Regime of the Stanford Aquifer, South Africa. *M.Sc. thesis Lunds universitet*, Nr .291, 40 sid. 45 hp.

Abstract: This study focuses on the Stanford Aquifer which is located in the Overberg region in the Western Cape of South Africa. The 'Eye', a captured spring, is used as source for potable water for the local municipality and extraction have in recent years exceeded the sustainable yield of 33 000 m^3/month and a supplementary source is therefore needed.

The aim of this study is to develop a conceptual model of the aquifer by analysing and compiling years of monitoring data as well as results from previous studies and field investigations. The aquifer is primarily formed within the gravelly Klein Brak Formation and to a lesser extent also within the overlying sandy Waenhuiskrans Formation. Extensive calcrete lenses within the Waenhuiskrans Formation are having a semi-confining effect on the aquifer, evident from long-term monitoring data. Therefore it is suggested that the aquifer is a confined but leaky type of aquifer. Furthermore, two palaeochannels (Klein River and Koue Vlakte Palaeochannel) have been identified within the study area, filled with the Klein Brak Formation they are expected to be high yielding hydrogeological features. The hydraulic parameters of the Koue Vlakte Palaeochannel were examined through a pump test, which confirmed the expected high yield nature. Based on the result from the pump test it has been decided to use the Koue Vlakte Palaeochannel as an additional groundwater source.

Recharge have been estimated using the chloride mass balance and Breede River basin study methods and suggest that recharge occurs both through precipitation and lateral inflow from adjacent formations. The fact that the Stanford Aquifer is endorheic, has a large infiltration potential, suggests that recharge through precipitation is significant. Furthermore, isotopic analysis confirms a meteoric origin of the water within in the Stanford Aquifer.

Keywords: Stanford Aquifer, Conceptual model, Klein Brak Formation, Palaeochannels, Hydraulic parameters, Recharge, Lateral inflow.

Sören Östergaard Holm, Department of Geology, GeoBiosphere Science Centre, Lund University, Sölvegatan 12, SE-223 62 Lund, Sweden. E-mail: hsoeren@hotmail.com

Hydrogeologi och Grundvatten Förhållande i Stanfordakvifären, Sydafrika

Sören Östergaard Holm

Holm, S.Ö., 2011: Hydrogeologi och Grundvatten Förhållande i Stanfordakvifären, Sydafrika. *Examensarbeten i geologi vid Lunds universitet*, Nr. 291, 40 pp. 45 hp.

Sammanfattning: Stanford, ett mindre samhälle 150 km väst om Kapstaden, har under de senaste åren sett en ökad turism och utveckling, vilket har medfört ett ökat behov av färskvatten. I dagsläget används en naturlig källa som täkt för kommunens vattenbehov, men källans hållbara vattenavgivningsförmåga på 33 000 m^3/månad är otillräcklig och en kompletterande täkt är nödvändig.

Stanfordakvifären består av två formationer, den grovkorniga Klein Brakformationen och den finkorniga Waenhuiskransformationen. Klein Brakformationen utgör den större delen av akvifären, medan Waenhuiskransformationen fungerar som semi-tätande lager för akvifären, samtidigt som en del av den också är vattenbärande och utgör en del av akvifären. Hydrogeologin är stark präglad av de sediment som avsatts i de två äldre flodfårorna (Klein River och Koue Vlakte vari Klein Brakformationen är deponerad) som nu fungerar som en form av flödeskanaler i akvifären. Särkilt sedimenten avsatta i Koue Vlakte-fåran anses vara hydrogeologisk viktiga och ett provpumpningstest utfördes för att utvärdera dess hydrogeologiska egenskaper. Baserat på provpumpningsresultaten har man beslutat att använda området vid Koue Vlakte-fåran till kompletterande täkt för kommunens behov.

Genom att upprätta en vattenbalans för akvifären, har vi kunnat kvantifiera mängden vatten som tillförs akvifären lateralt från omkringliggande formationer. Den totala mängden uppskattas till 21 840 000 m^3 årligen varav 3 900 000 m^3 från nederbörd. Detta innebär att det laterala tillflödet och ytavrinningen från omkringliggandes formationer är betydligt större än vad man hittills har trott.

Nyckelord: Stanfordakvifären, Sydafrika, Klein Brakformationen, halv-sluten, flodfåror, lateralt tillflöde.

Sören Östergaard Holm, Geologiska Institutionen, Centrum för GeoBiosfärsvetenskap, Lunds Universitet, Sölvegatan 12, 223 62 Lund, Sverige. E-post: hsoeren@hotmail.com

List of Abbreviations:

a - annum

^{o}C - Degrees Celsius

CRT - Constant Rate Test

DWAF - Department of Water Affairs and Forestry

DWA - Department of Water Affairs

K - Hydraulic conductivity (m/s)

km - Kilometre

Ma - Million years ago

mamsl - Metres above mean sea-level

MAP - Mean Annual Precipitation

mbgl - Meters below ground level

Ml - Million litres

mm- millimetre

mm/a - Millimetre per annum

My - Million years

m^3/a - Cubic meter per annum

PET - Potential Evapotranspiration

S - Storativity

TMG - Table Mountain Group

T -Transmissivity (m^2/s)

WRC - Water Research Commission

1. INTRODUCTION

1.1. BACKGROUND

Stanford, a small town approximately 150 km east of Cape Town (figure 1-1), have in recent years experienced increased tourism and a development boom. Furthermore, the municipality is currently in negotiation with local landowners in an attempt to acquire land for construction of additional RDP-housing (Rural Development Plan – a governmental scheme for relocating populations living in informal settlements into proper housing). Subsequently, the water demand has increased significantly over the last years and is expected to double within the next thirty years (Umvoto, 2009). Currently, a captured natural spring, the 'Eye', is being used as a source for potable water for the community and informal settlement and the sustainable yield of 33 000 m^3/month is no longer sufficient. Umvoto Africa has since 2004 continuously monitored the aquifer and in 2007 plans were initiated to locate a suitable locality for a new well field. A study located two suitable localities within the Stanford Aquifer, the Middelberg Farm and the Koue Vlakte Palaeochannel. The study concluded the Koue Vlakte Palaeochannel as the most favourable option, in terms of long-term sustainability and cost efficiency. In early 2010, two new drill wells were developed within the Koue Vlakte Palaeochannel in the southern part of the aquifer but remained untested until March 2011.

The initial plan is to use the new wells as an augment source for potable water in addition to the 'Eye' to fulfil the town water demand and thereby avoid over-exploitation of the 'Eye'. If needed it is possible to develop the wellfield further, as water demand increases.

1.2. AIM AND STRUCTURE OF REPORT

The aim of this report is to develop a conceptual hydrogeological model of the Stanford Aquifer by compiling and analyzing both previously collected and new data. The study was carried out as a desk-top study and supplemented with field investigation. Two major topics have been the focus throughout the study, one being the water balance and recharge estimations, especially the extent of lateral inflow from adjacent formations. It has previously been assumed that lateral inflow is nominal and thus has been ignored in previous models. However, no actual studies have been done to verify this. The second topic has evolved around the occurrence of palaeochannels. Previous studies have confirmed the existence of two palaeochannels within the study area but due to insufficient data the exact course of these channels have not been established.

The structure of this report is as follows:

1. Firstly, is the topography and climate of the study area, the Stanford Aquifer, briefly described based on previous collected and new data. A more detailed description of the geology and hydrogeology of the aquifer then follow. The geological description is mainly based on literature and to a lesser extent also on field observation. The hydrogeological model has been compiled using monitoring data collected since 2004, literature, previous in-house studies as well as new data collected in the field.
2. Hydrochemical data from samples collected from the aquifer dating back from 2005 have been analysed with respect to drinking water suitability, while new samples were collected from the aquifer in December 2010 and analysed for oxygen and hydrgen isotopes.

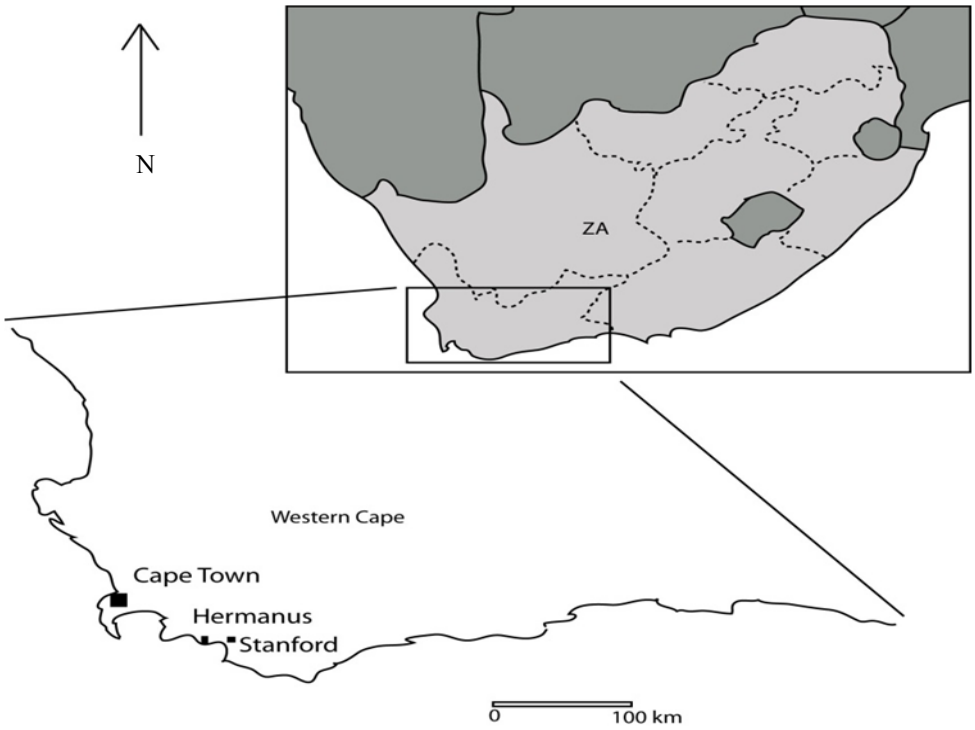

Figure 1-1. Regional map.

3. The results from a pump test carried out in March 2011 is analysed in order to estimate the performance of two new wells drilled into the Koue Vlakte Palaeochannel.
4. Finally, a mass balance is compiled using monitoring data collected since 2004. The mass balance is a useful management tool but also have other applications. The recharge is calculated using several methods in order to evaluate the main mode of recharge, precipitation or lateral inflow. An effort to determine the mode and volume of discharge has also been done. An attempt to estimate the volume of recharge which potentially can reach the saturated zone and form groundwater, groundwater potential, has been done using estimates of recharge and discharge

2. DESCRIPTION OF STUDY AREA

2.1. LOCALITY

Stanford is located within the Overberg region in the Western Cape of South Africa, approximately 150 km east of Cape Town. The study area, covering the Stanford Aquifer, is wedged between the Kleinriviersberge to the north and the Swartkransberg to the south and southeast and is sealed off from the coast by the sand dunes of the Walker Bay Nature Reserve (figure 1 in appendix A). The Klein River originates to the northeast of the Kleinriviersberge and runs along the northern boundary of the aquifer before reaching the Klein Lagoon. Stanford town is located in the northern part of the study area on a low-lying coastal plain, on the southern bank of the Klein River, approximately ten km east of Walker Bay.

Hermanus, a major stopover for the many thousands of tourists travelling along the Garden route each year and a popular spot for whale watching, is located 20 km northwest of Stanford. The close proximity to Hermanus has led to increasing numbers of tourists visiting Stanford over the last few years and subsequently put the aquifer under increasing stress.

2.2. DRAINAGE, TOPOGRAPHY AND LAND USE

The Stanford Aquifer lies within the G40L subcatchment area, an area covering roughly 385 km^2, which is divided into two sections (Midgley et al., 1994). The northern section consists of the southern slopes of the Kleinriviersberge and the northern banks of the Klein River while the southern section consists of the area south of the Klein River and north of the Swartkransberg. The main part of the study area is covered by 1:50 000 topographic map sheets; 3419AD Stanford and 3419CB Gansbaai and, to a lesser extent, by the 3419BC Jongenklip and 3419D Baardsheerderbos maps.

The topography of the Stanford area is relative flat. It slopes gently from approximately 350 meters above mean sea level (mamsl) in the south to approximately five mamsl in the north. To the west the sand dunes of the Strandveld Formation, protected by the Walker Bay Nature Reserve, reach a maximum elevation of approximately 150 mamsl to the south and 20 mamsl to the north and form a natural hydraulic divide, separating the study area from the coast. To the north of the Klein River the west-east striking mountains of the Kleinriviersberge reaches an elevation of 964 mamsl and to the south and south-east the Swartkransberg mountains reaches an elevation of 514 mamsl (figure 1 in appendix A).

The study area is mainly covered by native vegetation, dominated by coastal fynbos and pampus grass, while cultivated crop is nearly absent due to the sandy nature of the soil. Large populations of introduced blue gums (*Eucalyptus globalus*) are located in the northern region of the study area, where the groundwater level is in close proximity to the ground level. Farmland is used for chicken farming, small-scale livestock and game farming, vineyards and flower plantations although the majority of the land is uncultivated.

2.3. CLIMATE

Regional Climate

The climate of the Western Cape is comparable to that of the Mediterranean, with windy, wet and cold winters and dry and warm summers (Diamond and Harris, 2000). Along the coastal regions the winter temperatures averages at around 10 ^{0}C during the day. During the summer the day temperature lies on average around 25 ^{0}C but can rise to 30 ^{0}C on hot days (Diamond and Harris, 2000). The winter months (June to August) receives the larger parts of the annual precipitation (80%), with a monthly mean of 40-100 mm on the coastal plains and up to 200 mm in the mountains, while the monthly mean for the summer months (December to March) is between 10 and 50 mm, (Diamond and Harris, 2000).

Local Climate

The undulating topography of the Western Cape results in localized micro-climates. The close proximity to the Kleinriviersberge and Swartkransberg mountain ranges has an orographic effect on the climate of the Stanford area and in general is the climate less seasonal compared to the regional climate, with reduced temperature and precipitation fluctuations.

2.3.1. Precipitation

Precipitation data have been collected by a rain gauge monitored by Alexander Grier (local resident in Stanford) since 1983 and additional data have been gathered from weather stations located at Hermanus Magnetic Observatory (HMO), 20 km northwest of

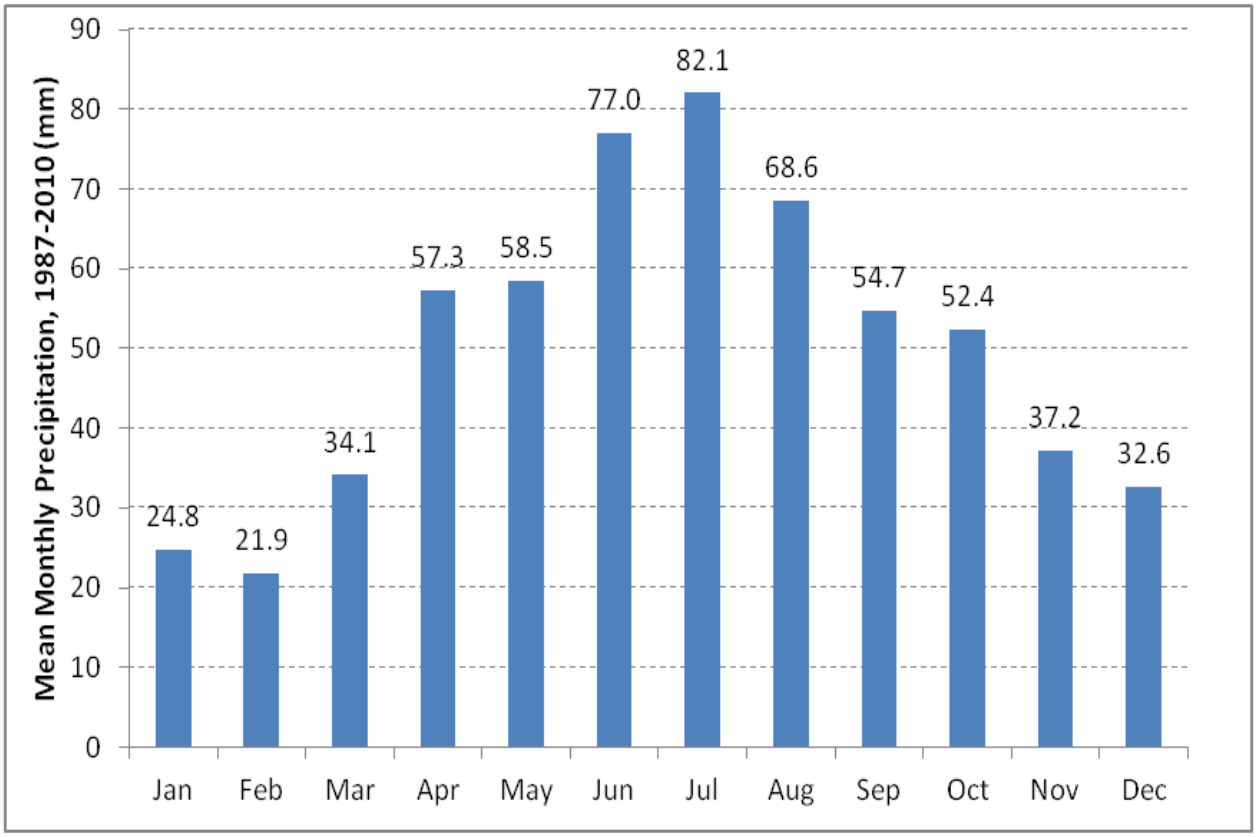

Figure 2-1. Mean monthly distribution of precipitation for Stanford, based on data for the period 1987 to 2010.

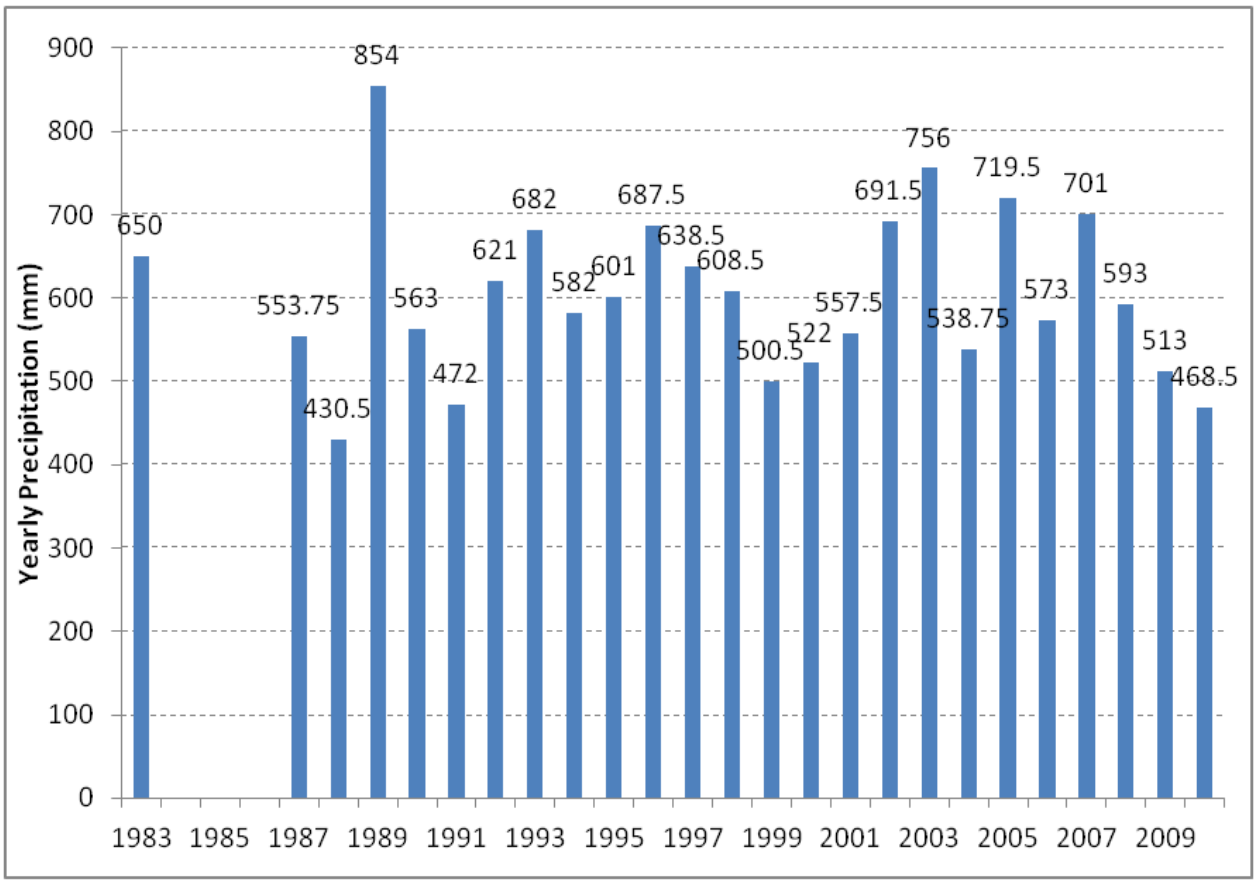

Figure 2-2. Annual historical precipitation. Data for the period 1984-86 is incomplete and is therefore not displayed.

Stanford, and at Walker Bay Nature Reserve, 10 km west of Stanford.

For the period 1987 to 2010 the mean annual precipitation (MAP) was 613 mm/a, with roughly 40 % of the precipitation falling during the winter months (figure 2-1). The yearly amount of precipitation has a broad spread but is normally between 550 to 700 mm. A yearly low was recorded in 1988 with 430.5 mm of precipitation, while a yearly high was recorded the year after in 1989 with 854.0 mm of precipitation (figure 2-2).

A mean annual precipitation (MAP) surface map was created using GIS software and shows the distribution of precipitation within the study area (figure 2 in appendix A). The main part of the area receives approximately between 500 and 575 mm of precipitation annual. A MAP of 534 mm was calculated using the MAP surface map, approximately 14 % lower than the actual measured MAP of 613 mm. The GIS software calculates the precipitation based on elevation and regional climatic factors but do not account for local geographical factors, which are thought to cause the inconsistency between the actual and calculated MAP.

2.3.2. Surface run-off

The regional mean surface run-off for the G40L subcatchment is estimated to 21.5 x 10^6 m^3/a (Midgley, 1994). However, in most parts of the study area no perennial surface water is present and the drainage of the Stanford Aquifer is considered to be endorheic, meaning most precipitation infiltrates or evaporates and very little surface run-off occurs (Umvoto, 2009). However, non-perennial streams are likely to occur during periods of heavy rain but drains quickly into the substrata and little water is drained into Klein River as surface run-off. Perennial streams originates from the Eye and Springfontein, two natural springs located in the northern part the study area, and drains into the Klein River (figure 2 in appendix A).

2.3.3. Evaporation and Evapotranspiration

The mean annual potential evapotranspiration (PET) have been estimated to approximately 1500 mm by Schulze (1997) for the coastal regions of the Western Cape. However, due to local climatic and hydrogeological conditions the actual evaporation for the study site is believed to be less than that. Evaporation is the most significant directly after a rainfall event when rain water is infiltrating the soil. The loss through evaporation can be estimated from evaporation pans or through calculation using parameters such as; solar radiation, wind speed and soil temperature. However, no such data have been collected for the Stanford Aquifer and it is therefore difficult to produce a representative estimation of evaporation. The Turc formula [1.1] estimates evaporation as a function of mean annual temperature and precipitation (MAP) (Umvoto, 2009):

$$Et = \frac{MAP}{\sqrt{0.9 + \frac{MAP^2}{L^2}}} \quad [1.1]$$

Where L is 300 + 25T+ 0.05T3 and T being mean annual temperature.

Using the Turc formula, evaporation is estimated to be in the order of 538 mm/a, using a mean annual temperature of 17.1 ^oC.

Evaporation can also occur directly from the groundwater table in areas where it is in close proximity to the ground. The loss through evaporation directly from the groundwater level is normally quite small and decreases with increasing depth to the water table. The groundwater table is in large parts of the study area located several ten's of meters below ground level and is therefore not directly subjected to evaporation or transpiration. Along the northern boundary of the aquifer, the groundwater table is in close proximity to the ground level, generally less than five meters, and evapotranspiration from the groundwater table is therefore considered to be the most significant in this part of the study area.

However, studies conducted using lysimeters show that evaporation decreases significant with increasing depth to the water table and at depths over two meters, evaporation is nearly insignificant (Todd and Mays, 2005). It is therefore assumed that evaporation occurring directly from the groundwater table is insignificant and is therefore not taken into further consideration.

3. GEOLOGY

3.1. REGIONAL SETTING

The geology of the Overberg region is dominated by the Cape Supergroup and Quaternary sediments. The sediments of the Cape Supergroup was deposited on a continental marginal setting during a 130 My long period of sea-level fluctuations during the Palaeozoic, 495 to 360 Ma (Thamm and Johnson, 2006). The sediments were deposited in various shallow marine and terrestrial environments and were subsequently uplifted and deformed during four deformation events of the Cape Orogeny (Late Permian to Early Triassic), resulting in the folded Cape Fold Belt (Thamm and Johnson, 2006). A 350 My hiatus separates the Cape Supergroup from overlying Quaternary sediments, creating an unconformity, during which rifting and igneous intrusions associated with the breakup of Gondwana occured (Thamm and Johnson, 2006). The Quaternary sediments of the Bredasdorp Group were deposited during Cenozoic sea-level fluctuations and consist of marine, fluvial and aeolian sediments (Thamm and Johnson, 2006).

3.2. LOCAL GEOLOGY

Within the study area the geology consists of the Table Mountain Group (TMG), Bokkeveld Shale and the Quaternary formations of the Bredarsdop Group. Both the TMG and the Bokkeveld Shale are siliclastic members of the Cape Supergroup (Thamm and Johnson, 2006).

Table Mountain Group (400-495 Ma)

The cratonic, sandstone-dominated Table Mountain Group (TMG) was deposited during the Palaeozoic and consist of three major formations (Thamm and Johnson, 2006):

- The Graafwater Formation is between 300-450 meters thick and consists of interbedded sandstones and shales, indicating a flood plain to lagoonal depositional environment.
- The up to 2500 meter thick Peninsula Formation consists of sandstone and quartzite units, interrupted by layers of pebbles and conglomerate, suggesting a fluvial depositional environment in the form of river channels and sandbars (Thamm and Johnson, 2006).
- The thin glacial tillite of the Pakhuis Formation only occurs on the highest points of the Table Mountains due to its low preservation potential and consists of varved mudstone, mudstone with drop-stones and sandy diamicton. The Pakhuis Formation was deposited during the Ordovician glaciation (Thamm and Johnson, 2006).

Bokkeveld Shale (375-400 Ma)

The Bokkeveld Shale is of Early to Middle Devonian age and consists of offshore to deltaic fossiliferous shale and sandstone units, showing coarsing-upward cycles caused by repeated basin-ward progradation (Thamm and Johnson, 2006). The group is conformably overlying the TMG in an off-lapping sequence and reaches a maximum thickness of 3500 meters in the eastern part of the basin but rapidly thins out to the north (Thamm and Johnson, 2006).

3.3. STRUCTURAL GEOLOGY

During the Permian and Triassic, between 280 and 230 Ma, the Cape Supergroup was intensely deformed by several compressional episodes, the Cape Orogeny, which resulted in the Cape Fold Belt (Shone and Booth, 2005). The fold belt is recognized by north-verging thrusts and folds in the southern branch of the belt, while in the western branch open folds are typical and the two branches meets in a syntaxial zone (Shone and Booth, 2005). During the break up of Gondwana 184 Ma, the Cape Supergroup was subjected to tensional stress and a series of horst and graben structures formed (Shone and Booth, 2005).

Two major faults are located within the study area (figure 3 in appendix A); an easterly-striking fault that downthrows the Bokkeveld shale against the Cape Granite Suite and TMG north of the Klein River. The second fault runs in a north-easterly direction along the south-eastern and southern boundary of the aquifer and is down-faulting the Bokkeveld shale against the TMG of the Swartkransberg (Umvoto, 1998). Numerous minor faults run in a north-easterly direction in the TMG in the Kleinriviersberge and a larger north-easterly striking fault is found south of the study area.

3.4. QUATERNAY SEDIMENTS (0-2.5 Ma)

The Bredasdorp Group consists of coastal sediments deposited during a period of regression and transgression in the Late Cenozoic and comprises five formations (Roberts et al., 2006). The De Hoopvlei, Wankoe, Klein Brak, Waenhuiskrans and Strandveld Formation consists of littoral marine, estuarine, fluvial, lacustrine and aeolian sediments varying in thickness from about 10 to 300 m. Within the study area, covering the Stanford Aquifer, only the Klein Brak, Waenhuiskrans and Strandveld Formation are present.

Klein Brak Formation

The Klein Brak Formation is resting unconformably on top of the Bokkeveld Shale and reaches a maximum thickness of approximately 10-13 m within the palaeochannels incised into the basement. The formation consists of cemented and uncemented, fine to coarse grained, calcareous sand/sandstone with beds of gravel, conglomerate, limestone and siltstone (Malan, 1987; Roberts et al., 2006). The fossil fauna assemblage indicates a shallow marine, lagoonal to foreshore depositional environment and is thought to represent a period of transgression during the Late Pleistocene (Malan, 1987; Roberts et al., 2006). Unconsolidated fine- to mediumgrained gravel and coarse grained sand with a high abundance of shell fragments (figure 3-2) were encountered during drilling of two wells in the southern part of the area in January 2010. The lithology and fossil assemblages indicates an estuarine or littoral depositional environment.

Waenhuiskrans Formation

The Waenhuiskrans Formation is resting conformable on top of the Klein Brak Formation (Roberts et al, 2006), reaching a maximum thickness of approximately 200 - 300 m along the southern boundary and thins out to the north. It is an aeolian deposit, consisting of consolidated to semi-consolidated calcareous sand (figure 3-3) and calcarenite with layers/lenses of palaeosols and calcrete scattered throughout (Malan, 1989). The Waenhuiskrans Formation is overlain by a relative thin layer of top soil (figure 3-4).

Large-scale aeolian cross-beds are characteristic of the formation as well as the presence of terrestrial gastropods (Malan, 1989). The lithology consists of well sorted to very well sorted, fine to medium grained sand and is distinguish from the Klein Brak Formation by the absence of coarse grained layers (Malan, 1989).

Limestone units (aeolinite) have been encountered, both during drilling and in surface exposures (figure 3-5). The exposed units at ground level is intensively fractured (could be due to weathering) and will therefore have relative elevated porosity and hydraulic conductivity. It is also possible that a small scale karst system has developed within these units.

Strandveld Formation

The Holocene Strandveld Formation is restricted to the coastal zone of Walker Bay and forms a narrow (<200 m) band consisting of fossil and modern sand dunes. The lithology is described by Roberts etal. (2006) as calcareous, unconsolidated dune sand with a high percentage of shell fragments, both terrestrial and marine. The Walker Bay Nature Reserve is located 10 km west of the study area, along the western boundary, and aims to preserve the sand dune habitat of the Strandveld Formation.

3.5. GEOLOGY: ADDITIONAL COMMENTS

Along the southern bank of the Klein River and the lagoon, between Stanford town and Walker Bay Nature Reserve, the soil changes its character from being sandy and calcareous in the south to finer grained and dark coloured and appears to consist of a mixture of eroded shale, sand and modern estuarine sediments in the north. The southern extent of this clayey soil-type is believed to mark the northern boundary of the Waenhuiskrans Formation (figure 3 in appendix A). Furthermore, along the contact the topography is drastic dropping from approximately 20 mamsl to approximately 5 mamsl and this shift is thought to also represent the northern extent of the Waenhuiskrans Formation.

In the literature the Klein Brak Formation is generally described as sand-dominated with occasional layers of conglomerate, gravel, silt- and limestone (Malan, 1987). Drilling within the Middelberg and Koue Vlakte Farm has encountered an up to 13 m thick gravel/sand bed immediately above the Bokkeveld Shale. This coarse-grained bed has been interpreted to belong to the Klein Brak Formation, based on its stratigraphic position and fossil assemblage.

4. HYDROGEOLOGY

4.1.HYDROSTRATIGRAPHY

The Stanford Aquifer is primarily formed within the Klein Brak and to a lesser extent also within the lower part of the Waenhuiskrans Formation. The aquifer extends over an area of approximately 120 km^2 and is an intergranular type aquifer consisting of un- and consolidated sediments.

The Klein Brak Formation is hydrogeologically important due to its coarse grained nature and is expected to be high yielding. The areal distribution and thickness of the formation is partially controlled by the relief of the basement. It reaches a maximum thickness of approximately 13 m within the palaeochannels and thins out to a few meters or less outside of these. It

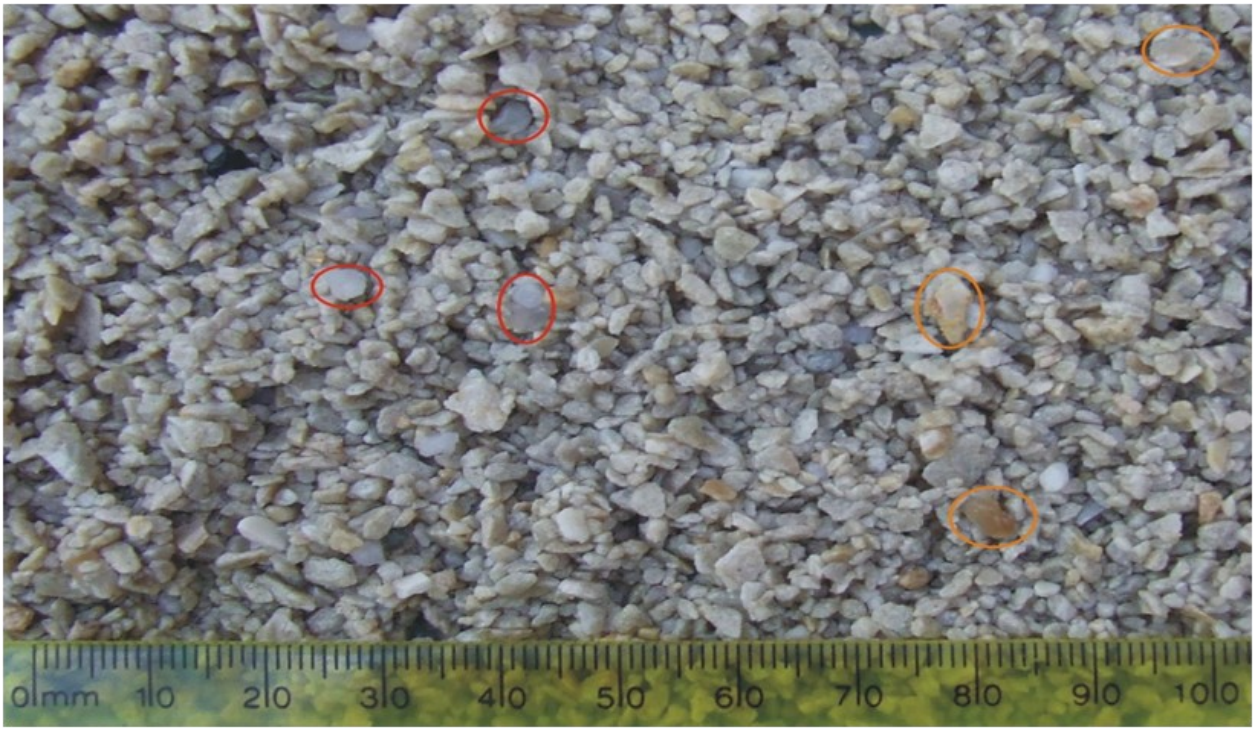

Figure 3-2. Unconsolidated coarse grained sand and gravel of the Klein Brak Formation. Large quartz grains are encircled in red and shell fragments in orange (photo by D. Blake, 2010).

Figure 3-3. Outcropping calcareous sandstone of the Waenhuiskrans Formation. Outcrop is ca two m high.

Figure 3-4. A relativ thin layer of top soil overlying the Waenhuiskrans Formation (Umvoto, 2011)

Figure 3-5. Exposed fractured limestone in the Waenhuiskrans Formation.

consists mainly of unconsolidated to semiconsolidated sand and gravel. The hydraulic conductivity of the unit is estimated to be in the range of 10^{-1} to 10^{-3} m/s due to the low degree of consolidation and heterogeneous nature of the formation.

The overlying sand-dominated Waenhuiskrans Formation is made up of consolidated to semi-consolidated, calcareous sand and sandstone, varying in thickness from a few meters in the north to a few hundreds of meters in the south. The hydraulic conductivity of consolidated sand is usually in the 10^{-2} to 10^{-6}m/s range (figure 4-1) (Todd and Mays, 2005) and thus has a substantially lower hydraulic conductivity than the Klein Brak Formation due to the calcareous nature and degree of cementation.

4.2. HYDRAULIC BOUNDARIES

The boundaries of the Stanford Aquifer are defined as follows:

- The Klein River and Lagoon is making up the north and north-western boundary, functioning as a local catchment area for water discharged from the aquifer as lateral outflow, perennial-streams and seasonal surface run-off.
- The north-eastern and eastern boundary is defined by outcropping Bokkeveld Shale (Figure 2 in appendix A).
- The Swartkransberg of the Table Mountain Group forms the southern boundary.
- To the west the aeolian sand dunes of the Strandveld Formation delineates the western extent of the aquifer.
- The aquifer is confined downwards by the Bokkeveld Shale, considered impermeable although proven waterbearing in certain areas.

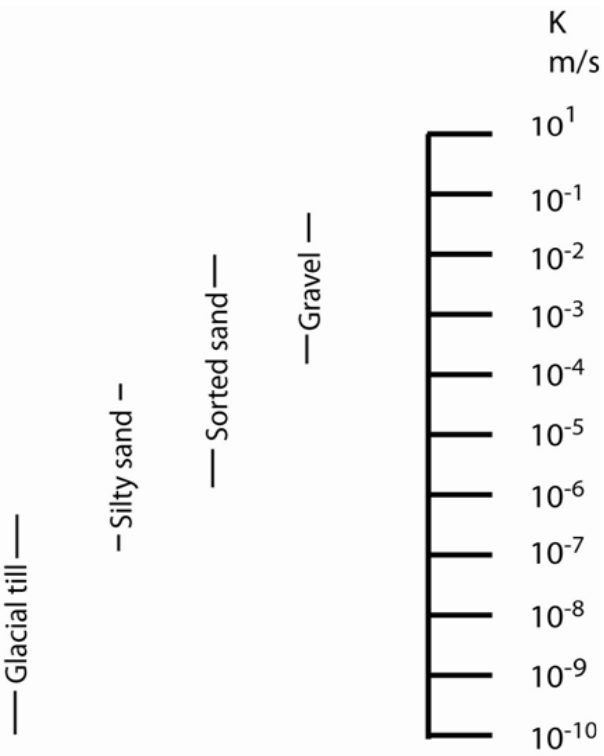

Figure 4-1. Hydraulic conductivity for a range of unconsolidated sediments (Todd and Mays, 2005).

4.3. SPRINGS AND PERENNIAL STREAMS

Two springs are located with the study area; the 'Eye' and the Springfontein. The 'Eye' is located southeast of Stanford and is used for extraction of potable water for the municipality and informal settlement, while the unexploited Springfontein is located on the Springfontein property, four km west of Stanford. One perennial streams originate from each of these springs and drains into the Klein River. The springs seem to appear at or near the boundary between the Bokkeveld Shale and the Quaternary sediments.

4.4. PALAEOCHANNELS

Palaeochannels have in previous studies proved important hydrogeological units with great potential for groundwater exploitation (Singh, 1995). The lithology of such palaeochannels is usually of coarse-grained sediments confined by finer grained deposits. The coarse-grained nature of palaeochannels usually means they are high yield aquifers but their limited lateral extent reduces the total amount of extractable water (Singh, 1995).

Previous studies have confirmed the presence of two palaeochannels within the study area; the Klein River Palaeochannel and the Koue Vlakte Palaeochannel (Umvoto, 2009). The palaeochannels were formed by a fluvial system eroding channels into the basement and subsequently filled by the sediments of the Klein Brak Formation. The marine fossil assemblage suggests that the Klein Brak Formation was deposited during a period of sea-level rise flooding the area, at which littoral and/or estuarine environments developed. This is further supported by the fact that the Klein Brak Formation is not just found within the palaeochannels but also in areas not being part of the channels. After the sea regressed to its present level, terrestrial conditions developed and subsequently the alluvial Waenhuiskrans Formation formed.

The course and extent of the palaeochannels have been inferred from drill-logs and a high resolution digital elevation model (DEM):

Drill-logs were used to confirm the presence of the gravelly Klein Brak Formation within the expected course of the palaeochannels. As palaeochannels are usually incised into the basement, and assuming the topography reflects the relief of the basement, the course of palaeochannels can be inferred from topographic data put into digital elevation models (DEM).

The Klein River Palaeochannel is located in the northern part of the study area and is running parallel to the present course of the Klein River. It is therefore believed to be an older course of that river

(figure 4-2). Well-logs confirm the presence of coarse grained sand and gravel within parts of the palaeochannel (figure 4-2 and table 4-1).

A long elongated depression has been identified from the high resolution DEM (3 m contours) in the southern part of the study area and is believed to represent the course of the Koue Vlakte Palaeochannel. The depression runs from the Swartkransberg in the south, through the centre of the aquifer, and onto the Wortel Gat property where it terminates near the Klein Lagoon (figure 4-3). Bore-logs from wells drilled into the inferred course of the Koue Vlakte channel intersects the Klein Brak Formation at several localities (figure 4-3). The Klein Brak Formation is found immediately above the basement and varies in thickness from a few meters up to ten meters. To the north-west the topographic depression branches out into two possible parallel paths.

4.5. GROUNDWATER LEVEL AND FLOW

The groundwater table is at approximately 20 meters above mean sea level (mamsl) in the south and slopes with the topography towards the north. The general flow direction is thus from south to north, but local diversions occur. Along the Strandveld Formation boundary to the west the flow is initially directed towards the east but eventually changes towards the north due to the difference in elevation between the two formations. A localised depression in the water table occurs in the Middelberg area (figure 4 and 5 in appendix A). This is believed to be caused by increased groundwater flow within the palaeochannels with subsequent lowering of the water table. The water flow in the vicinity of this depression is directed towards the centre of the depression.

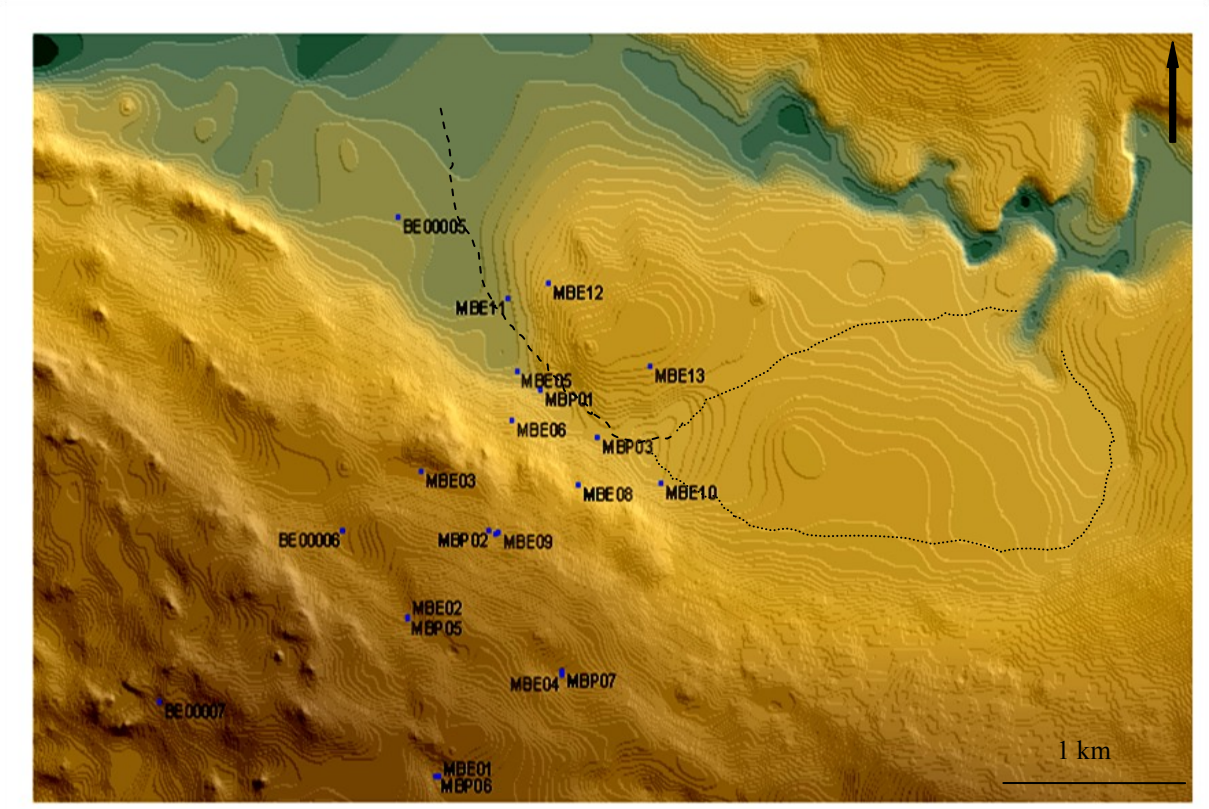

Figure 4-2. Dashed line outlines the estimated course of the Klein River Palaeochannel referred from surface topography. Wells (bold) confirm the presence of a gravel bed varying in thickness between 1.5 and 10 m in and around the proposed course of the channel. The two dotted lines to the east represent two possible paths of the palaeochannel.

Table 4-1. Table over wells located along the proposed course of the Klein River and Koue Vlakte Palaeochannels. The thickness of the Klein Brak Formation varies in thickness between 2 and 11 m. The formation is also encountered outside of the palaeochannels suggesting a littoral/ eustarine depostional environment instead of a fluvial one.

Well Id	Thickness of the Klein Brak Fm (m)	Well Id	Thickness of the Klein Brak Fm (m)
MBE02	4	MBP01	7.5
MBE03	0	MBP02	6
MBE05	9.5	MBP03	6
MBE06	9	MBP04	8
MBE08	13	MBP05	0
MBE09	11	BE00003	11
MBE10	1.5	BE00005	2
MBE11	3	BE00006	2
MBE12	0	KVE01	6
MBE13	8	KVE02	6

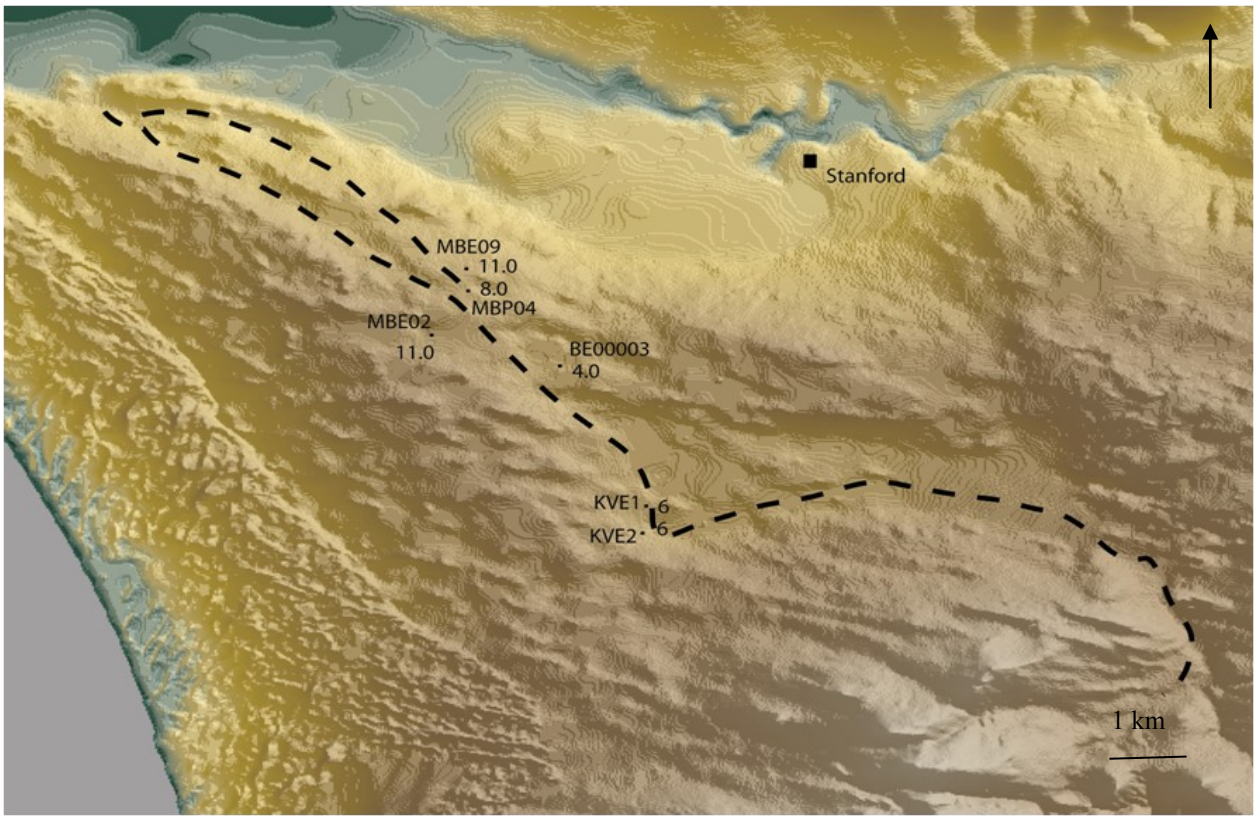

Figure 4-3. The depression in topography is thought to mark the course of the Koue Vlakte Palaeochannel (dashed line). Dots mark the location of wells located along the proposed course of the palaeochannel. The thickness of the Klein Brak Formation intercepted in these wells is also given.

Two piezometric maps have been created, one using water level measurements from the summer of 2010 (figure 4 in Appendix A) and one using measurements taken during the winter of 2010 (figure 5 in Appendix A). The two maps are nearly identical but a slightly lower water table is, as expected, seen from the summer values due to increased water extraction and decreased precipitation.

4.6. HYDROGEOLOGY: ADDITIONAL COMMENTS

The Waenhuiskrans Formation has a semi-confining effect on the Stanford aquifer despite also being part of the same aquifer. The calcareous nature and abundance of calcrete lenses reduce the vertical conductivity greatly and is believed to be near impermeable in some areas. When analysing long-term monitoring data from the Stanford aquifer, a relationship between changes in water level and atmospheric pressure was revealed, a phenomenon common in confined aquifers. The relationship is reversed; meaning an increase in atmospheric pressure causes a lowering of the water table (Todd

and Mays, 2005).

The magnitude of water level change due to barometric pressure variation is a function of the degree of confinement, rigidity of the aquifer matrix and specific weight of water (Spane, 1999). The ratio of water-level change to inverse change in barometric pressure is referred to as the aquifers barometric efficiency (BE) and can be as high as 75-80% (Todd and Mays, 2005) and is defined as:

$$BE = -\left(\frac{\Delta h_w}{\Delta P_a}\right) \quad [4.1]$$

Where:

Δh_w – Change in water level (m)

ΔP_a – Change in atmospheric pressure (m)

The minus reflects the inverse relationship existing between water level and pressure changes (Todd and Mays, 2005).

The change in water level caused by barometric pressure variation can be explained by considering aquifers as elastic bodies, where a change in barometric pressure, Δpa, will cause a change in the hydrostatic pressure, Δpw, at the top of the confined aquifer and subsequently an increase of the compressive stress, Δsc, acting on the aquifer:

$$\Delta p_a = \Delta p_w + \Delta s_c \quad [4.2]$$

At a well intersecting a confined aquifer, an increase in atmospheric pressure is transmitted directly to the aquifer via the water in the well and the water in the well will therefore be forced into the aquifer, causing a lowering of the water level within the well (Todd and Mays, 2005).

By analysing long-term fluctuations of the water table it was revealed that the water-level fluctuated with different magnitude across the Stanford aquifer due to changes in barometric pressure. It is therefore suggested that the degree of confinement varies across the aquifer as a result of the uneven distribution calcrete lenses. The calcrete lenses within the Waenhuiskrans Formation are thought to be the confining layers, which are not laterally continuous nor evenly distributed throughout the aquifer. The water level in a well located in an area where there are few calcrete lenses will show less fluctuation compared to the water level in a well drilled through several calcrete lenses (figure 4-4).

5. HYDROCHEMISTRY

5.1. WATER QUALITY

Water samples have been analyzed for chemical constituents (major anions and cations) since September 2009 on a monthly basis, and from time to time before then. The results have been compared to the guidelines for drinking water suitability set by the South Africa National Standards, document 241 (SANS-241) (table 5-1). The samples have also been compared to class 0 (ideal standard, comparable to international standards) of the South African Drinking Water guidelines (SADWG) set by the Department of Water Affairs (DWA) (2005).

The results from the analyses show that the

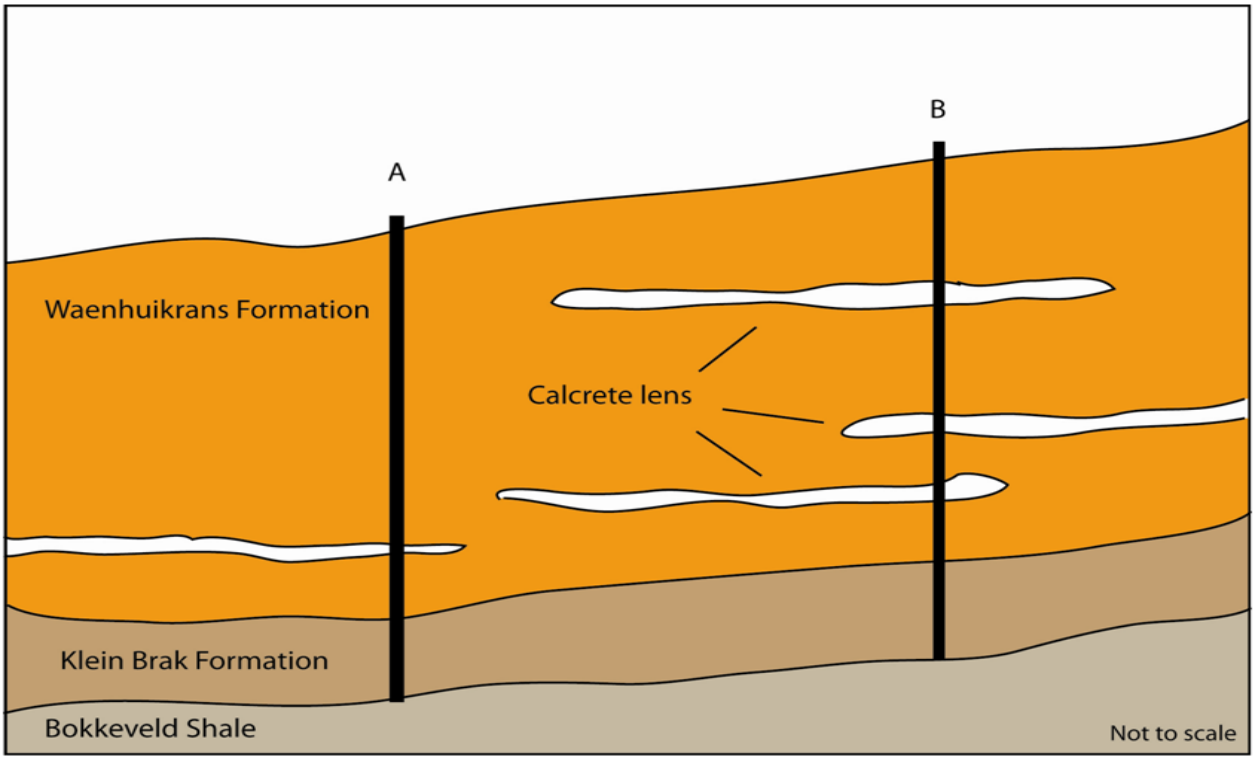

Figure 4-4. The water level in well A will fluctuate less than the water level in Well B due to the lower degree of confinement.

groundwater of the Stanford aquifer meets the overall criteria for class 1 water (acceptable as drinking water) set by SANS with mainly exceptions for fluoride, nitrate and ammonia (appendix B). The high levels of nitrate and ammonia is probably due to anthropogenic sources, such as use of fertilizers or leakage from septic tanks or alike. Fluoride is also used in fertilizers but is also a common element in many minerals.

Occasional high levels of iron have been recorded in some wells, e.g. KVE1 and KVE2 (August and December 2010), WF1 (September 2009 and December 2010) and MF1 (December 2010) (appendix B). This is possible due to the fact that these wells are not pumped on a regular basis which allow for iron to build up in the static water within the wells. If these are not purged sufficiently before sampling, the results will show elevated concentration of certain constituents.

High levels of iron and manganese have been recorded in WF1, KVE1 and KVE2. This can partly be explained by the extensive depth of KVE01 and KVE02 (> 90 m in KVE01 and KVE02) which allows for anaerobic condition to develop, causing manganese to remain in solution especially under carbonated conditions (Todd and Mays, 2000). The low pH level in KVE02 is considered to be the cause of the elevated aluminium levels.

A summary of the chemistry results is shown in figure 5-1 and 5-2, in which the data is plotted in Piper diagrams. Figure 5-1 plots results from samples collected during summer 2010 and figure 5-2 plots results from winter 2010. The diagrams clearly illustrates that the sampled water have an overall similar chemical fingerprint with a few exceptions. In figure 5-2 a sample from the Municipality Office plots abnormally once in the winter of 2010. However, the water from the Municipality Office has undergone treatment and will therefore be enriched in chloride.

The samples GB1 and TMG1 were collected from the Swartkransberg, to the south of the study site.

Table 5-1. South Africa National Standard guidelines for drinking water, (after SANS-241, 2005).

SANS-241	Unit	Class I	Class II (max. allowable for limited duration)	Class II water (max consumption period)
pH	-	5 – 9	4 - 10	-
EC	mS/m	< 150	150 - 370	7 years
Colour	Pt	< 20	20 – 50	-
Alkalinity	-	n/a	n/a	n/a
Total hardness	-	n/a	n/a	n/a
Magnesium	mg/L	< 70	70 – 100	7 years
Sodium	mg/L	< 200	200 – 400	7 years
Potassium	mg/L	< 50	50 – 100	7 years
Zinc	mg/L	< 5	5 – 10	1 year
Chloride	mg/L	< 200	200 – 600	7 years
Fluoride	mg/L	< 1	1 – 1.5	1 year
Sulphate	mg/L	< 400	400 – 600	7 years
TDS	mg/L	< 1000	-	-
Ammonia	mg/L	< 1	1 – 2	-
Nitrate/Nitrite	mg/L	< 10	10 - 20	7 years
Iron	µ/L	< 200	200 – 2000	7 years
Manganese	µ/L	< 20	100 – 1000	7 years
Aluminium	µ/L	< 300	300 - 5000	1 year

The fact that they plot similar to the water samples collected from the aquifer (figure 5-1) supports the idea of lateral inflow to the aquifer from the TMG. Also the rain water sample (GB1RG) shows a similar chemical fingerprint as samples from the aquifer. This indicates that little chemical absorption/dissolution occurs after rainwater once has infiltrated into the aquifer, possible due to the unreactive siliclastic nature of the sediments within the aquifer.

From the piper diagrams is can be observed that a slight enrichment in cations has occurred and is probably due to the calcium-rich nature of the Waenhuiskrans Formation. Thus the water is hard in nature and has Ca^{2+} as its dominant cation and HCO^{3-} and/or CO_3^{2-} as its dominant anion (Fetter, 2001). The clustering in the diamond diagram indicates a similar origin from the samples collected from the aquifer, that they belong to the same hydrochemical facie, as expected (Fetter, 2001).

5.2. STABLE ISOTOPES

5.2.1. Background

Hydrogen (H) and oxygen (O) isotope studies are readily used for determine origin and undergone processes of groundwater. During processes such as evaporation, condensation or interaction with geothermal heat, do the hydrogen and oxygen isotopes fractionate into light or heavy fractions. The degree of fractionation is determied by (Fetter, 2001):

$$\delta = \frac{Rsample - Rstandard \times 1000}{Rstandard} \quad [3.1]$$

Where R is the ratio of heavy to light isotopes.

The results are given in ‰ relative to V-SMOW (Vienna Standard Mean Ocean Water), a standard consisting of distilled seawater as defined by the International Atomic Energy Agency (SAHRA, 2011).

A positive value indicates that an enrichment of the heavy isotopes relative to the standard have occur-

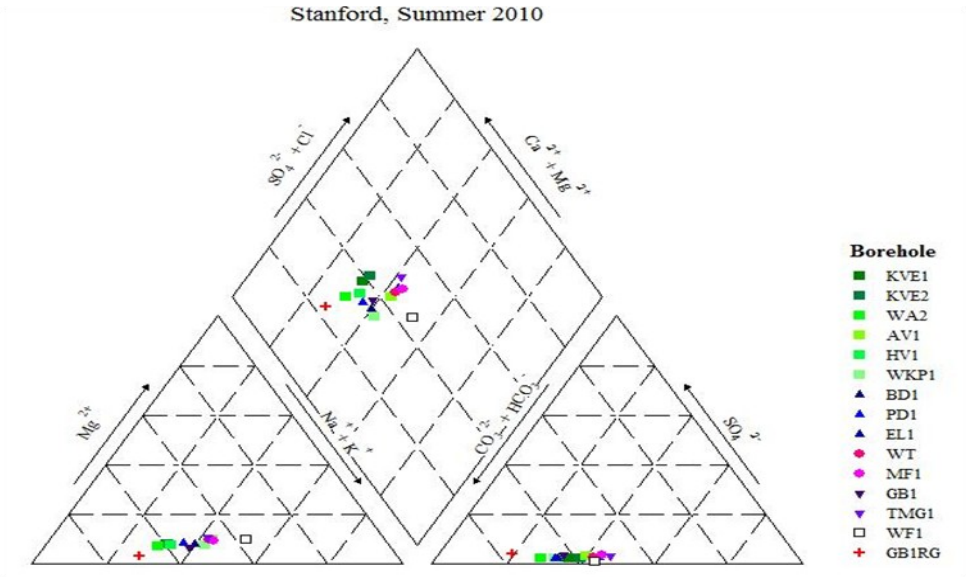

Figure 5-1. Chemistry data from samples collected during the summer of 2010, plotted in a Piper diagram. A general enrichment in cations has occurred, probably due to the calcium-rich nature of the Waenhuiskrans Formation.

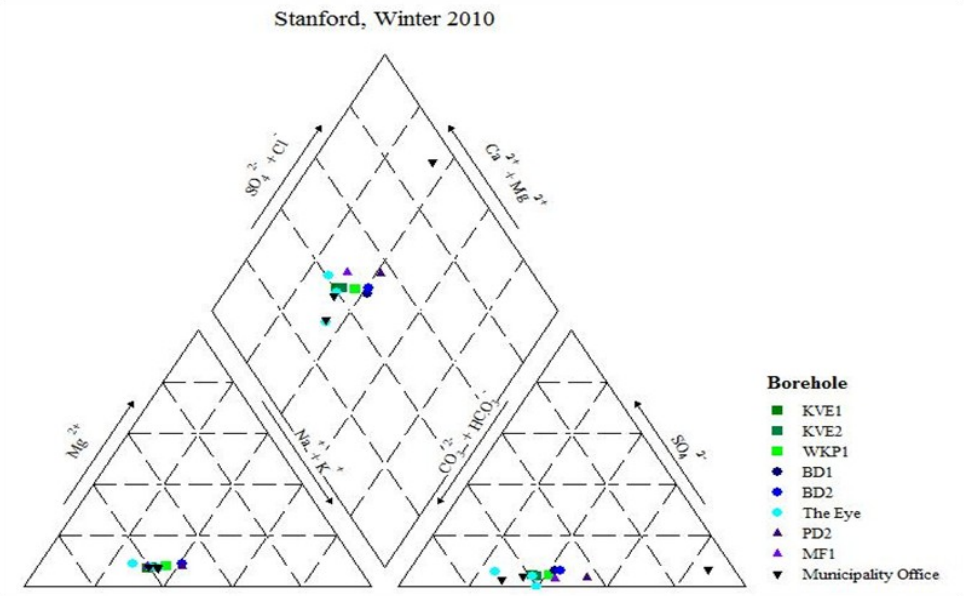

Figure 5-2. Chemistry data from samples collected during the winter of 2010, plotted in a piper diagram.

red, while a negative value means an enrichment of the light isotopes have taken place (Fetter, 2001). Fractionation can occur during evaporation at which the lighter isotopes, ^{1}H and ^{16}O, are concentrated in the vapour phase and the heavier molecules, ^{2}H and ^{18}O, are concentrated in the liquid phase, while during precipitation the heavier isotopes falls to the ground with the rain and the lighter isotopes remain in the vapour in the atmosphere (Fetter, 2001).

There are several factors influencing the isotopic composition of rainwater as well as groundwater. Altitude, latitude, humidity, continentality and season of the year are all influential, besides evaporation and condensation. Figure 5-3 summarises these processes effects on the isotopic composition

5.2.2. Sampling

Samples from selected wells across the Stanford Aquifer were collected in December 2010 and analyzed for stable isotopes at the Department of Geological Sciences at University of Cape Town (appendix C for details). For comparison, two samples, TMG1 and GB1, were collected from the Table Mountain Group south of the study area.

5.2.3. Results

Thirteen samples were analyzed for isotopic composition, of which ten samples derived from the Stanford Aquifer, two from the Table Mountain Group and one of precipitation. $\delta^{2}H$ values range between -29 and -20 ‰ while $\delta^{16}O6$ values range between -5.8 and -5.09‰ relative to V-SMOW, respectively. It can thus be concluded that a depletion in heavy isotopes has occurred.

In figure 5-4 and 5-5 is $\delta^{2}H$ versus $\delta^{16}O$ plotted against the Global Meteoric Water Line (GMWL) and the Cape Town Meteoric Water Line (CMWL). Sample TMG1 and GB1 were not collected from the Stanford Aquifer but plots similar to the samples from the aquifer. GB1RG is a rainwater sample collected from the Swartkransberg; a rainfall sample was also collected from the Stanford Aquifer but due to contamination, it has not been used.

It is interesting to note that the water does not appear to have had undergone a large degree of fractionation due to evaporation. If it had it would be been expected that the samples would plott below the GMWL (figure 5-3). The reason could be (*i*) the majority of the precipitation occurs during the winter were evaporation is at is lowest, (*ii*) most of the water in the aquifer comes from the Swartkransberg and enters the aquifer as lateral inflow and the if the Swartkransberg is highly fractured the rainwater will enter the system rapidly and therefore not be subjected to evaporation.

5.2.4. Conclusion

From the isotope data it can be concluded that:

- Samples from the aquifer plot in close proximity of the GMWL and are most likely of meteoric origin.
- The isotopes have undergone some degree of fractionation.
- Samples TMG1 and GB1 consist of water collected from the Swartkransberg, south of the

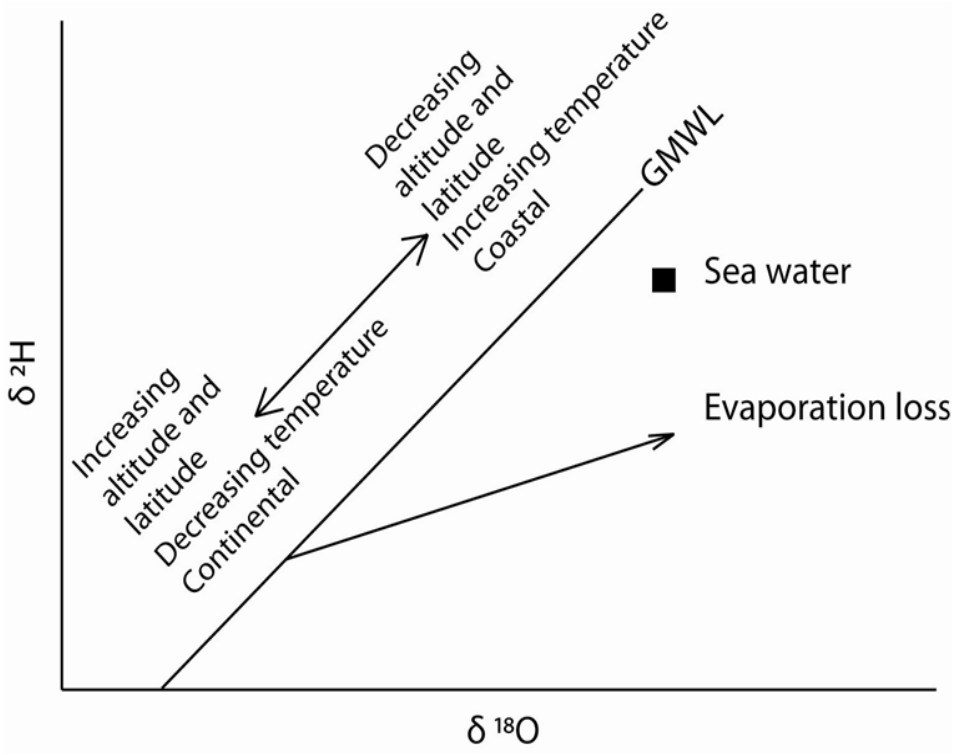

Figure 5-3. Schematic illustration summarizing how hydrological processes affect isotopic composition of ground- and rainwater (after SAHRA, 2011).

aquifer, and as shown in figure 5-5 they plot similar to the samples collected from the aquifer itself, which could be indicative of an inflow from this formation into the aquifer.

6. CONCEPTUAL MODEL

The Stanford Aquifer is formed within both the Klein Brak and Waenhuiskrans Formation with the Klein Brak Formation resting directly on top of the basement, the Bokkeveld Shale. The thickness of the Klein Brak Formation is partially controlled by palaeochannels eroded into the basement and usually varies between one meter at the edge of the channels and ten meters in the centre of the channels. The aquifer is partially confined by calcrete lenses within the Waenhuiskrans Formation and is therefore classified as a leaky type aquifer. Two palaeochannel have so far

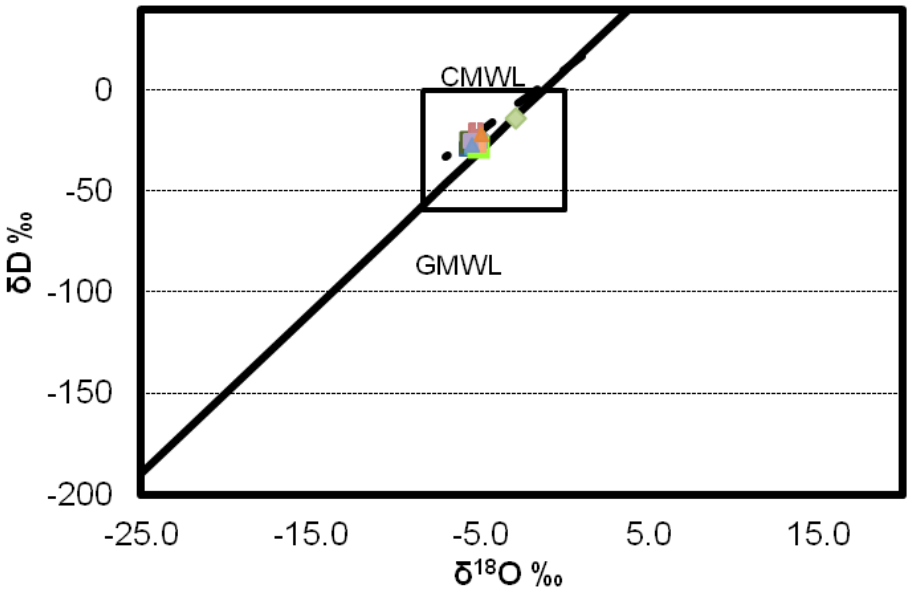

Figure 5-4. Stable isotopes plotted against Cape Meteoric Water Line (CMWL) and Global Meteoric Water Line (GMWL).

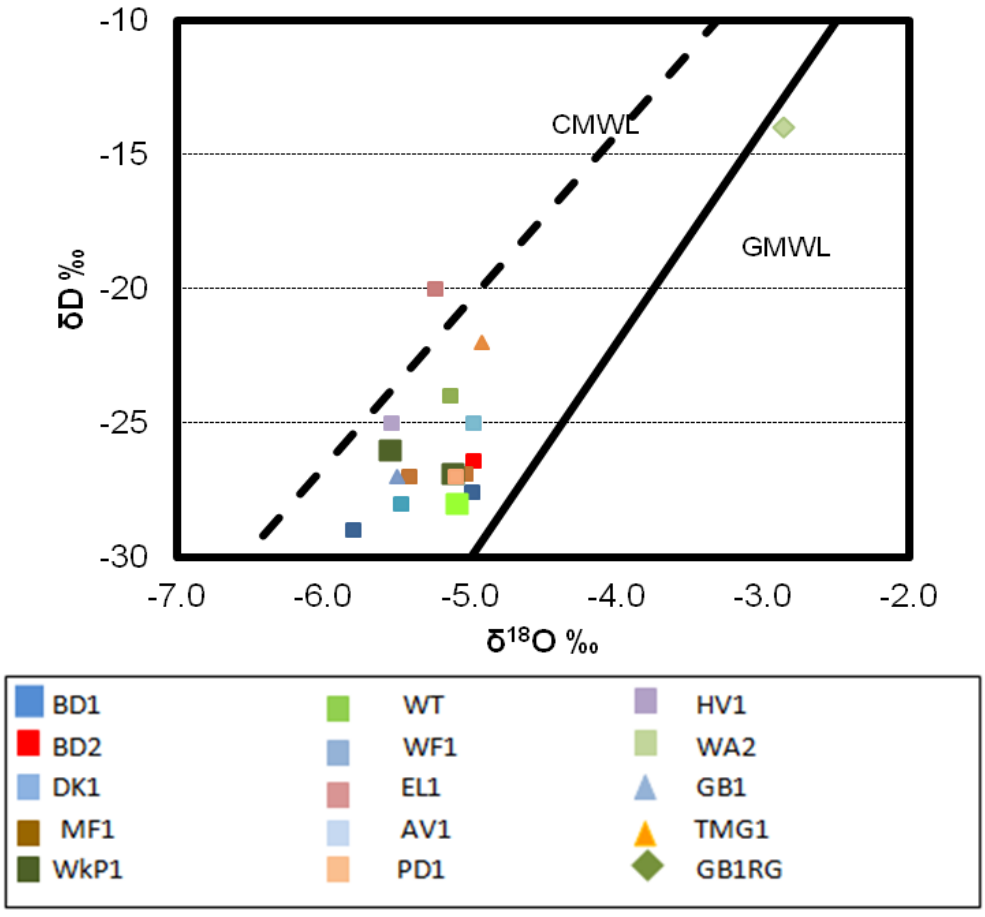

Figure 5-5. Stable isotopes plotted against CMWL and GMWL, a close-up of fig. 5-4.

been identified within the aquifer, the Klein River and Koue Vlakte Palaeochannel.

Groundwater flow is in general from south towards north but local diverts occur. Along the western aquifer boundary the flow has a north-eastern direction. In the central parts of the aquifer a groundwater depression is present, thought to be caused by rapid groundwater flow within the palaeochannel due to coarse grained nature of the Klein Brak Formation.

Surface waters are restricted to two springs (the 'Eye' and the Springfontein) located in the northern part of the aquifer, from where two perennial streams originate and drains into the Klein River and lagoon. Surface run-off is otherwise limited due to the endorheic nature of the Stanford Aquifer.

The 'Eye' (a natural spring) has been captured and is being used as a source of potable water for Stanford town and the informal settlement. Surplus water is being lead through the town before being discharged into the Klein River via the Leiwater channel. Numerous private wells are located throughout the aquifer from which extraction occurs.

Isotopic analysis indicates a meteoric origin of the water within the aquifer, with recharge occurring both through infiltrating precipitation, lateral inflow and surface run-off. Inflow and surface run-off is thought to occur primarily from the Swartkransberg, located south of the aquifer.

Figure 6.1 sums up the conceptual model as a schematic cross-section taken in north to south direction.

7. PUMP TEST

7.1. INTRODUCTION

7.1.1. Background

Pump tests are used to evaluate aquifer parameters, such as transmissivity (T) and storativity (S) among others, as well as well performance. From this, conclusions can be made on what effects the pumping will have on the aquifer and neighbouring wells.

Groundwater extraction from the 'Eye' has in previous years exceeded the estimated sustainable yield of c. 400 Ml/a (Umvoto, 2009) and an additional source of extraction is therefore needed for augmentation. Exploration of the groundwater potential in the Kouevlakte area was initiated in November 2009, starting with a gravity survey conducted by Cape Geophysics. The aim of this survey was to locate and determine the lateral extent of the Koue Vlakte Palaeochannel in the southern part of the study area. Based on the results from the gravity survey two new boreholes (KVE01 and KVE02) were sited and drilled in February 2010 by SA Rock Drills (Pty) Ltd.

7.1.2. Well Specifications

KVE01 and KVE02 are located approximately 6 km south of Stanford, adjacent to the R43 towards Gansbaai and were drilled into the expected course of the palaeochannel. The wells were drilled at a diameter of 300 mm to a depth of 110 and 114 meters below ground level (mbgl) for KVE01 and KVE02, respecti-

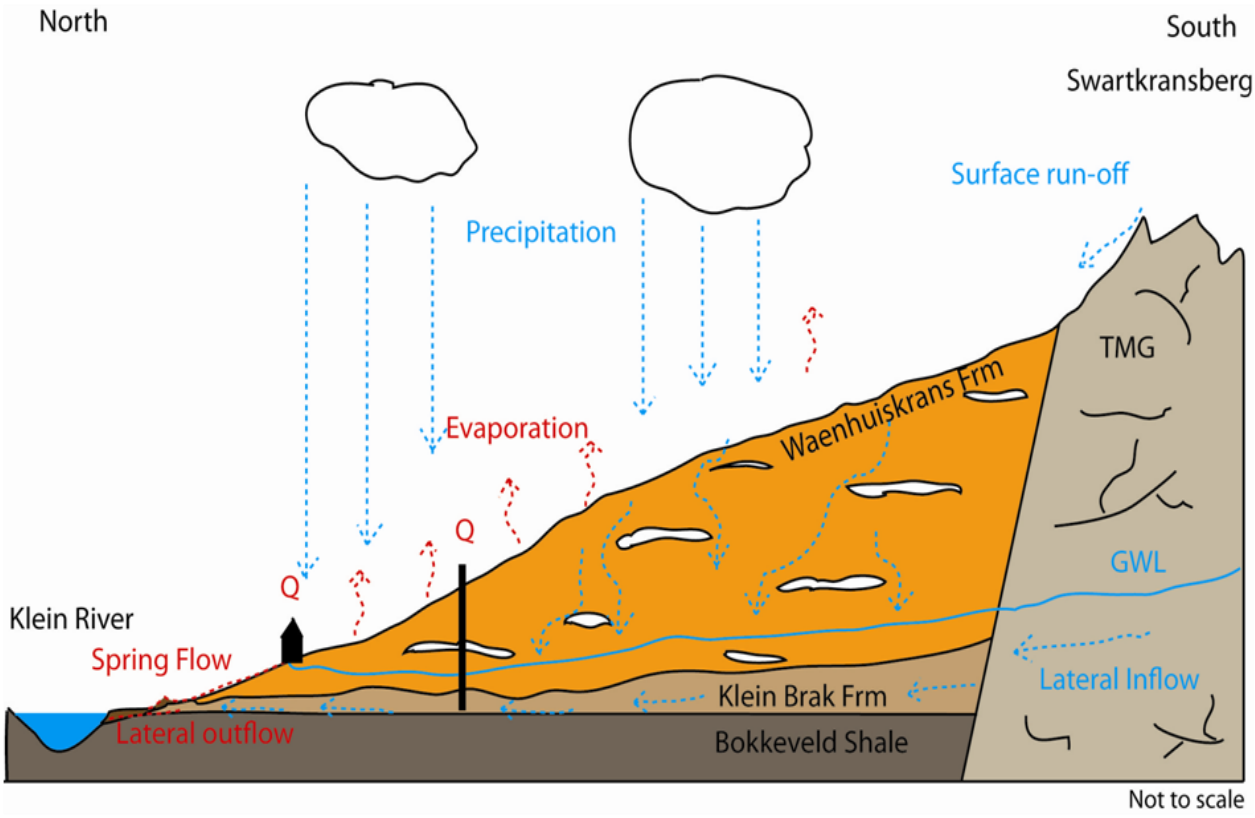

Figure 6-1. Schematic cross-section summarising the conceptual model.

vely (table 7-1). The coarsegrained Klein Brak Formation was encountered at approximately 105 and 110 mbgl for KVE01 and KVE02 (appendix D for details), respectively (Umvoto, 2010).

7.1.3. Monitoring network

The location and observations made in the observation wells are given in table 7-2. The position of the observation wells are shown in figure 7-1.

7.1.4. Pump Installment

In order to prevent discharged water to recharge the aquifer, the discharge point has to be positioned down-gradient from the well. During the Step-down test of KVE01 and KVE02 the discharge point was positioned 100 m down-gradient of the wells, making it possible to monitor the sediment load in the discharged water more efficiently. During the constant rate test the discharge point was positioned 300 m down-gradient from the wells.

Pump and pump installation specification are given in table 7-3 and figure 7-2.

7.2. METHODOLOGY

7.2.1 PUMP TEST PROCEDURE

The pump test planned and conducted on KVE01 and KVE02, consisted of a step-down test, followed by a constant rate test and finally a recovery test. The testing of KVE01 was commenced on March 16 2011 at 13:55 and was completed on March 21 at 08:00. The testing of KVE02 was commenced on March 21 at 11:22 and was completed on March 26 at 08:00. The pump test was conducted by contracted Pumpcor under the supervision of Umvoto.

Step-Down Test

The aim of the step-down test (SDT) is to evaluate the performance of the well and aquifer parameters as well as to determine the needed extraction rate for the constant rate test. The minimum requirements for a step-down test are four steps of at least one hour duration for each step (SANS, 2003).

The initially planned step-down test was of 8 steps of one hour duration each and with increasing pumping rates from 5 to 22.5 l/s. However, due to technical issues the planned step-down test could not be executed fully and only the first six steps were completed. The reason for this is thought to be partially due to the fact that the boreholes were slightly curving and therefore causing the pump to rest on one side against the casing and subsequently partial obstructing the pump inlet. The relatively short head in the boreholes is also thought to be limiting the pump rate, as insufficient water was being 'fed' to the pump and therefore causing the pump to work at higher amplitude causing the generator to work above its capacity. During step six of the test, the generator was working at its maximum capacity and it was not possible to continue with step seven and eight.

Figure 7-1. Pump installation at KVE02. The blue pipe is the mechanical flow meter and the white pipe behind it is the digital flow meter. The water level was monitored manually with a dip meter through the black hose coming up to the right.

Specification	Unit	KVE01	KVE02
Elevation	mamsl	106	110
End of hole	mbgl	110	114
	mamsl	-4	-4
Static water level	mbgl	91.6	96.55
	mamsl	14.4	13.45
Casing diameter	mm	200	200
Length of solid casing	m	102	101
Length of slotted casing	m	9	14

Table 7-1: Drilling and well specifications for the tested wells (Umvoto, 2010).

Table 7-2. Details of monitoring netwok.

Borehole ID	Borehole purpose	Distance/direction from KVE01	Measurements
KVE01	Pump test/observation	-	Automatic logger: hourly. Manual measurements: Frequently for the first 200 minutes, thereafter regularly.
KVE02	Pump test/observation	134 m/190° (S)	Automatic logger: hourly. Manual measurements: Frequently for the first 200 minutes thereafter regularly.
DP1	Observation	480 m/49° (NE)	Automatic logger: hourly.
AV1	Observation	560 m/216° (SW)	Automatic logger: hourly.
LT2	Observation	1880 m/19° (NNE)	Automatic logger: hourly Manual measurements: Daily during pump test

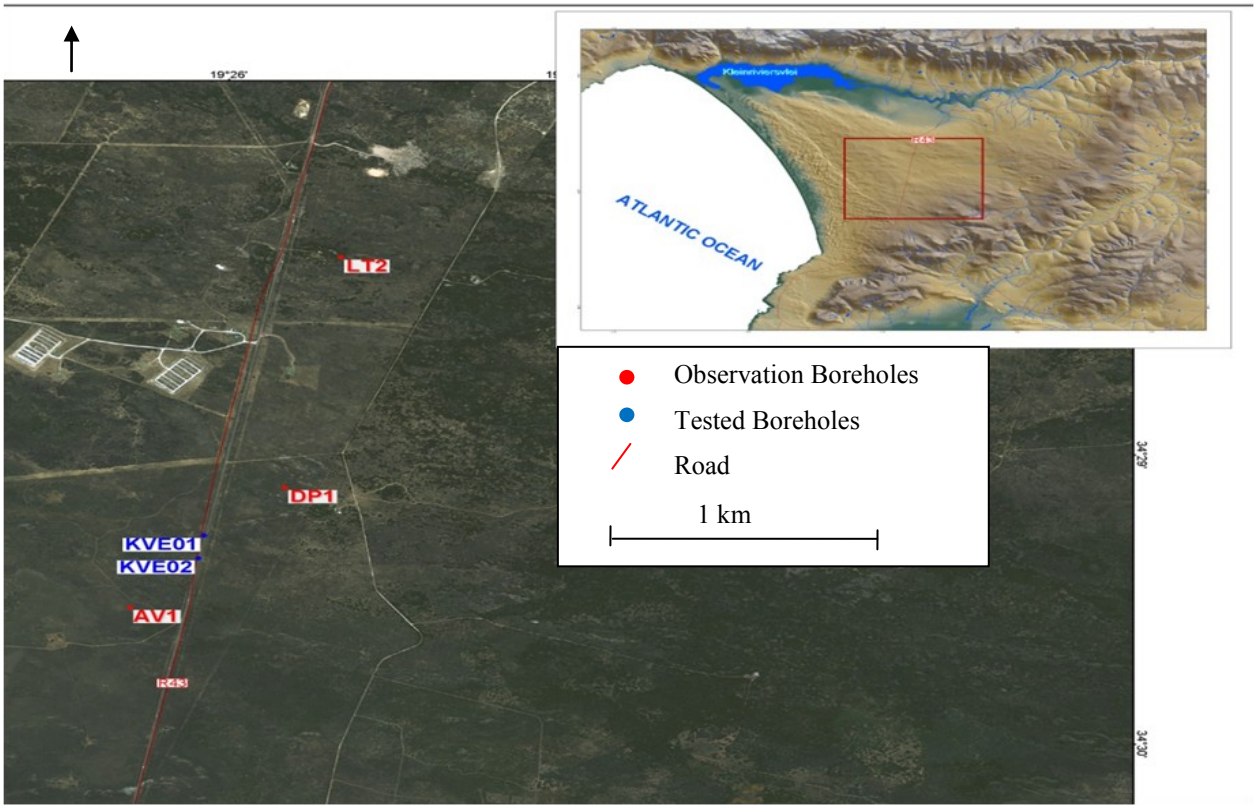

Figure 7-2. Map over monitoring network. Tested wells in blue and observation wells in red.

Constant Rate Test

The purpose of the constant rate test (CRT) is to evaluate transmissivity and storativity of the aquifer and determine the long-term sustainable yield of the aquifer (SANS, 2003). The duration of the CRT depends on the intended usage of the well, the aquifer type tested and can vary in time in the order of 24 hours to 30 days, the longer the test the more reliable data (SANS, 2003). It is important that the pump rate remains constant throughout the duration of the test and it is a requirement that the fluctuations in rate during the test is less than ±5% and should be monitored regularly (on a hourly basis) during the duration of the test (SANS, 2003). The discharge rate is determined from the SDT and should be such that the water level is not drawn down below the pump inlet. Preferably should the drawdown not exceed three-quarters of the available drawdown in the borehole (SANS, 2003).

The discharge rate for the planned CRT for KVE01 and KVE02 was to be determined from the result from the step-down test, as explained above. But due to the technical issues encountered (see above),

the CRT was conducted at the pumps maximum capacity, 16.2 l/s, for a duration of 72 hours (table 7-4 for specification).

Recovery test

A recovery test is useful to further evaluate aquifer parameters as the test result is not affected by equipment or human errors. The test is performed immediately after the CRT and it is a requirement that the pump is fitted with a non-return valve, as the results otherwise would be erroneous (SANS, 2003).

A recovery test is considered complete when:

- The water level have recovered to less than 5% of the total drawdown of the constant rate test,
- At least three successive readings are identical, or
- the recovery test have been going on for a duration equal to the duration of the CRT.

(SANS, 2003)

The actual performed pump test deviated somewhat from the initially planned test due technical difficulties, as described above. A summary of the test specifications are outlined in table 7-4.

Table 7-3. Pump and installation specifications.

	KVE01	KVE02
Pump inlet depth (mbgl)	107.5	110.5
Static water level (mbgl)	91.6	96.55
Available drawdown (m)	15.9	13.95
Pump model	Brisan Q90/14	

7.2.3. PROCEESING OF DATA

7.2.3.1. Masking of atmospheric pressure

As mentioned earlier, changes in the atmospheric pressure causes fluctuations of the water table which in turn can result in somewhat obscure pump test result. Before the results from the pump test could be processed and analysed it was necessary to adjust for the effect caused by the fluctuation of the atmospheric pressure.

The factor by which the boreholes respond to changes in pressure was determined by using long-term pressure and water level data (January – March, 2011) and assuming that a direct linear relationship exists between the two. The influence by precipitation and pumping is expected to be nominal due to (i) that the majority of rainfall occurs during the winter months and (ii) that no pumping occurred in the near vicinity of the tested and monitored wells.

By using Excel Solver it was possible to partially smooth out the water table and remove the fluctuations caused by changes in atmospheric pressure. However, the water level is still fluctuating (see figures 7-3, 7-4, 7-5 and 7-6), which can be due to several factors: measurement errors, inconsistent pumping rate or that the assumed linear relationship between changes in atmospheric pressure and fluctuation of the water table is not completely true. In figures 7-3 and 7-4 are the observations made in KVE01 and KVE02 during the constant rate test (CRT) of KVE01 plotted. In figures 7-5 and 7-6 are the observations taken in KVE01 and KVE02 during the CRT of KVE02 plotted, respective. Figures 7-3 and 7-5 shows that the water level in the tested wells rises to above the initial static water level (SWL) after the completion of the test before levelling out. The reason for this is a small hole in the non-return valve, which allows water to be drained from the boreline and run back into the well. Unfortu-

Table 7-4. Summarization of planned and actual performed test program.

Step	Test type	Planned test		Performed test	
		Rate (l/s)	Duration (hours)	Rate (l/s)	Duration (hours)
1	Step-down	5	1	5.4	1
2	Step-down	7.5	1	7.5	1
3	Step-down	10	1	10	1
4	Step-down	12.5	1	12.5	1
5	Step-down	15	1	15.2	1
6	Step-down	17.5	1	17.5	1
7	Step-down	20	1	-	-
8	Step-down	22.5	1	-	-
9	Recovery	0	6	0	6
10	Constant rate	*	72	16.2	72
11	Recovery	0	72	0	24

nately, it also means that the recovery test cannot be analysed as the data is obscured by the water returning from the boreline.

The water level in observation wells AV1, DP1 and LT2 showed no or little drawdown during the pump test, possible due to that the pump test was not long enough for the radius of influence to reach the observation wells. Furthermore, the effect of atmospheric pressure complicates detail analyse of these wells. Therefore, the observations made in these wells have not been further analysed.

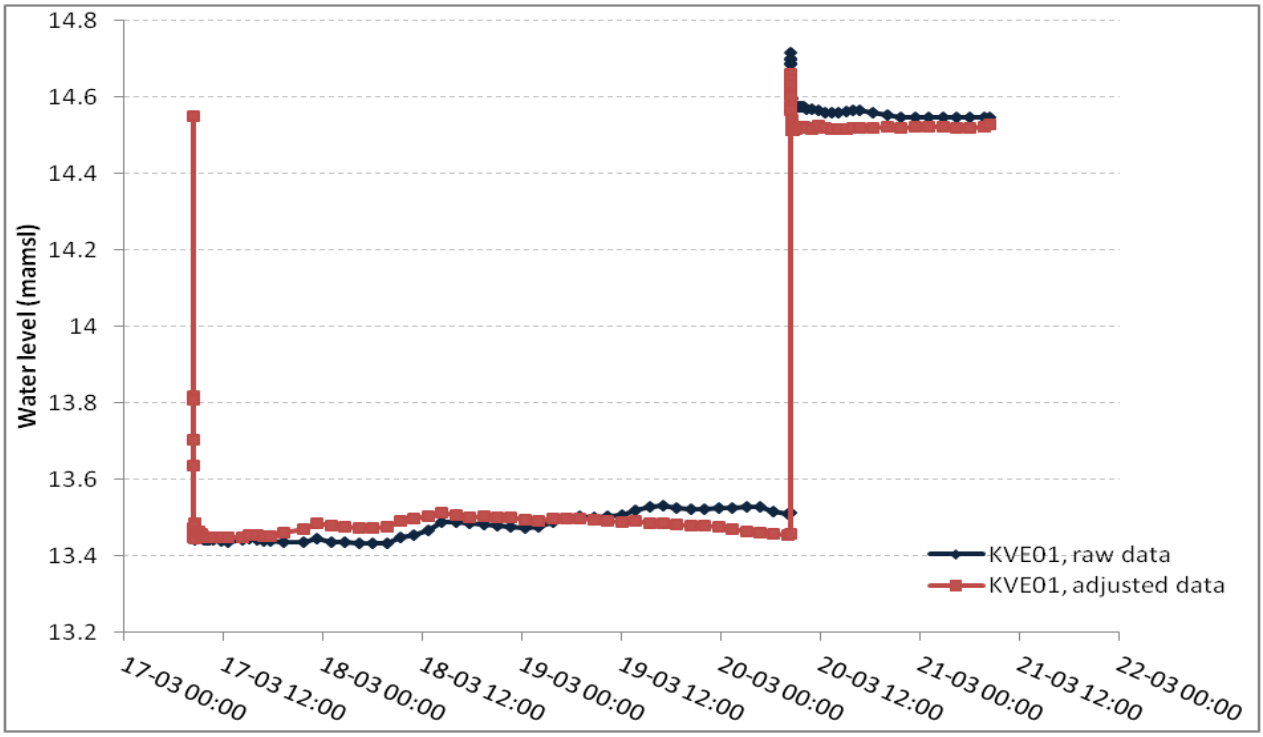

Figures 7-3. Raw and adjusted observations taken in KVE01 during the constant rate test of KVE01. Despite being adjusted the water level is still fluctuating. Pump started at 08:00 on March 17 2011.

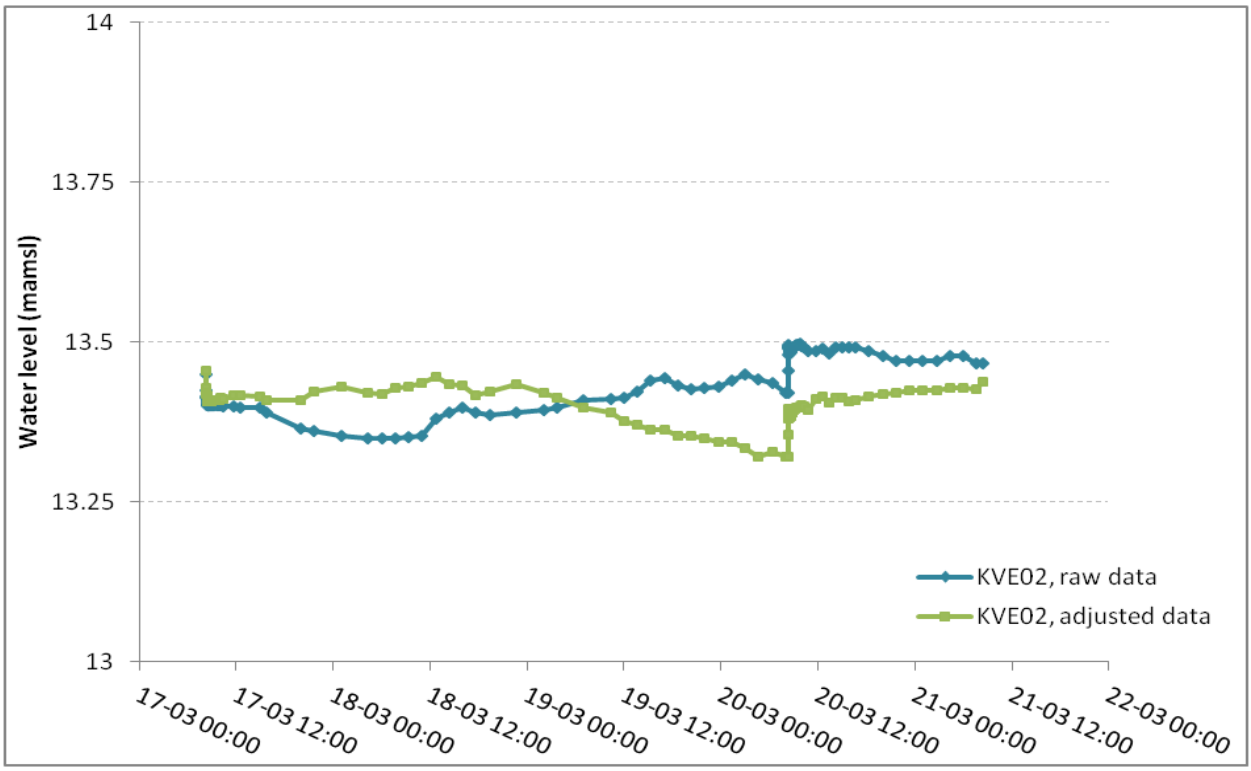

Figure 7-4. Raw and adjusted observations taken in KVE02 during the constant rate test of KVE01. Note the abnormal fluctuations of the adjusted data.

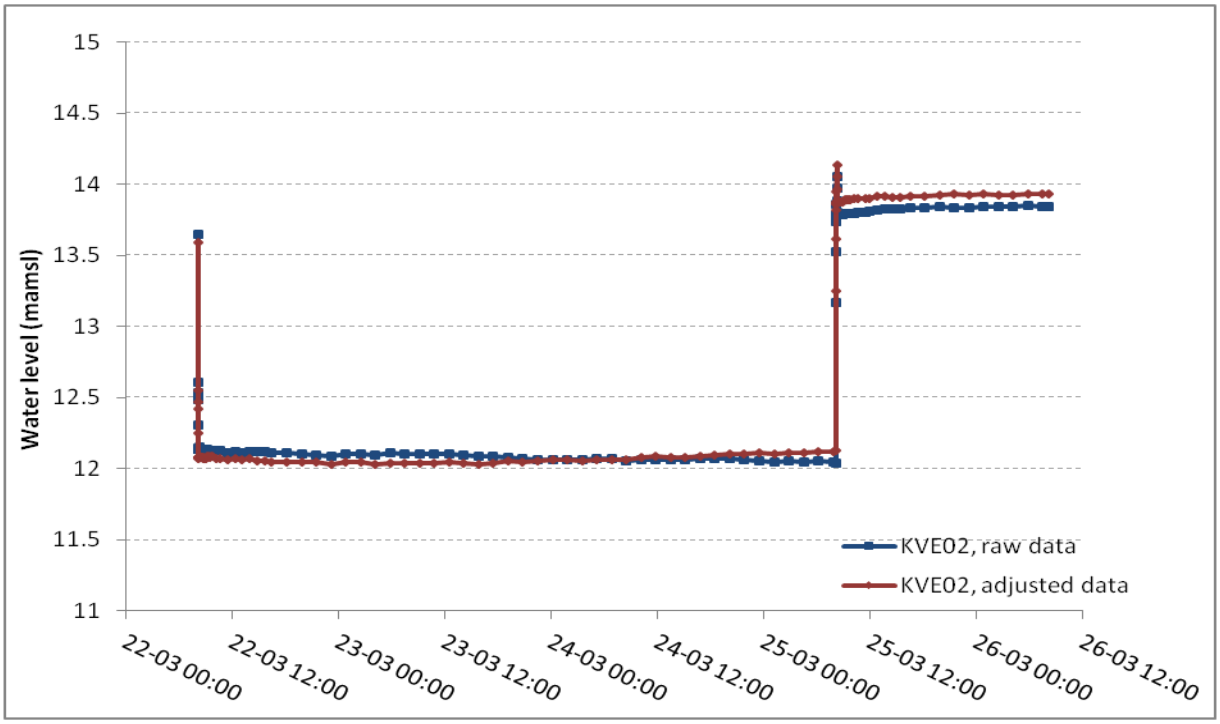

Figure 7-5. Raw and adjusted observations taken in KVE02 during the constant rate test in KVE02. Test commenced at 08:00 on March 22 2011.

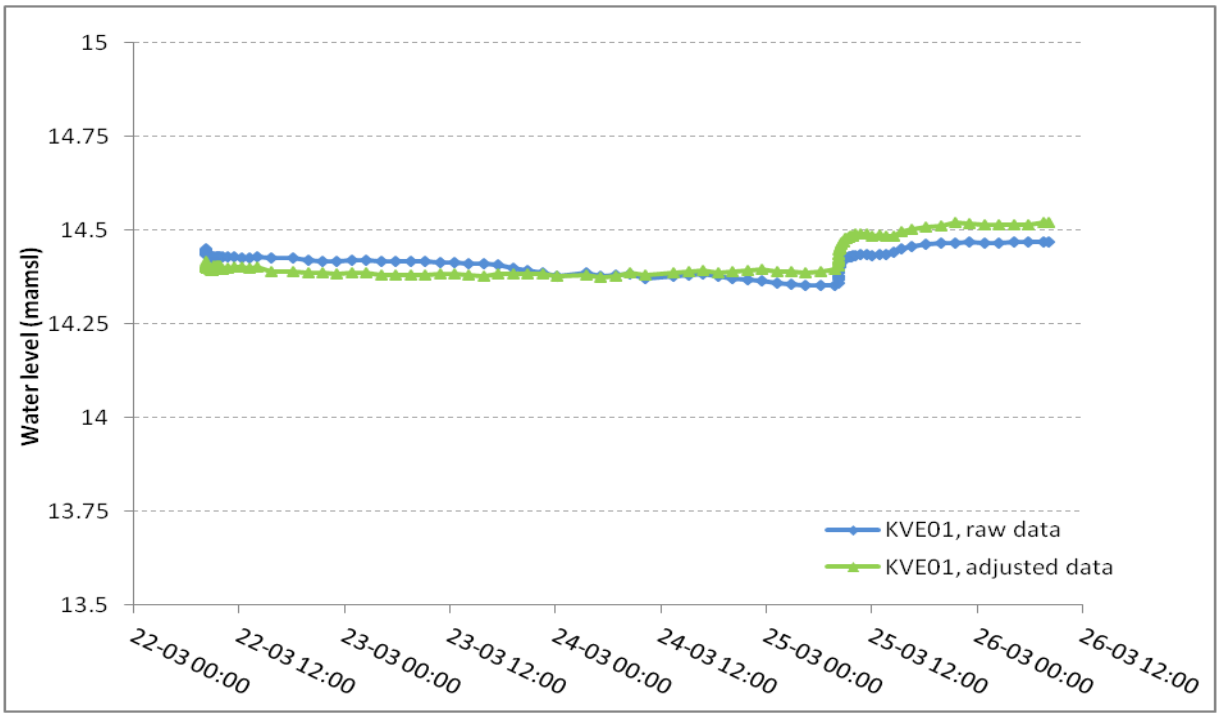

Figure 7-6. Raw and adjusted observations taken in KVE01 during the constant rate test of KVE02.

7.2.3.2. Analytical Interpretation

AQTESOLV, version 4.5 (a software developed by HydroSOLVE), was used to analyse the results and estimate values of Transmissivity (T) and Storativity (S). The method of Hantush-Jacob for leaky aquifers was chosen when analyzing the data as this method seems to best represent the condition prevailing in the system. Furthermore, the Theis-Boulton method for unconfined aquifers with delayed yield was manually used to produce estimates of T and S. The radius of influence was determined using Jacobs drawdown-distance method.

Hantush – Jacob Method - Leaky Aquifer: De Glee derived a formula based on the steady-state drawdown occurring in an aquifer with leakage from an aquitard proportional to the hydraulic gradient across the aquitard (Kruseman & de Ridder, 2000), written as:

$$s_m = \frac{Q}{2\pi T} K_0\left(\frac{r}{L}\right) \qquad [7.1]$$

where:
s_m - Steady-state drawdown in meters in a piezometer at distance r in m from well.
Q - Pumping rate (m^3/d)
T - Transmissivity (m^2/d)
L - $\sqrt{KDc}$ (leakage factor in m)
c - D´/K´ (hydraulic resistance of the aquitard in d)
D´ - Saturated thickness of the aquitard (m)
K´ - Hydraulic conductivity of the aquitard for vertical flow (m/d)
$K_0(x)$ - Modified Bessel function of the second kind and of zero order.

Hantush and Jacob later noted that if r/L is less than 0.05, De Gees equation can be written as:

$$s_m \approx \frac{Q}{4\pi T} W(u, r/B) \qquad [7.2]$$

and

$$u = r^2 S/4Tt \qquad [7.3]$$

Where the integral expression W(u,r/B) is referred to as the Hantush well function and:
s_m – drawdown since pumping started (m)
Q – pumping rate (m^3/d)
T – Transmissivity (m^2/d)
r – distance from pumping well (m)
B – leakage factor (determined by AQTESOLV)
S – Storativity
t – time since pumping started (min)

The assumption and conditions underlying the method are as follows:

- The aquifer is leaky.
- Confining bed(s) has infinite areal extent, uniform vertical hydraulic conductivity and uniform thickness.
- The aquifer have infinite lateral extent.
- The aquifer is homogenous, isotropic and of uniform thickness over the area influenced by the test.
- The aquifer is compressible, and water drains instantaneously.
- Prior to pumping the piezometric surface is horizontal.
- The well is pumped at a constant rate.
- The pumping and observation wells penetrates the entire aquifer.
- The flow to the well is in an unsteady state and is radial (aquifer has radial symmetry).
- The diameter of the pumping well has an infinitesimal diameter so that well storage can be neglected.
- The aquitard is incompressible and no water is being released from storage during the test.
- Flow is vertical in aquitard.
- The aquitard is overlain by an unconfined aquifer, the source bed.
- The water level in the source bed is horizontal and no lowering of the water table occurs during the test.
- Groundwater flow within the aquifer is vertical
- Darcy's law is valid
- Groundwater has a constant density and viscosity
- Aquifer is bounded on the bottom by a confining layer.

(Kruseman and de Ridder, 2000; Fetter, 2001)

Theis-Boulton Method-Unconfined Aquifer with delayed yield: The Theis-Bouton method has its origin in the Theis method for unconfined aquifers, which later was developed further by Boulton in order to accompany for delayed yield. The Theis-Boulton type curve consists of three phases, phase I and III derived from Theis and phase II from Boulton (Kruseman and de Ridder, 2000). During phase I does the radius of influence grow quickly through momentary water release. However, water remained in the pores within the radius of influence do eventual start to move downward under the influence of gravity. When the radius influence reaches a certain size, the volume of downward moving porewater is equal to the volume of extraction (Q). After which temporary stationary conditions develops, phase II, and the radius of influence ceases to expand. After some time nearly all water within the radius of influence has been drained and the radius of influence continues to expand due to momentary water release, phase III (figure 7–7) (Kruseman and de Ridder, 2000).

Transmissivity and storativity is derived from:

$$T = \frac{Q}{4\pi s_m} W\left(\frac{1}{u_y}, r/D\right)_m \qquad [7.4]$$

and

$$S_{ya} = \frac{240 T t_m u_{ym}}{r^2} \qquad [7.5]$$

where:
W(1/uy,r/D) is the Boulton well function and can simply be written as W(u)m.
u_{ym} is a dimensionless helpfactor.
r/D is the delay factor and is a function of the relationship between the horizontal drainage and vertical transmissity (D) and the distance from the pumped well (r).
s_m is drawdown after time t_m in minutes.

s_m and t_m is determined graphically by curve fitting using a match point at which W(u)m and u_{ym} equals

one.

The conditions and assumptions underlying the Theis-Boulton method are as followed:

- The aquifer is unconfined.
- The aquifer is confined downwards by an impermeable unit.
- The aquifer has infinite horizontal extent.
- The aquifer is homogenous and isotropic.
- Groundwater flow is horizontal.
- The pumping well is infinite small and penetrates the entire aquifer.
- Drawdown is insignificant compared the initial thickness of the saturates zone.

(Fetter, 2001)

Fitting of the Theis-Boulton type curve involves five steps:

1. Adjustment of observations (s) due to decreasing thickness of the saturated zone if $s_{max} \geq 0.02H_i$ (H_i is the initial thickness of the saturated zone while smax is the maximum drawdown encountered during the pump test).
2. Fitting of Type A curve, obtain r/D.
3. Fitting of Type B curve, obtain s_m and t_m graphically using match point at which W(u)m and uym equals one. Transmissivity and Storativity is calculated using s_m and t_m.
4. Correction of S_{ya} if corrections of s have been done. The correction is done by:

$$S_{ya} = S_{ya}^{\wedge}\left(\frac{H_0 - s_D}{H_0}\right) \quad [7.6]$$

5. Control of curve fitting has been done after the effect of delayed yield has ceased. Done by:

- Calculate index for delayed yield (α): $\alpha = \frac{(\frac{r}{D})^2}{4t_m u_{ym}}$ [7.7]
- Calculate a theoretical time delay (twt): $t_{wt} = (\alpha t_{wt})/\alpha$ [7.8]

(αtwt is obtained graphically, using r/D.)

If $t_D \geq t_{wt}$ then the fitting is satisfactory. tD is the time (in minutes) into the pump test at which point the transition from phase II of the Theis-Boulton type curve into phase III occurs, determined graphically during step 3 (see above).

Radius of Influence - Jacobs method: Jacobs equation for determining radius of influence in a confined aquifer was used to estimate the radius of influence based on the parameters obtained from the above methods. The equation is derived from the Jacob distance-drawdown method and is written as:

$$r = \sqrt{\frac{2.25Tt}{S}} \quad [7.9]$$

where:

R is the radius of influence

T is transmissivity (m^2/s)

t is time in minutes

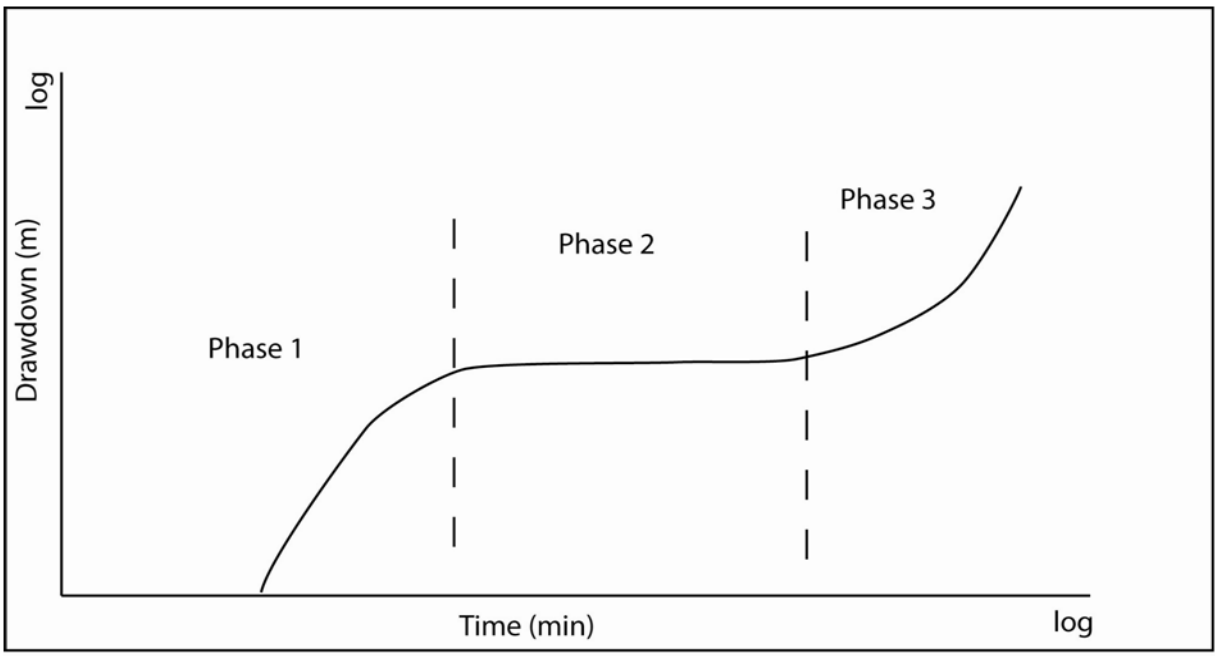

Figure 7-7. The three different phases of the Theis-Boulton type curve.

S is storativity

7.3. RESULTS

7.3.1. Hantush-Jacob

Step-down test

The drawdown vs. time for the KVE01 and KVE02 step-down (S-D) tests is plotted in figures 7-8 and 7-9, respectively. The data is plotted against time in accordance with the Hantush-Jacob method and manually fitted to the type curve to produce estimates of T and S.

The step-down test of KVE01 returned estimates of Transmissivity (T) and Storage (S) in the order of 0.014 m^2/sec and 0.029, respectively. The KVE02 step-down test produced estimates of T and S in the order of 0.012 m^2/sec and 0.048.

Constant rate test

Drawdown vs. time is showed in figure 7-10 from the KVE01 constant-rate test (CRT), and curves fitted and aquifer parameters calculated using the Hantush-Jacob method. T and S were estimated to 0.021 m^2/sec and 0.00022, respectively.

The data from the KVE02 constant rate test is plotted in figure 7-11 and fitted to the curve according to the Hantush-Jacob method. T is here estimated to 0.0132 m^2/sec and S to 0.00056.

7.3.2. Theis-Boulton

Constant rate test

The Theis-Boulton method could only be used on one of the observation sets, the observations made in KVE02 during the constant rate test of KVE01. The reason being that stationary conditions did not develop in the system as the pump test was not long enough. The corrected observation made in KVE02 is plotted

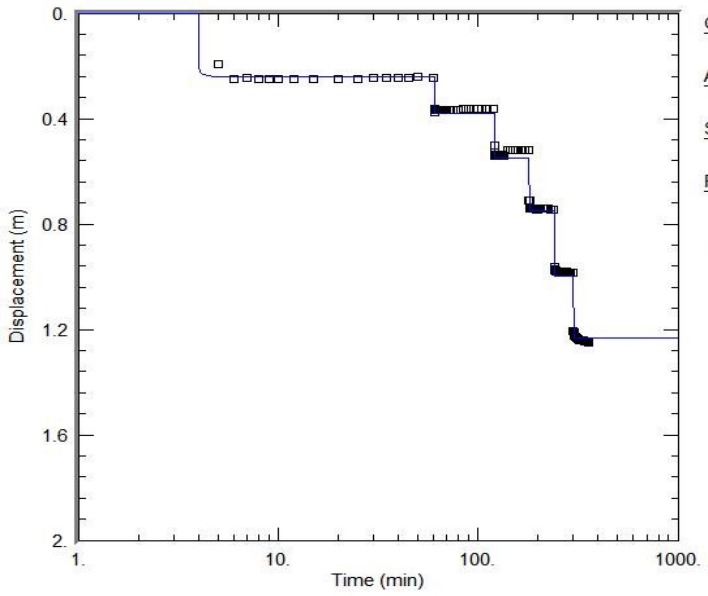

Figure 7-8. Drawdown vs. time in KEV01 during the step -down test of KVE01.

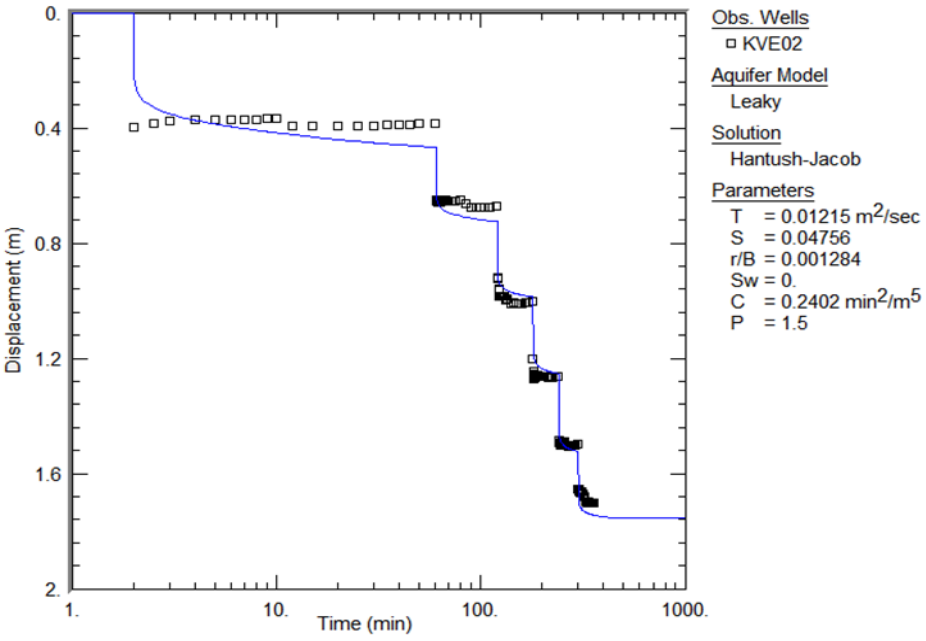

Figure 7-9. Drawdown vs. time in KVE02 during the step -down test in KVE02.

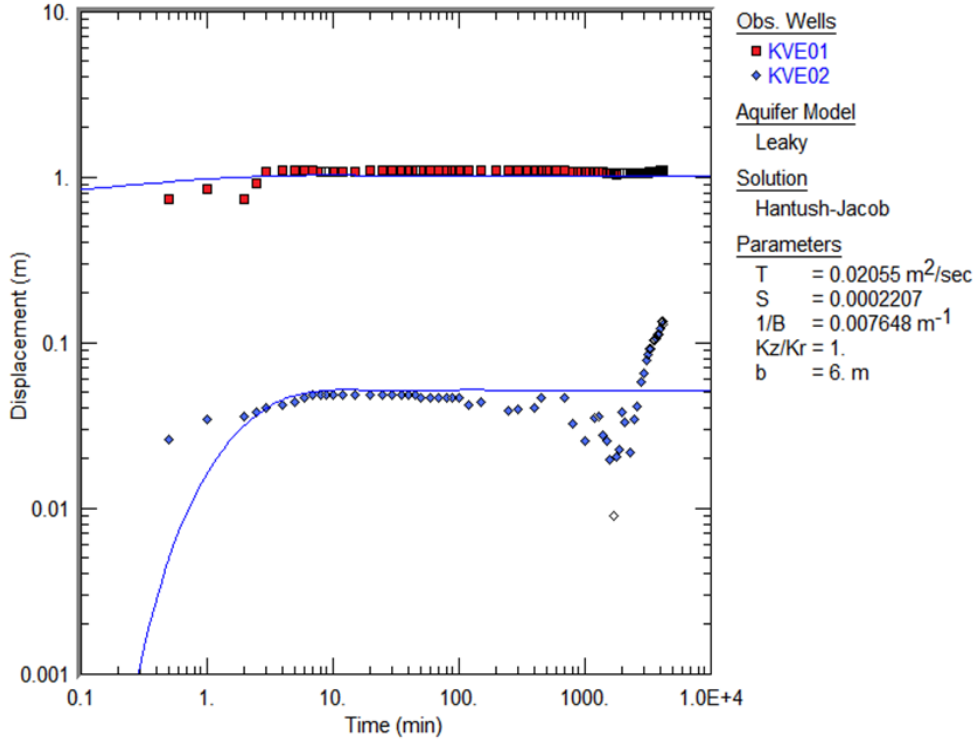

Figure 7-10. Drawdown in KVE01 and observation well KVE02 during the constant rate test of KVE01. Observe the increase in drawdown in KVE02 towards the end.

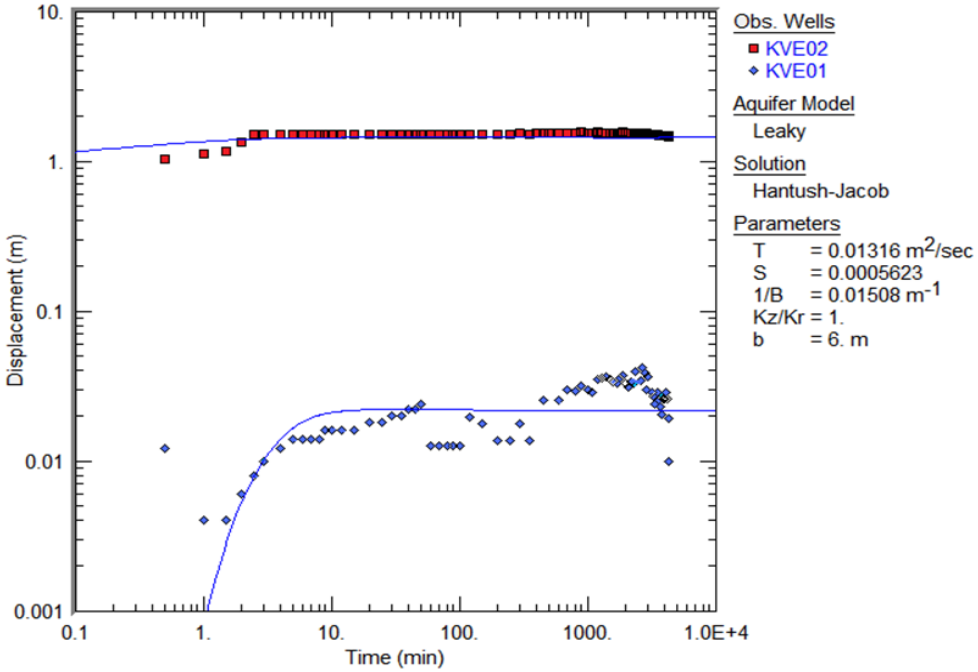

Figure 7-11. Drawdown versus time in KVE02 and observation well KVE01 during the constant rate test of KVE02.

against time on a log/log graph in figure 7-12. A value for t_m and s_m was obtained graphically and T and S calculated (table 7-5 for specifications).

Since the pump test was not conducted over a long enough period to determine s_D and tD it has not been possible to check if the curve fitting was done satisfactory.

7.3.3. RADIUS OF INFLUENCE

The radius of influence was determined using estimates of T and S as produced by the Hantush-Jacob method, as well as those produced by the Theis-Boulton method after one and five years of pumping

Table 7-5. Estimates of T and S based on the Theis-Boulton method.

Parameter	
Q (m^3/sec)	0.0162
t_m (min)	4100
s_m (m)	0.17
r/D	2.5
r (m)	134
T (m^2/s)	0.0076
S	0.42

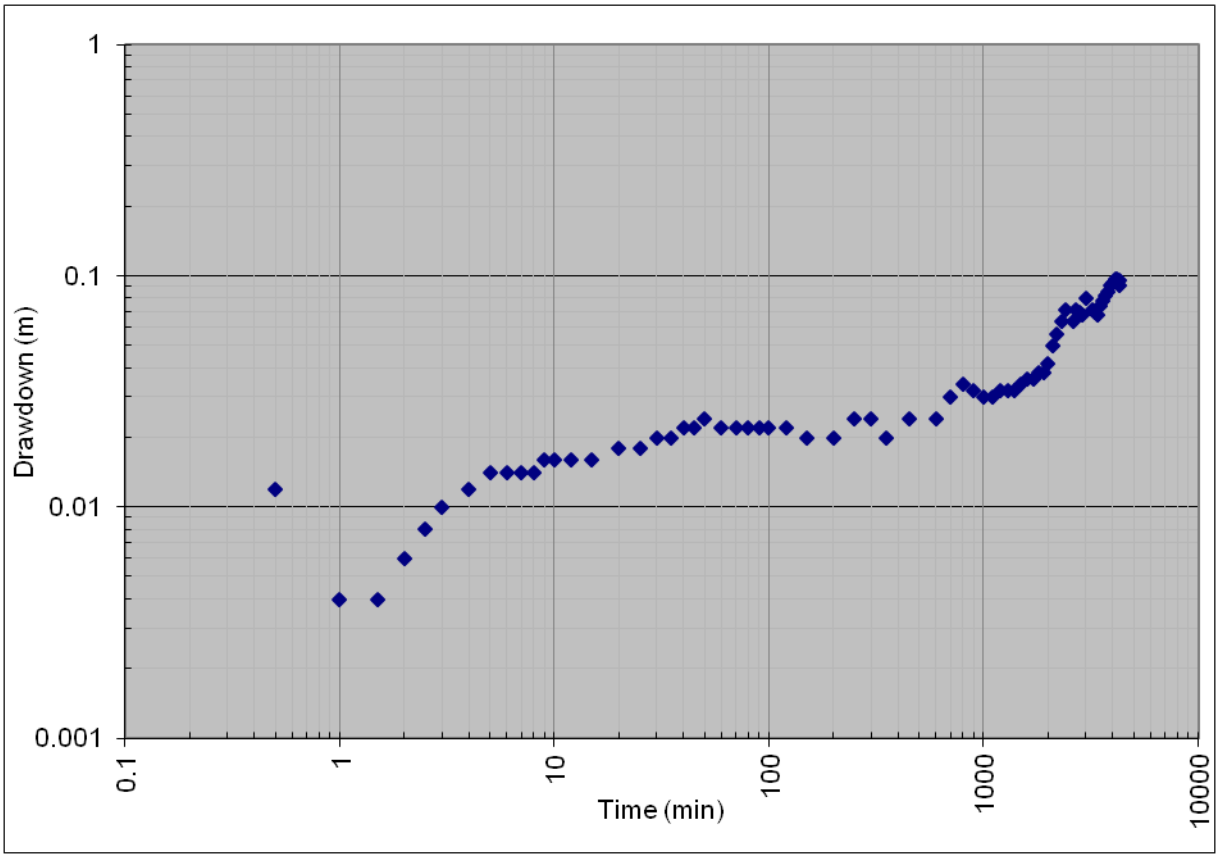

Figure 7-12. Drawdown vs. time after correction. Observations are taken in KVE02 during the constant rate test of KVE01.

(table 7-6).

Table 7-6. Estimations of the radius of influence after one and five years of pumping based on approximation of T and S using the Hantush-Jacob and Theis-Boulton method.

Method	1 year	5 years
Hantush-Jacob	2978 m	6659 m
Theis-Boulton	146 m	327 m

7.4. SUMMARY

Estimates of aquifer parameters, as given in previous chapters 7.1 – 7.3, are summarized in table 7-7. Based on the calculated values, transmissivity (T) is believed to be in the range 0.01 - 0.02 m^2/sec and storativity (S) in the range 0.0002-0.05. The hydraulic conductivity (K) was calculated by:

$$K = T/b \qquad [7.10]$$

where b is the thickness of the saturated zone.

An aquifer thickness of six meters has been used for calculating K, which is the thickness of the Klein Brak Formation in KVE01 and KVE02. It is, however, unclear if this is the correct value for b. The available drawdown in KVE01 and KVE02 was before the commencement of the pump test at 15.9 and 13.95 mamsl (table 7-2), respectively. Since the aquifer is semi-confined, can the thickness of the saturated zone in theory be considerable thicker than the thickness of the Klein Brak Formation. It is, however, uncertain how thick the saturated zone actual is and a theoretical value of b has been set to six. This creates a certain degree of inaccuracy in the estimated hydraulic parameters.

7. 5. PUMP TEST EVALUATION

It proved difficult to select an appropriate method to evaluate the pump test due to a number of factors. Firstly, the effect of change in barometric pressure on the water table obscured the observation made, which had to be adjusted for. Despite this smoothing on the curve the result was not completely satisfactory.

Secondly, the selection of the analytical method is done based on the conceptual hydrogeological model. However, the analytical method is created based on a number of conditions which rarely is fulfilled in the geological reality. The heterogeneous and anisotropic nature of the Stanford Aquifer and especial the Waenhuiskrans Formation made it diffecult to select a suitable method. The Hantush-Jacob method was selected as it is thought to best represent the conditions existing in the system. The Theis-Boulton method was tested based on how the observations taken in KVE02 during the pump test of KVE01 plotted. However, the Theis-Boulton method could only be used on these observations due to insufficient observations and it can

Table 7-7. Summary of estimates of hydraulic parameters.

Test	Borehole	Method	Transmissivity (m^2/sec)	Storativity	Hydraulic Conductivity (m/sec)
KVE01 S-D test	KVE01	Hantush-Jacob	0.014	$2.9*10^{-2}$	$2.3*10^{-3}$
KVE02 S-D test	KVE02	Hantush-Jacob	0.012	$4.8*10^{-2}$	$2.0*10^{-3}$
KVE01 CRT	KVE01	Hantush-Jacob	0.021	$2.2*10^{-4}$	$3.5*10^{-3}$
KVE02 CRT	KVE02	Hantush-Jacob	0.013	$5.6*10^{-4}$	$2.2*10^{-3}$
KVE01 CRT	KVE02	Thies-Boulton	0.0076	0.42	$1.3*10^{-3}$
Estimation based on results from both	KVE01		0.01 – 0.02	0.03 - 0.0002	$1.7 – 3.3*10^{-3}$
	KVE02		0.01 – 0.02	0.05 – 0.0005	$1.7 – 3.3*10^{-3}$

thus be concluded that the constant rate test of KVE01 and KVE02 should have had been longer than 72 hours.

The delayed yield that can be observed in KVE02 during the pump test of KVE01 can be explained by a number of scenarios:

- It is possible that a dual-pore system exists in the Stanford Aquifer, which would produce pump test results similar to those obtained from an unconfined aquifer with delayed yield when pump tested (Singhai and Gupta, 1999). As the name suggests a double porosity aquifer has two pore systems, often a normal matrix pore system divided by a fracture pore system (Singhai and Gupta, 1999). This type of systems does often exist in fractured aquifers and less often in primary (sedimentary) type aquifers. When pump tested, the water in the fractures in the vicinity of the well is first removed from storage (phase I), thereafter follows a period of more or less constant drawdown as matrix water is released from storage, phase II. The final phase, phase III, is due to removal of water from both the fractures and matrix (Singhai and Gupta, 1999). It is, however, unlikely a fracture system exists in the Klein Brak Formation due to its unconsolidated nature. It is possible that a fracture system has developed in the more consolidated and cemented sections of the Waenhuiskrans Formation, especially in the limestone units. The three-phase drawdown curve can be explained by initial removal of water stored in the coarse grained Klein Brak in the vicinity of the well (phase I). Thereafter follows a period constant drawdown when water in the Waenhuiskrans and Klein Brak Formations is released from storage (phase II). If the radius of influence encounters a heavily fractured section of limestone, a second momentary release of water will occur (phase III).
- Another scenario that could explain the observation made in KVE02 is the existence of a karst system. This scenario is very similar to that above, but were the karst system will behave as a fracture system and when reached by the radius of influence it will result in momentary release of water in storage from the karst system (phase III).
- A third scenario is illustrated in figure 7-13. During phase I is the well being emptied while extracted water is being replaced by water infiltrating the well from the Klein Brak Formation. At the transition into phase II, do the flow rate from the Klein Brak Formation in the well equal the pumping rate and stationary conditions develops. As the radius of influence increases water from the Waenhuiskrans Formation starts to move downwards due to the influence of gravity. As the water reaches the well a secondary state of momentary release of water occurs, delayed yield, (phase III). It is, however, peculiar that a similar drawdown curve cannot be seen from the observation from the pumped well. It is possible that if the pumping duration had been longer that a similar behavior could have been observed in KVE01. At this stage no apparent reason behind the differences between the observations made in the two wells can be given.

Variable estimates of storativity were produced depending on the method or pump test used. Estimates of storativity obtained from analysing the results from the step-down test are greater compared to the estimates derived from the constant rate tests. The reason for this is probably that the step-down test is of a too short

duration for the system to reach steady-state conditions and hence is the estimated values of T and S are not completely representative of the system.

The Theis-Boulton method returned a larger estimate of S as compared to estimates obtained from the Hantush-Jacob. This is not unexpected as the Theis-Boulton method is used on the assumption that the aquifer is unconfined and such have in general a much greater yield (however, a storativity value in the order of 0.42 is even for an unconfined aquifer unrealistic). It is difficult with the available data to determine what value of S is the most representative of the aquifer. In order to carry out a more accurate evaluation of the pump tests it should have been substantially extended in time.

Also the estimates of the radius of influence turned out to be quite variable depending on which method and approximations of T and S was used. Again is it difficult to determine which estimation is the most correct. Also, the Jacob method, based on conditions existing in a confined aquifer, contributes to an error as the Stanford Aquifer is considered to be only semi-confined. The actual radius of influence will probably somewhere in between the estimations presented in table 7-6.

8. RECHARGE & DISCHARGE

8.2. RECHARGE

Recharge occurs through precipitation, lateral inflow from adjacent formations, lakes and rivers and can to a lesser extent also occur through irrigation. Precipitation is often being the most significant source. However, the amount of rainfall that actual infiltrates the ground and form groundwater depends on:

- Topography and slope
- Soil type and vegetation cover
- Geology
- Evaporation/temperature, and
- Amount of rainfall

Estimates of recharge through precipitation have in previous studies been proven successful (Bredenkamp et al., 1995) with the help of GIS software and natural tracers (chloride). Each method has however limitations and it is therefore wise to use several methods to estimate the recharge.

8.2.1. Chloride Mass Balance Method

A common used method is the Chloride Mass Balance Method (CMB method). Since chloride is an environmental tracer that once it has entered the aquifer with precipitation is not subjected to absorption or degradation, it can be used to calculate recharge through precipitation (Bredenkamp et al., 1995).

The chloride mass balance (equation 8.1) is rearranged and recharge is calculated through equation 8.2.

$$MAP \times [Cl_{pre}] = R \times [Cl_{gw}] \qquad [8.1]$$

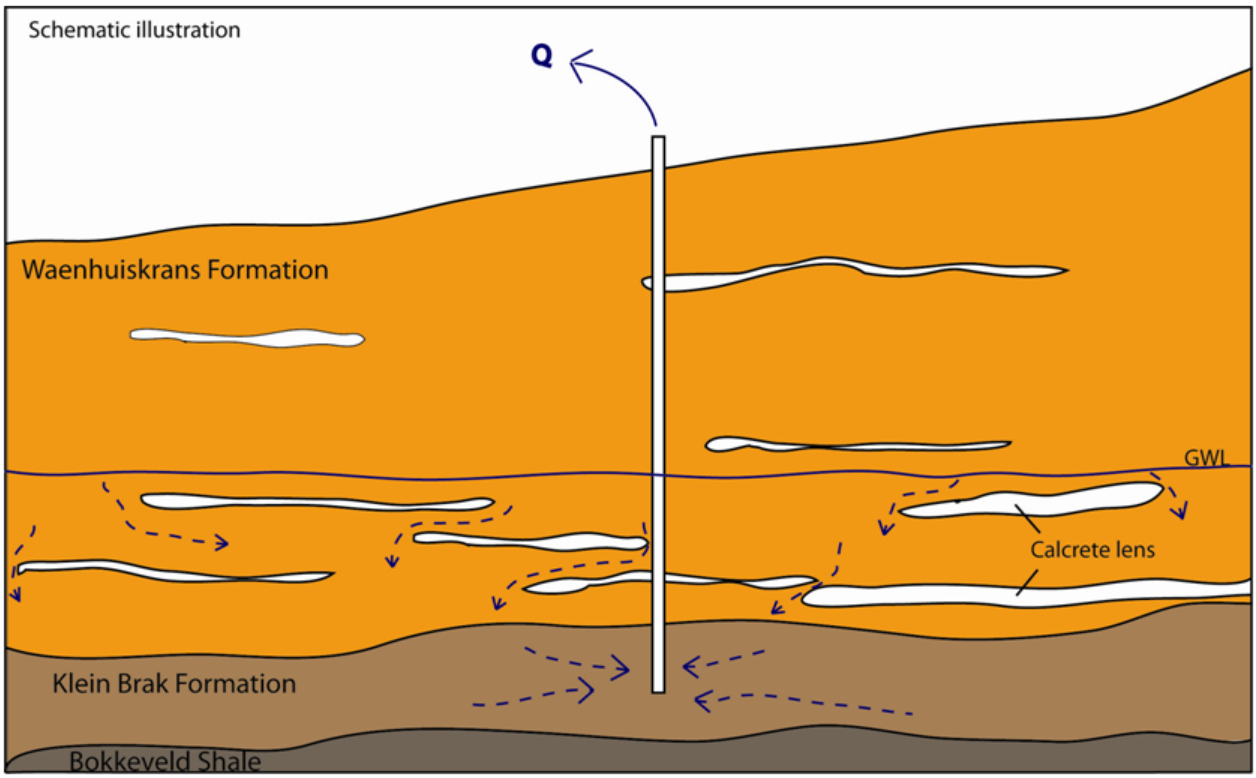

Figure 7-13. Schematic illustration of the groundwater flow within the Stanford Aquifer when being pumped. The impermeable calcrete lenses forces water to flow around them and a delay in release of stored water occur.

$$R\ (mm/a) = (MAP \times Cl_{pre} + D) / Cl_{gw} \quad [8.2]$$

Where:
MAP is the mean annual precipitation
Cl_{pre} is the chloride concentration in precipitation
D is the amount of dry outfall of chloride, and
Cl_{gw} is the chloride concentration in groundwater.

The amount of dry outfall of chloride has not been measured but is usually very small and can be ignored and recharge is calculated by:

$$R\ (mm/a) = (MAP \times Cl_{pre}) / Cl_{gw} \quad [8.3]$$

where:
MAP is mean annual precipitation (mm), 613 mm/a.

Table 8-2. Summary of parameters used for calculating recharge using the CMB method.

	MAP (mm)	Cl_{pre} (mg/l)	Cl_{gw} (mg/l)
Average	613	38.9	132
max	-	45.1	216
min	-	32.7	85.3

Water samples collected from the Stanford Aquifer since 2009 have been analysed for major cations and ions, including chloride concentration (mg/l). A total of 26 samples have been collected from wells scattered throughout the aquifer and used to determine recharge. Two samples of precipitation were collected, June and October 2010, from a rain gauge located on the Middelberg property and was analysed for chloride concentration and used to calculate recharge.

The recharge rate was calculated to 182 mm/a and with a catchment area of approximately 120 km^2, the volume of water entering the aquifer is approximately 21 840 000 m^3/a. It should be noted that the CMB method gives an estimation of all water entering the aquifer, through rainfall and from lateral inflow and surface run-off from adjacent formation.

8.2.2. Breede River Basin Study (BRBS) Method

The BRBS Method was developed by the South African Department of Water Affairs and Forestry (DWAF) for the Breede River Basin Study in 2002 and was used as a preliminary method to calculate recharge from rainfall by the use of GIS software (Umvoto, 2007). It is not within the scope of this study to go into details behind the application of this method besides a brief explanation. Recharge is assumed to be a function of infiltration potential for rainfall and a recharge factor (Umvoto, 2007). The infiltration potential has been determined as a percentage of the mean annual precipitation from a GIS software and varies between 3 and 21 percent depending on the MAP and regional factors (e.g. altitude and slope) (table 8-3) (Umvoto 2007). The recharge factor accounts for different rock types ability to absorb water, where a low value (<0.5) is given to rock types with a poor infiltration potential (crystalline) while a large value (1.5) is given to rock types with a good infiltration potential (sedimentary) (table 8-4).

Table 8-3 Mean annual infiltration (MAI) as a percentage of MAP (Umvoto, 2007; DWAF, 2002).

MAP Range (mm/a)	MAI % of MAP
0 - 300	3
300 - 600	6
600 - 900	9
900 - 1200	12
1200 - 1500	15
1500 - 1800	18
1800 - 2100	21

Table 8-4: Recharge factor for various types of aquifers (After Umvoto, 2007 and DWAF, 2002).

Aquifer Type	Recharge Factor
Primary Sedimentary Aquifer	1.5
Fractured Crystalline Aquifer	0.8
Weathered Fractured Crystalline Aquifer	0.7
Crystalline Aquifer	0.5

Based on the BRBS method the recharge have been estimated to approximately 3 960 000 m^3/a (computed from a GIS software). However, the BRBS method was developed to determine recharge on a regional scale and might not be applicable on a single aquifer study, as local factors like soil type and vegetation cover is not being considered.

8.2.3. Additional Comments: Recharge

The CMB and BRBS methods use different parameters and approaches for the determination of recharge. The CMB method estimates recharge from hydrochemical data and recharge is estimated not just from precipitation falling onto the aquifer but also from rainfall entering the aquifer as lateral inflow and surface run-off from adjacent formations. The BRBS method determines recharge solely from rainfall falling onto the

aquifer based on geological factors and do not account for lateral inflow.

In theory should the difference between recharge derived from the CMB method and the BRBS method account for the lateral inflow from the Swartkransberg to south of the study area and other formations bordering the Stanford Aquifer. If this is the case then the volume of water entering the aquifer as lateral inflow and surface run-off will be in the order of approximately 17 880 000 m^3/a. A better understanding of the hydrogeological properties of the Swartkransberg is required before it is possible to determine if this is the case.

Another factor that must be considered, is the potential of chloride enrichment due to seawater spray. Seawater contains higher concentrations of chloride compared to freshwater and the relative close proximity of the Stanford Aquifer to the sea could cause elevated levels of chloride. This in turn would mean that the CMB method will return an overestimation of recharge. This enrichment can somewhat be adjusted for by measuring the dry outfall of chloride.

8.3. Discharge

8.3.1. Natural Discharge

Natural discharge can occur as evapotranspiration, surface run-off and base-flow and can vary greatly over time. Furthermore, diffuse discharge can make it hard to accurately determine discharge rate, often the case for base flow.

Evaporation has been estimated to be in the range of 538 mm/a using the Turc formula (see section 2.3.2). It is, however, unclear how accurate this estimation is and further investigation into water loss through evaporation is recommended. Transpiration is another parameter that is hard to determine without sufficient data.

Two natural springs occurs within the Stanford Aquifer from where groundwater is discharged, the Eye and the Springfontein. The Eye is located approximately 1 km southeast of Stanford and the Springfontein is located approximately 4 km west of Stanford (figure 1 in appendix A). As no long-term monitoring data exist for the springs, the discharge rates are circa estimations and is likely to show both seasonal and yearly variation.

The Eye

The Eye is being used as a source of water for the town and informal settlement, while excess water is diverted through town before discharged into the Klein River via the Leiwater channel. A flow-meter has since October 2010 measured the amount of water being discharged into the Leiwater channel at the 'Eye'. Based on the data from the flow-meter the flow-rate appears to vary between 6 and 24 l/s depending on if water is pumped from the Eye. For the period 11/11-2010 to 27/2-2011 a total of 80 000 m^3 of water was discharged into the Leiwater, with an average flow-rate of approximately 8.7 l/s. If the flow-rate is assumed to be constant throughout the year, a total of approximately 270 Ml of water is being discharged from the 'Eye' into the Leiwater channel (the flow rate will obvious increase during the winter months due to increased precipitation).

The Springfontein

The flow-rate at the Springfontein was estimated in the field using the bucket method. The bucket method is a simple field method used for estimating flow rate of water being discharged from e.g. a spring, creek or pipe. By timing how long it takes to fill a container with a known volume the flow rate can be estimated. Several measurements should be done to obtain a more reliable estimation.

The flow rate was estimated to 1.5 l/s using the bucket method. This estimation is based on measurements taken in December 2010, in the middle of summer when the flow rate is at its minimum due to lack of precipitation.

Based on available data, the total natural discharged from the two springs is estimated to lie in the range of approximately 325 000 m3 (see table 8-7). However, due to missing long-term data and the fact that this estimation is based on data collected during the summer, the actual discharge is believed to be significantly greater.

Table 8-7: Summary of natural spring discharge.

Spring	Flow rate (l/s)	Yearly discharge (m^3)
Eye	8.7	274 400
Springfontein	1.5	47 300
Total	10	321 700

8.3.2. Groundwater Extraction

Groundwater extraction occurs through a number of private wells distributed throughout the aquifer and through pumps installed at the 'Eye' providing water to the town and informal settlement. Umvoto have monitored groundwater extraction since 2002 for the municipality, informal settlement and a number of the major farms. A summary of the largest water consumers are given in table 8-8 below.

The data provided is in some instances incomplete or completely missing. According to the data provided by County Fair, local chicken farm, is their average annual groundwater use approximately 350 m^3. This value is thought to be erroneous as the Elite Farm, also a chicken farm, is using on average 9 600 m^3 yearly. Furthermore, no data have been provided by the Arabie Woeste Farm and the Mosaic Farm.

Based on available data the total annual extracted volume is approximately 519 000 m^3/a, however due to missing and erroneous data the actual total extracted

Table 8-8: Summary of major groundwater consumers.

Establishment/ Property	Source	Average Yearly Extraction (m^3)
Stanford Town	The 'Eye'	432 500
Informal settlement	The 'Eye'	11 500
Birkenhead Brewery	Borehole BD1	57 000
Wortelgat Farm	Borehole WT4	7 800
Elite Farm	Borehole EL3, EL4	9 600
County Fair		*350*
Arabie Woeste Farm		No data available
Mosaic Farm	Borehole MF1	No data available
Minor users		420*
Total		***519 000***

* Based on ten households consisting of two adults and three children with an average monthly water consumption of 3.5 m3 per household (WRC, 2008). The data provided by County Fair is abnormally small and is believed to be incomplete.

volume is estimated to be in the order of 550 000 to 560 000 m^3/a.

The monthly extraction rate fluctuates with the season and is greatest over the summer and decreases in the winter (figure 8-1).

8.4. Summary

If the amount of water entering and leaving a system is known, it is possible to estimate the amount of water that potentially can reach the saturated zone and form groundwater. This is done by quantifying all components of inflow and outflow to and from the system (Kumar, unknown):

Groundwater potential = Inflow—Outflow [8.4]

where:

- Inflow is the sum of all water entering the system and can be from precipitation, lateral inflow and surface runoff from adjacent formation, inflow from surface waters, from field irrigation and artificial recharge.
- Outflow is the sum all water leaving the system and can be from evaporation, transpiration, lateral outflow to adjacent formations and surface waters and groundwater extraction.

For the Stanford Aquifer all the above mentioned parameters are not applicable or been possible to quantify but it is still possible to roughly estimate the groundwater potential by:

Groundwater potential = (Recharge from precipitation + Recharge from lateral inflow) - (Natural dischagre + Groundwater extraction) [8.5]

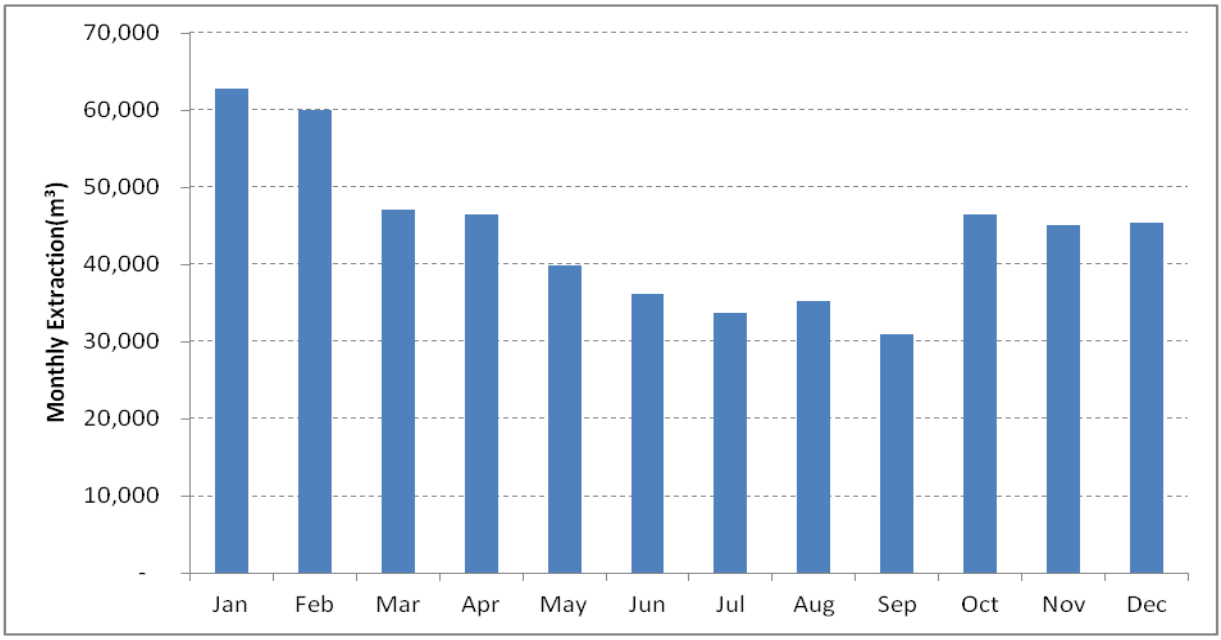

Figure 8-1. Average total monthly extraction.

Which gives:

Groundwater potential=(3 960 000+14 740 000) - (321 700+560 000)

Groundwater potential = 17 818 300 m^3/a

As mentioned earlier this is a rough estimate of the groundwater potential as it is missing one important component, lateral outflow. It is believed that the Stanford Aquifer is in hydraulic connectivity with Klein River and Klein River Lagoon along the northern boundary of the aquifer. Water is therefore being discharged as diffuse seepage and is thought to be greatest where the palaeochannels terminates.

9. CONCLUSIONS, DISCUSSION & RECOMMENDATIONS

9.1. CONCLUSIONS

- The Stanford Aquifer is formed within two formations with distinct different lithology. The lower coarsegrained Klein Brak Formation and the upper fine, heterogeneous Waenhuiskrans Formation.
- The Waenhuiskrans Formation is besides being part of the aquifer also forming the confining layer. Numerous calcrete lenses within the Waenhuiskrans Formation are drastic reducing the vertical hydraulic conductivity of the formation and hence is the Stanford Aquifer considered to be a semi-confined pore type aquifer.
- Groundwater flow is in general from south towards north.
- Two palaeochannels have so far been identified within the Stanford Aquifer, the Klein River and Koue Vlakte Palaechannel. Filled with the Klein Brak Formation they were expected to be high yielding formations. A pump test conducted on two wells located within the Koue Vlakte Palaeochannnel returned an estimate of hydraulic conductivity in the order of 9-10x10^{-4} m/s
- Oxygen and hydrogen isotopic composition suggest a meteoric origin of the water in the aquifer.
- Recharge occurs through both precipitation and lateral inflow. With lateral inflow being the primary source of recharge.

9.2. DISCUSSION

In order to create a representative and accurate conceptual and numerical groundwater model, high quality and long-term continuous monitoring is needed. By developing a model that explains and reproduces the observations made, an overall understanding of the system develops and enables more efficient management. Despite the fact that the Stanford Aquifer has been partly monitored since 2004, continuous monitoring data is limited to a few wells and only go back a few years. Furthermore, monitoring is only carried out in the most accessible wells and larger parts of the aquifer are therefore not monitored.

Climatic monitoring stretches back several decades and is generally of good quality in regards to precipitation and temperatures. However, very little data is actually available in terms of evaporation and transpiration across the aquifer and it has therefore been assumed that these factors are nominal and have been neglected. This might be partially true but it is not confirmed and does therefore need further examination. Several methods have in the past been successfully used for monitoring of evapotranspiration rates, either by comprehensive climatic monitoring using weather stations or by using field apparatus (such as lysimeters). However, the implementation of this type of monitoring will require daily readings and therefore a financial burden.

The geological understanding of the area is limited due to inadequate data. Approximately 60 boreholes have been located within the aquifer but bore logs is only available for 15 of these, whereof nearly all of them are clustered on the Middelberg property. The majority of the boreholes were drilled by private landowners or contracted drillers without practice for creating logs or keeping record and the geological understanding of the area is therefore rather generalised. The aquifer has, besides a pump test carried out on the Middelberg Farm, which produced rough and questionable estimates of hydrological properties, remained untested until March 2011 and hence very little hydrogeological data is available for analyses. An alternative procedure would have been to conduct laboratory studies on samples collected in the field but these methods tend not to produce representative estimates. The hydraulic conductivity can be estimated using a falling-head or constant-head permeameter where sediments from the formation of interest are used (Fetter, 2001). However, the transport and recompaction of the sediments alters the original sorting and degree of compaction and will therefore only produce approximations of the hydraulic conductivity (K) of the sediments (Fetter, 2001).

The palaeochannels, especially the Koue Vlakte Palaeochannel, are important hydrogeological landforms but the limited available data made it difficult to determine their course and thickness. A geophysical survey was conducted in 2010 but only covered a limited part of the aquifer and was of little use. Instead a digital elevation model and bore logs were used to determine the possible course of the palaeochannels, as this type of data is readily available. However, due to a limited number of bore logs it has not been possible to check if the proposed course is correct. Another important aspect of the palaeochannels is the thickness of the Klein Brak Formation which is known to vary greatly even over short distances. There are no data available from the eastern third of the aquifer regarding the extent and thickness of the Klein Brak Forma-

tion and it has therefore been assumed that the formation is present throughout the entire aquifer.

An attempt was made to quantify and determine the mode of recharge by utilizing two different methods. The methods used are quite generalised and more advanced methods, such as the Saturated Volume Fluctuation method and Cumulative Rainfall Departure method (Bredenkamp et al., 1995), usually return more accurate estimations. However, these methods require long-term monitoring data of the watertable fluctuation from representative wells.

9.3. RECOMMENDATIONS:

- Instalment of a weather station in order to acquire needed data to accurately estimate evapotranspiration.
- A better understanding of the geology and hydrogeology can be accomplished by drilling a number of monitoring wells in the eastern part of the Stanford Aquifer. The drilling of more wells will accomplish several purposes: (i) the lateral extent and thickness of the Klein Brak Formation in the eastern part of the aquifer can be determined. (ii) The proposed course of the Kouevlakte Palaeochannel can be verified. (iii) The new wells can complete the existing monitoring network.
- Improvement of the monitoring practice of groundwater levels. Gaps in monitoring data have made it difficult to use the water level data. Continuous data is needed when attempting to estimate recharge and compiling a water balance using methods such as the Cumulative Rainfall Departure method and the Saturated Volume Fluctuation method. If continuous (over several years/decades) data collected from wells throughout the entire aquifer can be provided a more accurate mass balance can be compiled.
- A flowmeter at the V-notch (a triangular section of the discharge channel) at Springfontein should be installed as soon as possible. A flowmeter will provide a better estimate of the volume of water being discharged at this point compared to the bucket method.
- Continuous communication and improved relationships with major water uses will be beneficial. It has been proven difficult to acquire water consumption data from a number of the major consumers, which is needed for the mass balance and management plan.

10. ACKNOWLEDGEMENTS

I would like to thank Umvoto Africa for taking me in and giving me this opportunity, it has been a vast learning experience as well as a great chance to explore Cape Town and its great people. I would especially like to thank Sheila, Helen and Emilie for their help, guidance and patience throughout my stay and beyond. Also a big thanks to Alex and Nizberth for their help with maps and the fun soccer games. Finally, I would also like to thank Per and Lotta for their help finalising my thesis.

Ajoba!!

11. REFERENCES:

Blake,D.2010: Photo.

Bredenkamp, D.B., Botha, L.J., van Tonder, G.J. and van Rensburg, H.J., 1995: *Manual on Quantitative Estimation of Groundwater Recharge and Aquifer Storativity.* Water Research Commission Report, Pretoria.

DWAF (Department of Water Affairs and Forestry, South Africa), 2002: Groundwater Assessment. Prepared by J Papini of Groundwater Consulting Services as part of the Breede River Basin Study. DWAF Report.

DWAF (Department of Water Affairs and Forestry, South Africa), 2008: The Assessment of Water Availability in the Berg Catchment (WMA 19) by Means of Water Resource Related Models: Groundwater Model Report Volume 3 – Regional Conceptual Model. DWAF Report

DWA (Department of Water Affairs), 2005: *Drinking Water Quality Management Guide for Water Servi ces Authorities.* http://dwaf.gov.za/Documents/ other/DWQM/DWQMWSAGUIDESept05.pdf [Accessed 14 January 2011]

Diamond, R.E. and Harris, C., 2000: Oxygen and hyd rogen isotope geochemistry of thermal springs of the Western Cape, South Africa: recharge at high altitude? *Journal of African Earth Sciences 43*, 467-481.

Fetter, C.W., 2001: *Applied Hydrogeology*. 4th Ed. Prentice-Hall, New Jersey. 598 pp.

Kruseman, G.P. and de Ridder, N.A., 2000: *Analysis and Evaluation of Pumping Test Data.* International Institute for Land Reclamation and Improvement, Wageningen. 370 pp.

Kumar, C.P., unknown: *Assessment of Ground Water Potential.* Online publicattion. http://angelfire. Com/nh/cpkumar/publication/Lgwa.pdf [Accessed 21 May 2011]

Malan, J.A., 1989: *Lithostratigraphy of the Waen huiskrans Formation (Bredasdorp Group).* Lithostratigraphic Series, South African Committee for Stratigraphy No 8, 10 pp. Pretoria.

Midgley, D.C., Pitman, W.V. and Middleton B.J., 1994: *Surface Water Resources of South Africa 1990*. Water Research Commission Report. Pretoria.

Roberts, D.L., Botha, G.A., Maud, R.R. and Pether, J., 2006: Coastal Cenozoic Deposits. In M.R Johnson, C.R. Anhaeusser and R.J. Thomas (Eds.): *The Geo logy of South Africa.* Geological Survey of South Africa, Johannesburg/Council for Geoscien-

ce, Pretoria, 605-628.
SAHRA (Sustainability of semi-Arid Hydrology and Riparian Areas). http://web.sahra.arizona.edu/programs/isotopes/oxygen.html [Accessed 21 February 2011]
SANS, 2003:Part 4:Testpumping of water boreholes.Development, maintenance and management of groundwater resources. South African National Standards, Pretoria.
Schulze, R.E., 1997: *South African Atlas of Agrohydrology and –Climatology.* Water Research Commission report, Pretoria. 276 pp.
Shone, R.W. and Booth, P.W.K., 2005: The Cape Basin, South Africa: A review. *Journal of African Earth Sciences 43*, 196-200.
Singh, K.P., 1995: Significance of Palaeochannels for Hydrogeological Studies - A Case Study of Punjab and Haryana, India. *Water Science and Tecknology Library 16,* 245-249.
Singhai, B. B. S. and Gupta, R. p., 1999: *Applied Hydrogeology of Fractured Rocks.* Kluwer, Dordrecht. 408 pp.
Spane, F.A., 2002: Considering barometric pressure in groundwater flow investigations. *Water Resource Research, 38*. No 6.
Thamm, A.G. and Johnson, M.R., 2006: The Cape Supergroup. In M.R. Johnson, C.R. Anhaeusser And R.J. Thomas. (Eds.): *The Geology of South Africa.* Geological Survey of South Africa, Johan-Nesburg. Council for Geoscience, Pretoria, 443-460.
Todd, D.K. and Mays, L.W., 2005: *Groundwater Hydrology*. 3rd Ed. Wiley, New Jersey. 636 pp.
Umvoto Africa, 1998: *Water Resource Development and Management Plan for the Greater Hermanus Area Overstrand Municipality, Stanford: The Groundwater Regime and Aquifer Management in the Stanford Area.* Internal Report.
Umvoto Africa, 2009. *Water Source Development and Management Plan for the Greater Hermanus Area Overstrand Municipality, Stanford: Options Analysis of future water supply options.* Internal Report
Umvoto Africa, 2010: *Water Source Development and Management Plan for the Greater Hermanus Area Overstrand Municipality. Stanford: The Groundwater Regime and Aquifer Management in the Stanford Area.* Internal Report.
Umvoto Africa, 2010: *Water Source Development and Management Plan for the Stanford Area Overstrand Local Municipality. Kouvelakte Exploration Siting and Drilling Report.* Internal Report.

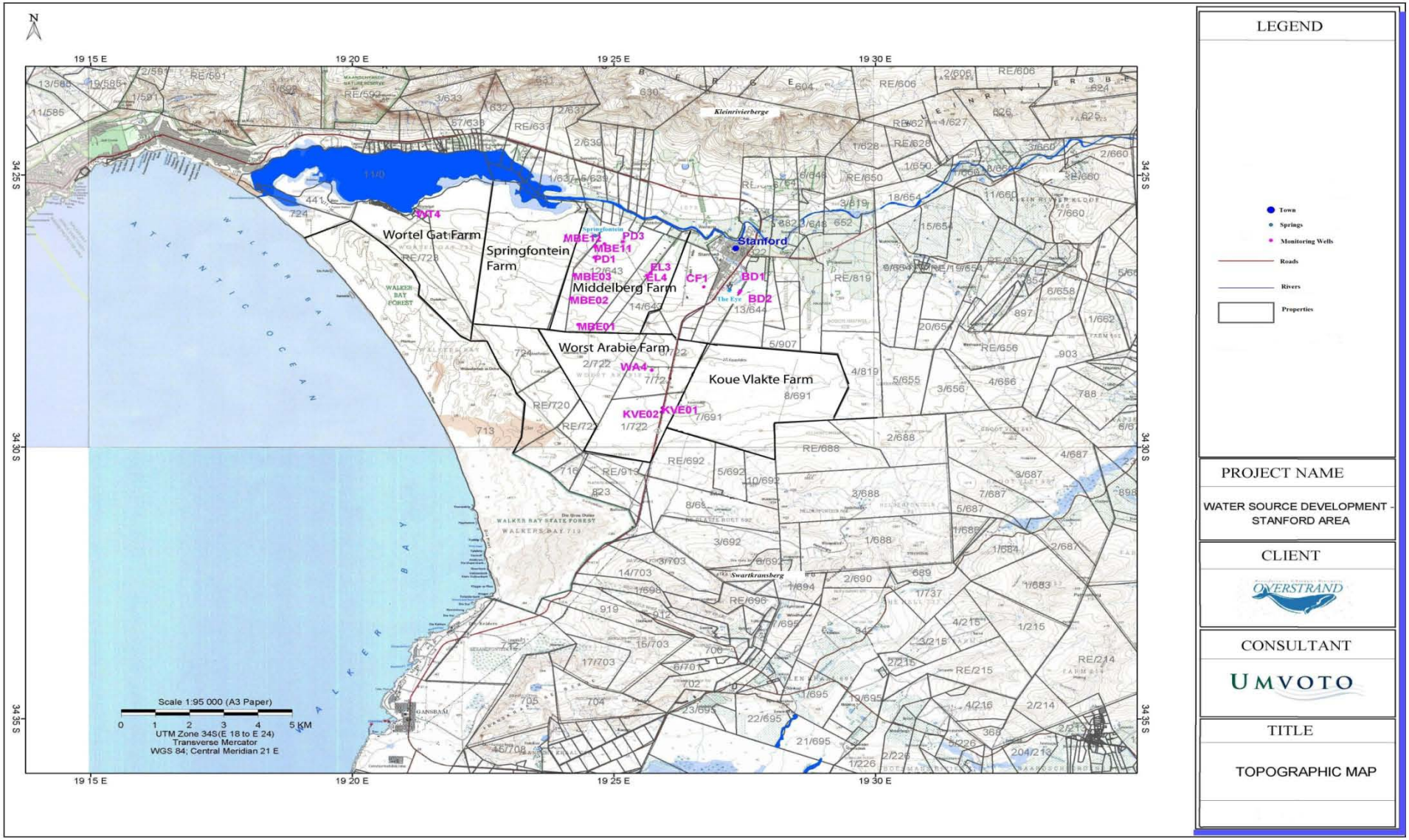

Appendix A. Figure 1. Topographic map over the study area.

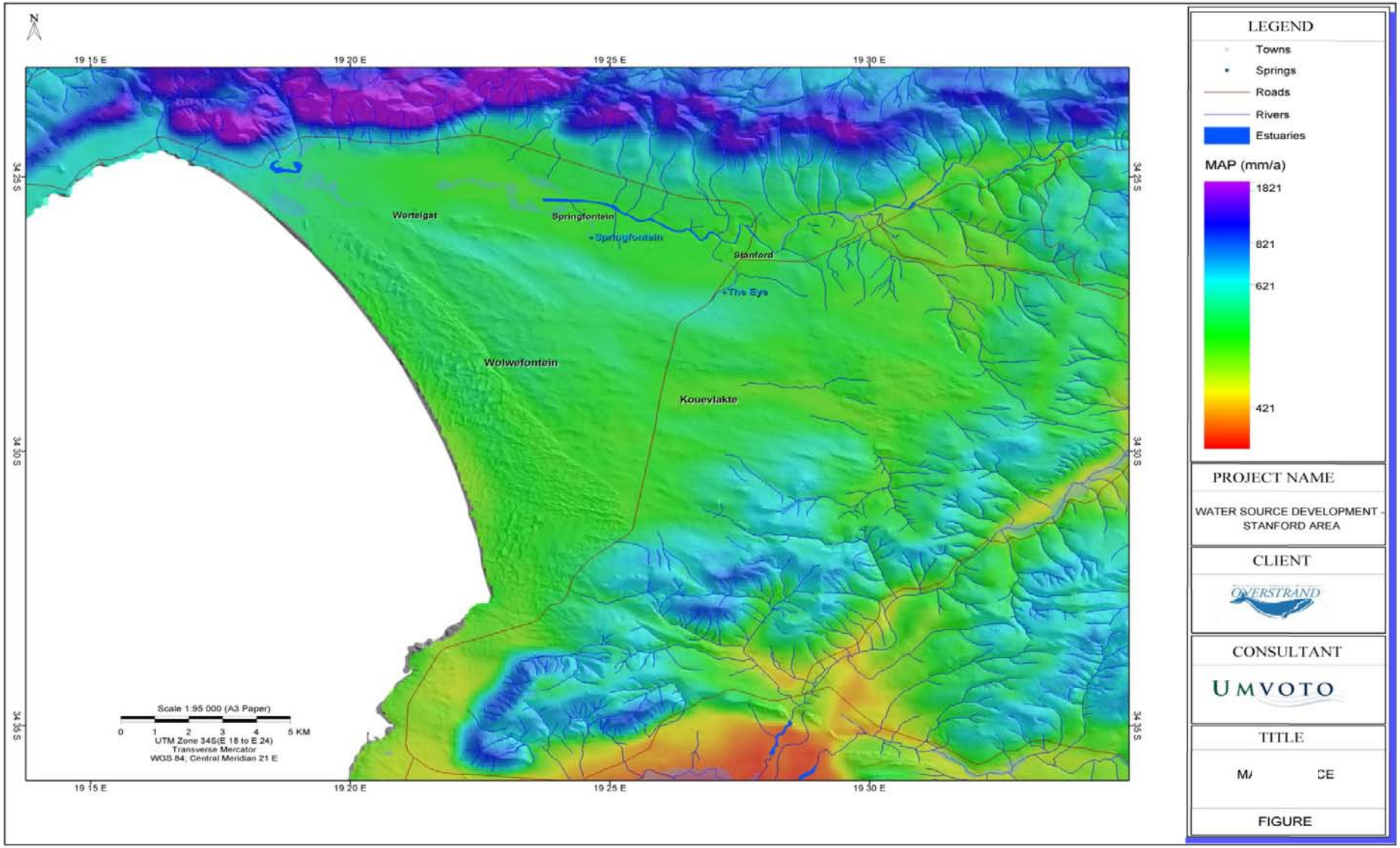

Appendix A. Figure 2. Mean Annual Precipitation (MAP) surface map.

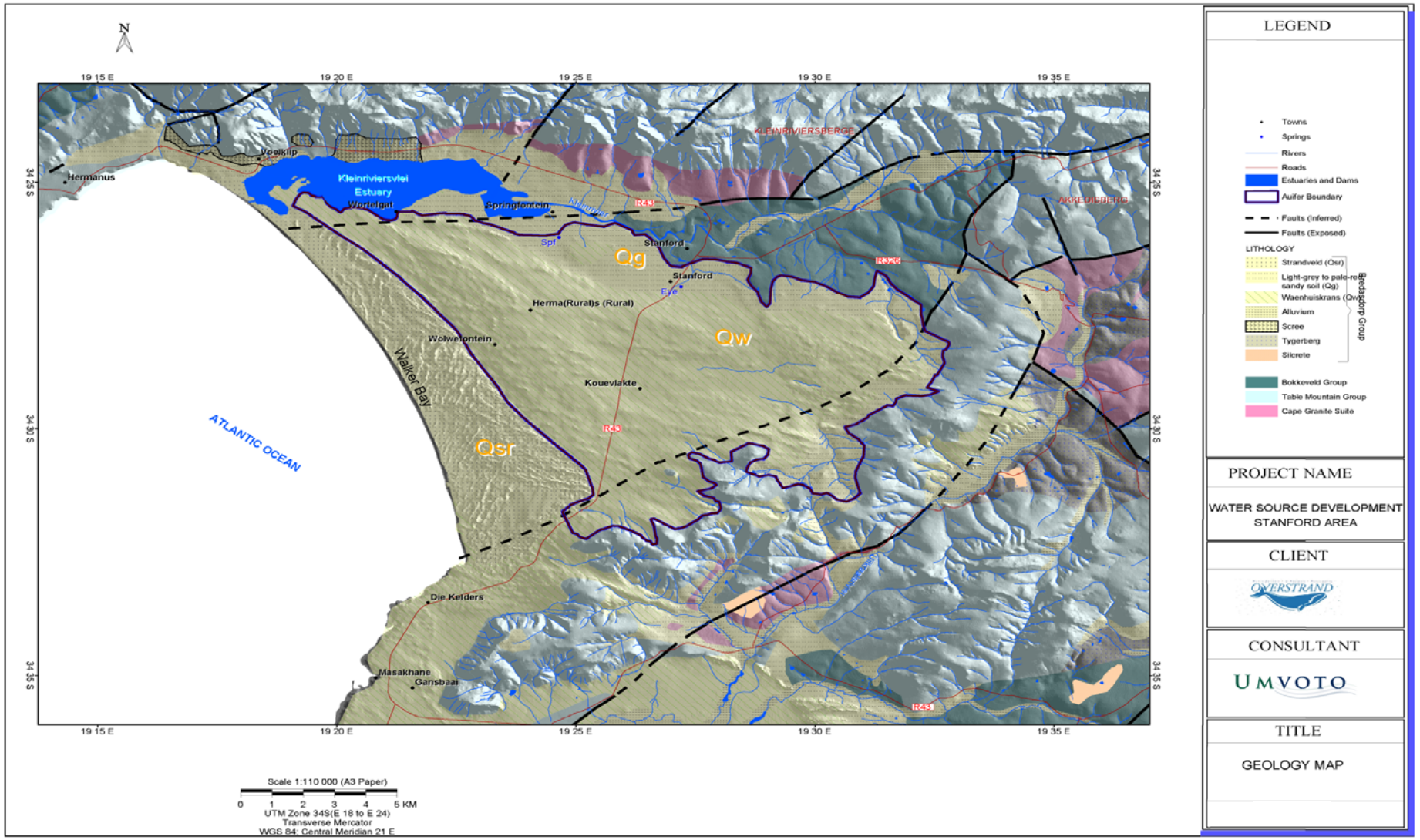

Appendix A. Figure 3. Geological map.

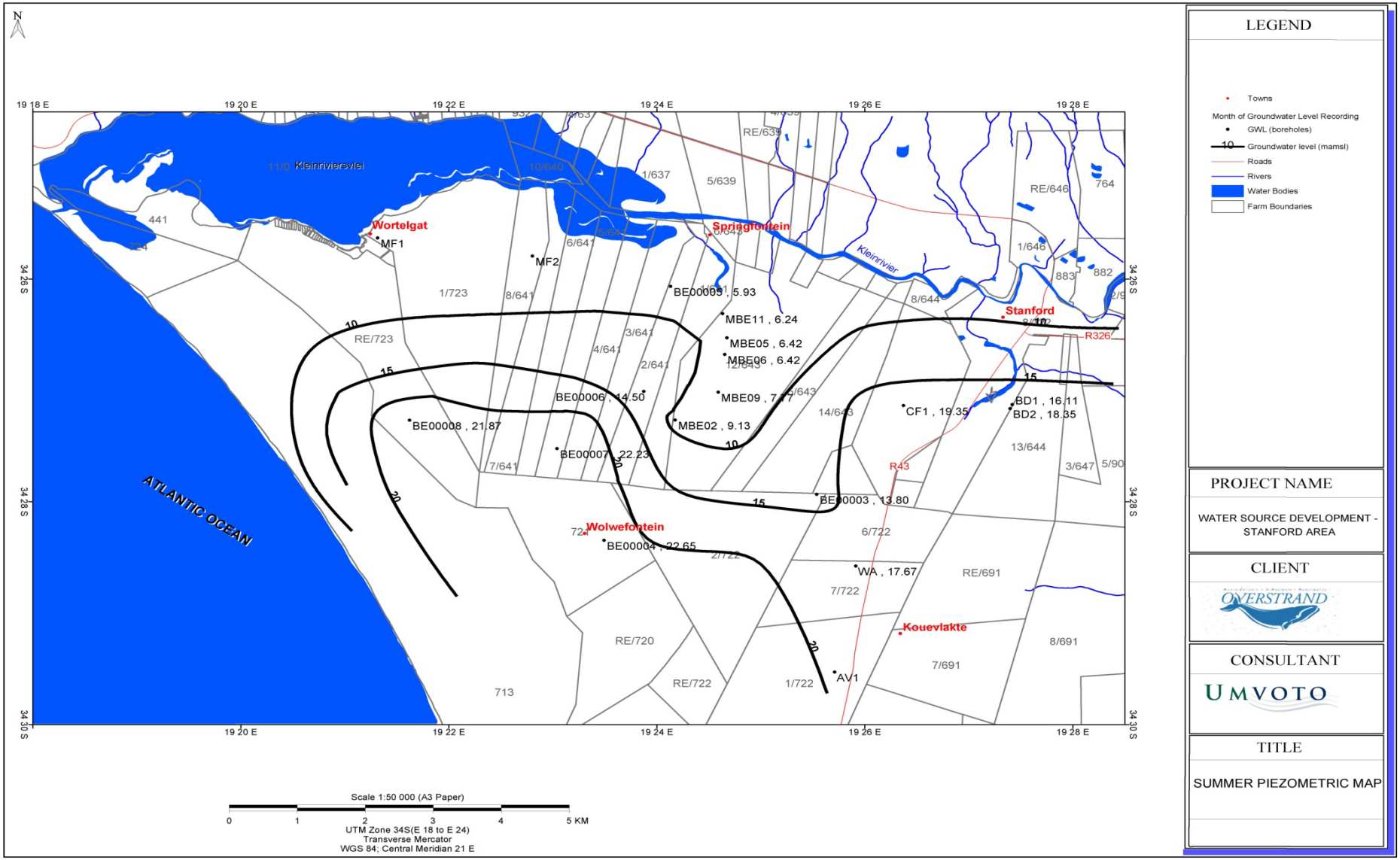

Appendix A. Figure A4. Piezometric map, summer 2010.

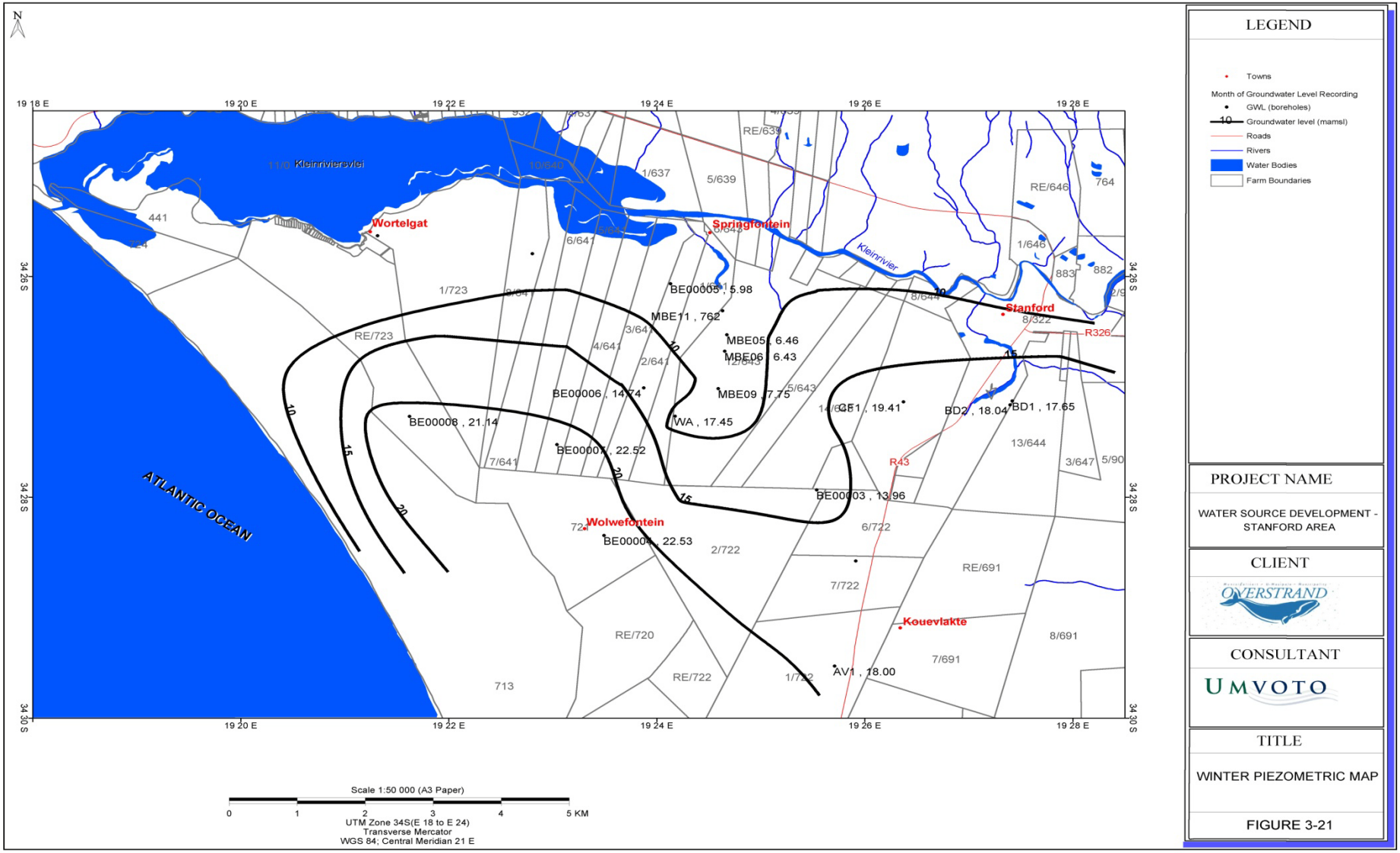

Appendix A. Figure 5. Piezometric Map, Winter 2010.

Appendix B. Chemical analysis results from samples collected between 2005 and 2010 from monitoring boreholes. Boxes highlighted in yellow is above recommended values for class 0 of South African Drinking Water Guidelines (SADWG) while boxes highlighted in red exceeds the recommended values of class 1 set by South African National Standards (SANS-241). Samples in *cursive* were bailed by hand and might not to truly representative of the aquifer.

Constituents	pH	EC (mS/m)		Alkalinity	Total Hardness	Calcium	Magnesium	Sodium	Potassium	Zinc	Chloride	Flouride	Sulphate	TDS	Ammonia	Nitrate/Nitrite		Iron	Manganese	Aluminium
Class 0 of SADWG	6.0-9.0	70	mg/l	n/a	n/a	80	70	100	25	3	100	0.7	200	450	0.1	6	µg/l	100	50	150
Class I of SANS-241	5.0-9.0	150	mg/l	n/a	n/a	150	70	200	50	5	200	1	400	1000	1	10	µg/l	200	100	300
The Eye May 2010	7.2	79	mg/l	196	281	99	8	69.4	1.2	<0.01	116	0.12	8	521	<0.15	2	µg/l	<10	<40	40
The Eye June 2010	7.36	76	mg/l	204	270	95.7		7.5	65.8	<0.01	101	<0.1	14	550	<0.15	2.1	µg/l	<10	<40	60
The Eye July 2010	7.23	73.3	mg/l	196	303	108	8	66.9	1.3	<0.01	100	<0.1	<0.15	500	17.3	2.5	µg/l	<10	<40	40
The Eye Aug 2010	7.68	76.6	mg/l	316	284	101	7.6	70.1	1.5	<0.01	101	<0.1	32	510	<0.15	19.3	µg/l	60	<40	20
The Eye Sept 2010	7.46	77.8	mg/l	212	290	102	8.6	69.4	1.2	<0.01	111	20.1	43	520	<0.15	1.7	µg/l	120	<40	60
The Eye Oct 2010	7.78	80.9	mg/l	240	224	74.8	9	91.3	1.2	<0.01	110	0.83	9	580	<0.15	2	µg/l	140	<40	40
The Eye Oct 2010	7.46	77.1	mg/l	248	247	84.7	8.5	91.3	1.3	<0.01	109	0.1	9	510	< 0.15	2.2	µg/l	< 10	< 40	< 14
Municipal Of. May 2010	7.22	78.4	mg/l	196	285	101	7.9	67	1.2	<0.01	110	0.36	8	517	<0.15	2.3	µg/l	<10	<40	48
Municipal Of. June 2010	8.12	75	mg/l	204	272	96.8	7.4	67.1	1.2	0.03	101	20.1	13	550	<0.15	1.9	µg/l	20	<40	40
Municipal Of. July 2010	7.7	74.8	mg/l	204	306	109	8	66.1	1.3	<0.01	100	<0.1	16.5	500	<0.15	2	µg/l	20	<40	40

Constituents	pH	EC (mS/m)		Alkalinity	Total Hardness	Calcium	Magnesium	Sodium	Potassium	Zinc	Chloride	Flouride	Sulphate	TDS	Ammonia	Nitrate/Nitrite		Iron	Manganese	Aluminium
Municipal Of. Aug 2010	7.91	76.9	mg/l	8	291	103	8	70.2	1.4	0.03	95.2	<0.1	10	510	<0.15	19.9	µg/l	<40	<14	
Municipal Of. Sept 2010	7.22	77.9	mg/l	208	292	103	8.4	69.4	1.3	0.02	109	<0.1	11	520	<0.15	1.9	µg/l	20	<40	60
Municipal Of. Oct 2010	7..8	80.2	mg/l	244	213	70.8	8.9	92.4	1.3	0.02	113	0.96	8	580	<0.15	21	µg/l	<10	<40	<14
EL1 Dec 2010	7,80	54.4	mg/l	120	176	58.2	7.3	60	1.4	0.32	92.5	0.13	8	370	<0.15	1.3	µg/l	20	<40	<14
MF1 Sep 2009	7.41	111	mg/l	216	321	109	11.8	107	2	0.01	191	0.34	16	740	< 0.15	1.6	µg/l	88	< 40	60
MF1 Jan 2010	7.27	118	mg/l	216	335	109	15	110	2.2	<0.01	194	<0.1	21	800	< 0.15	2.3	µg/l	< 10	< 40	120
MF1 Aug 2010	7,56	77.2	mg/l	176	329	116	9.4	68.9	1.9	0.02	122	0.17	11.3	530	<0.15	1.6	µg/l	<10	<40	40
MF1 Dec 2010	7,74	119	mg/l	256	352	117	14.4	129	2.4	<0.01	196	0.99	21	800	<0.15	2.9	µg/l	276	<40	20
WF1 Sep 2009	7.6	92.5	mg/l	188	287	99	9.5	99	1.5	0.34	156	< 0.1	14	620	< 0.15	1.8	µg/l	140	< 40	40
WF1 Dec 2010	7,70	69.9	mg/l	180	197	62.6	9.8	100	5	<0.01	126	<0.10	<4	480	7	0.31	µg/l	9300	168	40
WA2 Sep 2009	7.56	67.6	mg/l	192	259	94.1	5.8	50.2	0.55	0.08	85.3	0.16	8	450	< 0.15	1.6	µg/l	6840	< 40	< 14
WA2 Dec 2010	7,71	69.1	mg/l	236	236	100	6.8	56.2	0.77	<0.01	86.8	<0.1	9	480	<0.15	1.6	µg/l	<10	<40	<14

Constituents	pH	EC (mS/m)		Alkalinity	Total Hardness	Calcium	Magnesium	Sodium	Potassium	Zinc	Chloride	Flouride	Sulphate	TDS	Ammonia	Nitrate/Nitrite		Iron	Manganese	Aluminium
DK1 Sep 2009	7.81	69.1	mg/l	188	275	99	6.6	57.1	1.3	0.03	90.3	0.22	7	470	< 0.15	2	µg/l	180	< 40	< 14
DK1 Jan 2010	7.42	71.4	mg/l	188	273	96.8	7.6	61.6	0.88	0.07	88.1	<0.1	7	480	< 0.15	1.8	µg/l	< 10	< 40	160
AV1 Sep 2009	7.56	91.8	mg/l	188	285	97.9	9.7	100	1.4	0.35	172	< 0.1	14	610	< 0.15	1.6	µg/l	100	< 40	40
AV1 Dec 2010	7,94	54.2	mg/l	124	179	59	7.5	61.7	2.2	<0.01	90.6	<0.1	9	370	<0.15	1.2	µg/l	40	<40	120
HV1 Dec 2010	7,73	71.6	mg/l	208	277	97.9	7.7	64.2	1.1	<0.01	94.3	0.18	9	490	<0.15	2.2	µg/l	<10	<40	<14
HV2 Sep 2009	7.43	71.7	mg/l	188	259	92.3	6.7	62.7	0.99	< 0.01	100	0.31	11	480	< 0.15	1.6	µg/l	134	< 40	< 14
PD1 2005	7.5	75	mg/l	189	-	78	7.4	64	0.9	-	115	< 0.1	15	-	< 0.1	1.3	µg/l	< 50	< 50	-
PD1 Oct 2010	7.76	71.9	mg/l	220	223	73.7	9.4	93.5	1.3	0.02	115	0.13	11	480	< 0.15	1.4	µg/l	< 10	< 40	< 14
PD1 Dec 2010	7,86	73.8	mg/l	228	289	100	9.4	75.5	1.4	<0.01	109	0.94	11	500	<0.15	2.1	µg/l	60	<40	160
BD1 Oct 2009	-	-	mg/l	-	-	-	-	-	-	-	176	-	-	-	-	-	µg/l	-	-	-
BD1 Jan 2010	7.23	103	mg/l	244	328	109	13.3	100	2.4	0.01	147	0.44	19	700	< 0.15	2.7	µg/l	< 10	< 40	140
BD1 July 2010	7,45	101	mg/l	236	341	116	12.4	109	2.6	<0.01	156	0.31	31.5	700	<0.15	2.2	µg/l	50	<40	40
BD1 Oct 2010	7.66	101	mg/l	284	282	91.3	13.1	106	2.5	<0.01	161	0.28	19	680	<0.15	2.3	µg/l	< 10	< 40	< 14
BD1 Dec 2010	7,80	94.8	mg/l	280	334	116	10.7	101	1.9	<0.01	132	0.17	13	640	<0.15	2.8	µg/l	92	<40	20

Constituents	pH	EC (mS/m)		Alkalinity	Total Hardness	Calcium	Magnesium	Sodium	Potassium	Zinc	Chloride	Flouride	Sulphate	TDS	Ammonia	Nitrate/Nitrite		Iron	Manganese	Aluminium
BD2 Oct 2009	-	-	mg/l	-	-	-	-	-	-	-	125	-	-	-	-	-	µg/l	-	-	-
BD2 July 2010	7,15	102	mg/l	236	346	117	12.9	109	2.6	0.38	158	0.87	29.3	700	<0.15	2.2	µg/l	<10	<40	40
MBE03RG Oct 2010	7,29	79.1	mg/l	160	33,7	6.6	4.2	27	38.5	0.2	45.1	1.9	64	530	50	2.8	µg/l	472	<40	98
MBE03RG July 2010	-	-	mg/l	-	-	-	-	-	-	-	32.7	-	-	-	-	-	µg/l	-	-	-
WkP1 Sep 2009	7.55	86.2	mg/l	196	295	103	8.9	89.1	1.4	< 0.01	120	0.3	9	580	< 0.15	3	µg/l	34	< 40	< 14
WkP1 Jan 2010	7.36	76.8	mg/l	144	220	71.4	10	93.9	1.7	<0.01	121	<0.1	15	510	<0.15	1.3	µg/l	20	< 40	120
WkP1 July 2010	7,40	81.5	mg/l	196	292	102	9.1	78.2	1.7	<0.01	119	0.26	17.1	550	<0.15	2.8	µg/l	50	<40	60
WkP1 Oct 2010	7.67	79.7	mg/l	236	245	81.4	10	97.9	1.9	<0.01	130	0.1	14	530	0.19	2.2	µg/l	< 10	< 40	< 14
WkP1 Dec 2010	7,79	87.4	mg/l	260	298	103	9.7	100	1.9	<0.01	121	0.79	11	590	<0.15	3.1	µg/l	<10	<40	60
MBP02 Nov 2005	7.5	70	mg/l	178	-	77	7	59	1	-	106	-	12	-	< 0.1	1.5	µg/l	510	90	-
MBP05 Nov 2005	6.8	72	mg/l	170	-	76	6.9	67	1.1	-	119	-	15	-	0.12	0.75	µg/l	< 50	< 50	-
KVE01 Aug 2010	6.34	73.5	mg/l	204	289	103	7.5	61.2	1.3	0.02	90.4	< 0.10	14.4	500	< 0.15	1.3	µg/l	540	60	180
KVE01 Dec 2010	7,41	63.1	mg/l	-	192	91.3	7.4	56.3	0.77	0.01	90	<0.10	8	440	<0.15	1.5	µg/l	540	178	140

Constituents	pH	EC (mS/m)		Alkalinity	Total Hardness	Calcium	Magnesium	Sodium	Potassium	Zinc	Chloride	Flouride	Sulphate	TDS	Ammonia	Nitrate/Nitrite		Iron	Manganese	Aluminium
KVE02 Aug 2010	6.96	69.1	mg/l	184	272	96.8	7.4	61.8	0.99	0.02	88.5	< 0.10	13.2	480	< 0.15	2.6	µg/l	1180	< 40	660
KVE02 Dec 2010	5,79	57.8	mg/l	-	188	90.2	7.3	57.4	0.77	<0.01	90	<0.10	7	420	<0.15	2.2	µg/l	<10	<40	<14
KVE02 Dec 2010	5,85	57	mg/l	-	212	83.6	7.5	64.1	0.77	0.01	90	<0.10	20	420	<0.15	2.6	µg/l	5440	168	1260

WT Dec 2010	7,74	105	mg/l	236	327	108	13.8	112	2.5	0.07	164	0.75	15	450	<0.15	3	µg/l	<10	<40	20
PD2 Aug 2010	7,42	116	mg/l	220	443	153	14.5	143	2.4	0.02	222	<0.10	20.7	800	<0.15	2.5	µg/l	<10	<40	20
GB1RG Dec 2010	8,14	12.7	mg/l	48	53.6	20.5	0.55	8.9	0.55	0.02	15.1	0.32	<4	100	<0.15	0.34	µg/l	<10	<40	200
GB1 Dec 2010	7,70	96.4	mg/l	280	359	125	9.4	102	1.3	<0.01	136	0.29	19	650	<0.15	0.53	µg/l	100	<40	260
TMG1 Dec 2010	7,47	54	mg/l	132	179	58.2	8.1	58.5	1.5	<0.01	102	0.68	9	370	<0.15	0.71	µg/l	28	<40	<14

Appendix C: Isotopic Data

DEPARTMENT OF GEOLOGICAL SCIENCES
University of Cape Town
Rondebosch 7700
South Africa

Street address Room 409, 13 University Avenue
Phone +27 21 6502921/31
Fax +27 21 6503783
Email: chris.harris@uct.ac.za

Water samples submitted by for O and H isotope analyses, October 2010

Analytical methods

The stable isotope analyses were performed at the Department of Geological Sciences at the University of Cape Town. For oxygen, the CO_2 equilibration method of Socki et al. (1992) employing disposable pre-evacuated 7 ml glass vials. For hydrogen, 2 mg of water contained in a microcapilliary tube was dropped into a Pyrex tube containing approximately 100mg of Indiana Zn. The tube was attached to the vacuum line, frozen in liquid nitrogen, evacuated and then sealed using a torch. The tubes were then placed in a furnace at 450 ^{o}C to reduce the water to H_2. Isotope ratios of CO_2 and H_2 were measured using a Finnegan DeltaXP mass spectrometer, and the fractionation factor between CO_2 and water at 25 ^{o}C was assumed to be 1.0412 (Coplen, 1993). Data are reported in the familiar δ notation, relative to SMOW, where $\delta = (R_{sample}/R_{SMOW} - 1)*1000$, and $R = {}^{18}O/{}^{16}O$ or D/H. The long-term average difference between duplicates of our internal water standard (CTMP) are 0.48 ‰ for hydrogen (n = 23) and 0.10 ‰ for oxygen (n = 18). These correspond to values of 2 σ of 0.74 ‰ and 0.14 ‰ respectively. The standards V-SMOW and SLAP were analysed to determine the degree of compression of raw data and the equations of Coplen (1993) were used to convert raw data to the SMOW scale. Our internal water standard (CTMP3 δD = -7 ‰; $\delta^{18}O$ = -1.95 ‰), which had been calibrated against V-SMOW and SLAP, and independently analysed, was run with each batch of samples and used to correct for drift in the reference gases.

The precision of the analyses is approximately ±0.1-0.2‰ for $\delta^{18}O$ and 1.0‰ for δD, and accordingly $\delta^{18}O$ should be reported with 2 decimal places and δD to no decimal places.

Umvoto	δD	$\delta^{18}O$
635-BD1	-29	-5.80
635-WF1	-28	-5.47
635-WKP1	-26	-5.55
635-MF1	-27	-5.42
635-HV1	-25	-5.54
635-EL1	-20	-5.24
635-WT	-28	-5.09
635-TMG1	-22	-4.92
635-WA2	-29	-5.31
635-GB1	-27	-5.50
635-PD1	-27	-5.10
635-AV1	-25	-4.98
635-MBE03RG*	-2	-3.39
635-GB1RG	-14	-2.86

*samples contains oil and this may have affected the H-isotope analysis.

The charge for this is R350 per sample. There were 14 samples in this batch and this makes a total of R4900 excl VAT. Please would you send me a purchase order so that I can generate an invoice.

Please contact me if I can be of further assistance.

Yours sincerely

Chris Harris MA, DPhil (Oxford)
Professor, Stable Isotope Laboratory
(sent by email)

APPENDIX D: KVE01 Log

Project: Water Resource Development and Management Plan for the Standford Area

Borehole: **KVE01 - Kouevlakte Exploration 1**

UMVOTO

Drilling Method:	Rotary Mud	Rest Water Level: 91.6 mbgl	Longitude: S 34.48798	GPS
Drilling Dates:	02-04 February 2010	14.4 mamsl	Latitude: E 19.43209	GPS
Drilling Depth:	114 mbgl		Elevation: 106 mamsl	GPS

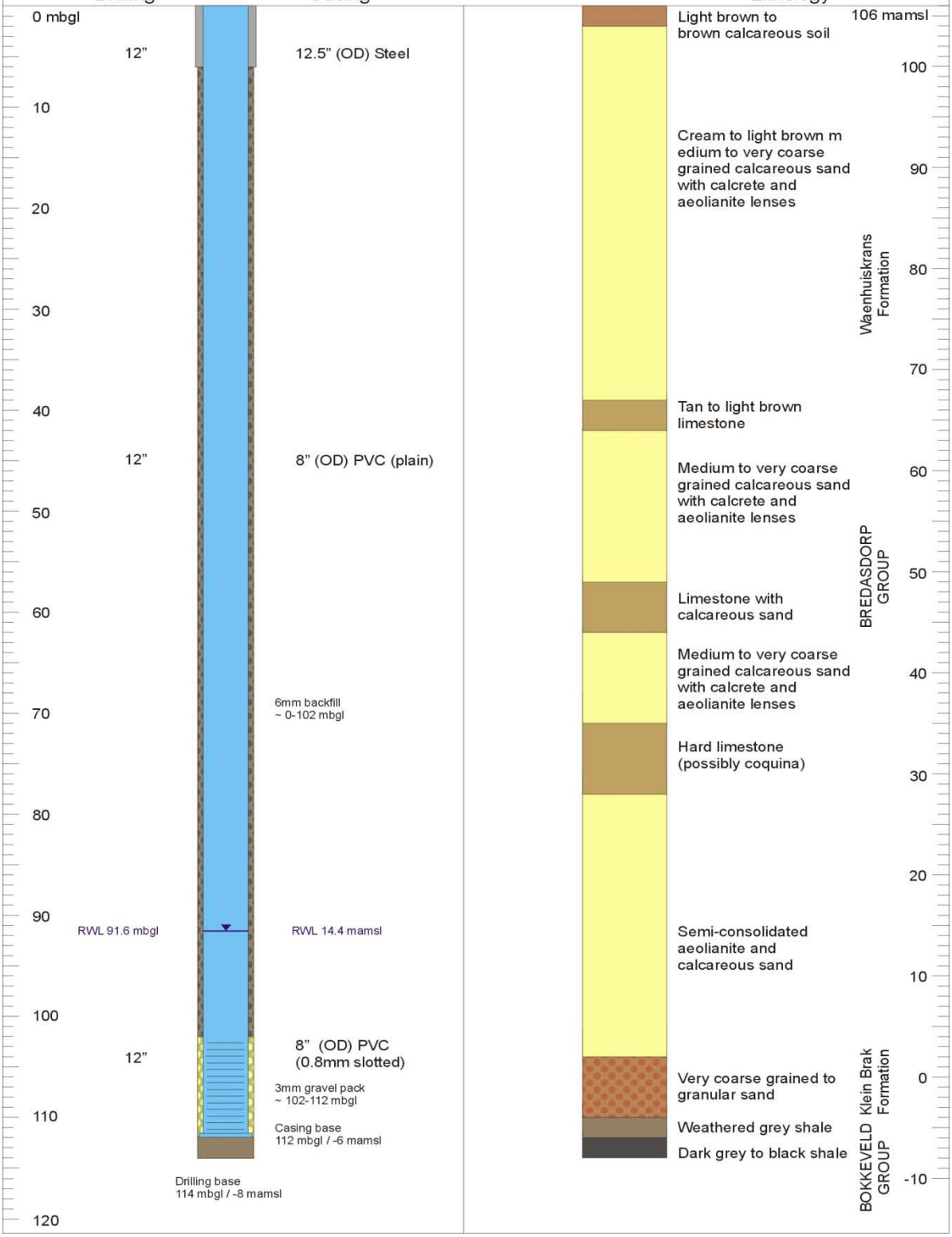

APPENDIX: KVE02 Log

Project: Water Resource Development and Management Plan for the Standford Area

Borehole: **KVE02 - Kouevlakte Exploration 2**

UMVOTO

Drilling Method:	Rotary Mud	Rest Water Level:	96.3 mbgl	Longitude:	S 34.48928 GPS
Drilling Dates:	09-11 February 2010		13.7 mamsl	Latitude:	E 19.43181 GPS
Drilling Depth:	117 mbgl			Elevation:	110 mamsl GPS

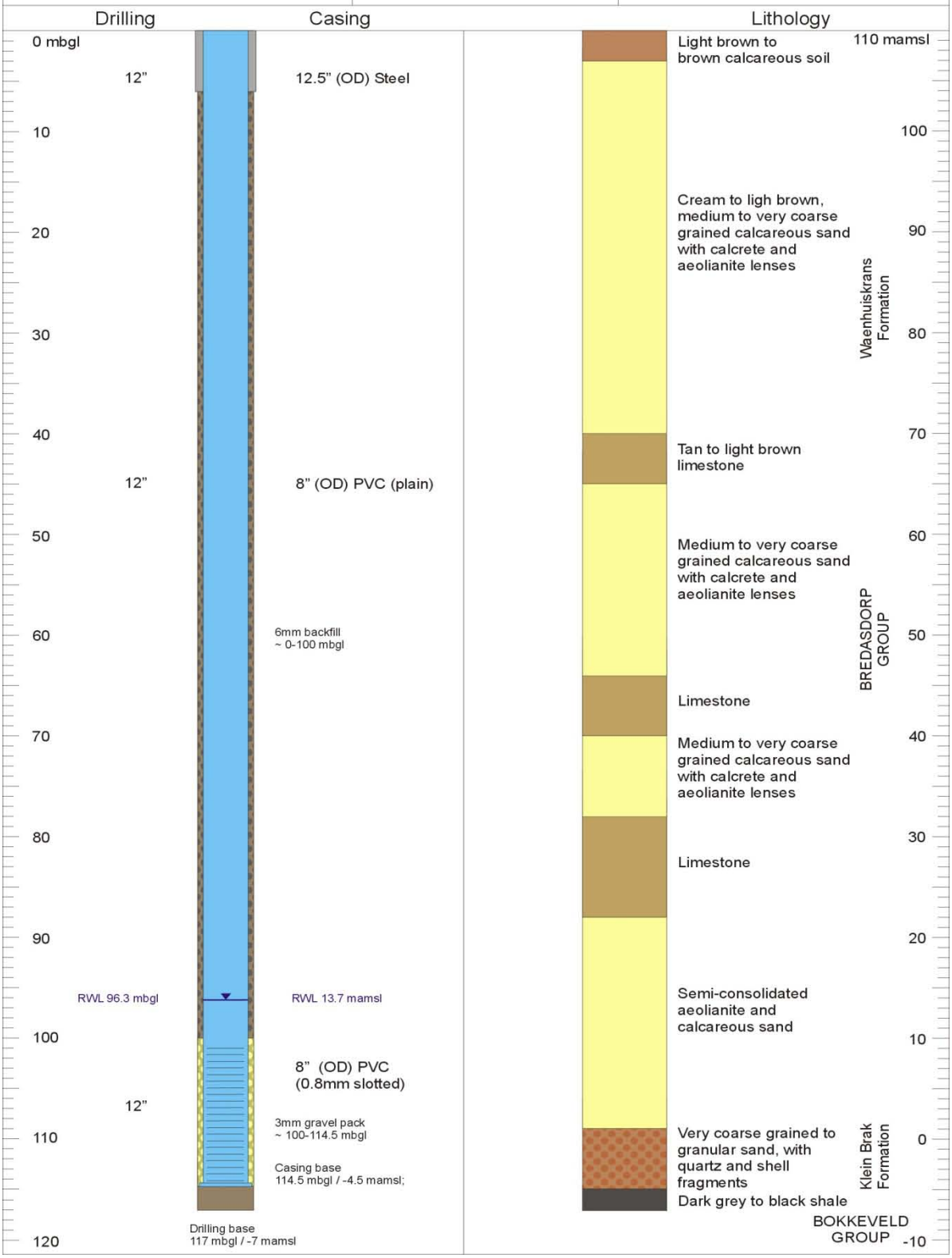

Tidigare skrifter i serien ”Examensarbeten i Geologi vid Lunds Universitet”:

241. Stenberg, Li, 2009: Historiska kartor som hjälp vid jordartsgeologisk kartering – en pilotstudie från Vångs by i Blekinge. (15 hskp)
242. Nilsson, Mimmi, 2009: Robust U-Pb baddeleyite ages of mafic dykes and intrusions in southern West Greenland: constraints on the coherency of crustal blocks of the North Atlantic Craton. (30 hskp)
243. Hult, Elin, 2009: Oligocene to middle Miocene sediments from ODP leg 159, site 959 offshore Ivory Coast, equatorial West Africa. (15 hskp)
244. Olsson, Håkan, 2009: Climate archives and the Late Ordovician Boda Event. (15 hskp)
245. Wollein Waldetoft, Kristofer, 2009: Svekofennisk granit från olika metamorfa miljöer. (15 hskp)
246. Månsby, Urban, 2009: Late Cretaceous coprolites from the Kristianstad Basin, southern Sweden. (15 hskp)
247. MacGimpsey, I., 2008: Petroleum Geology of the Barents Sea. (15 hskp)
248. Jäckel, O., 2009: Comparison between two sediment X-ray Fluorescence records of the Late Holocene from Disko Bugt, West Greenland; Paleoclimatic and methodological implications. (45 hskp)
249. Andersen, Christine, 2009: The mineral composition of the Burkland Cu-sulphide deposit at Zinkgruvan, Sweden – a supplementary study. (15 hskp)
250. Riebe, My, 2009: Spinel group minerals in carbonaceous and ordinary chondrites. (15 hskp)
251. Nilsson, Filip, 2009: Föroreningsspridning och geologi vid Filborna i Helsingborg. (30 hskp)
252. Peetz, Romina, 2009: A geochemical characterization of the lower part of the Miocene shield-building lavas on Gran Canaria. (45 hskp)
253. Åkesson, Maria, 2010: Mass movements as contamination carriers in surface water systems – Swedish experiences and risks.
254. Löfroth, Elin, 2010: A Greenland ice core perspective on the dating of the Late Bronze Age Santorini eruption. (45 hskp)
255. Ellingsgaard, Óluva, 2009: Formation Evaluation of Interlava Volcaniclastic Rocks from the Faroe Islands and the Faroe-Shetland Basin. (45 hskp)
256. Arvidsson, Kristina, 2010: Geophysical and hydrogeological survey in a part of the Nhandugue River valley, Gorongosa National Park, Mozambique. (45 hskp)
257. Gren, Johan, 2010: Osteo-histology of Mesozoic marine tetrapods – implications for longevity, growth strategies and growth rates. (15 hskp)
258. Syversen, Fredrikke, 2010: Late Jurassic deposits in the Troll field. (15 hskp)
259. Andersson, Pontus, 2010: Hydrogeological investigation for the PEGASUS project, southern Skåne, Sweden. (30 hskp)
260. Noor, Amir, 2010: Upper Ordovician through lowermost Silurian stratigraphy and facies of the Borenshult-1 core, Östergötland, Sweden. (45 hskp)
261. Lewerentz, Alexander, 2010: On the occurrence of baddeleyite in zircon in silica-saturated rocks. (15 hskp)
262. Eriksson, Magnus, 2010: The Ordovician Orthoceratite Limestone and the Blommiga Bladet hardground complex at Horns Udde, Öland. (15 hskp)
263. Lindskog, Anders, 2010: From red to grey and back again: A detailed study of the lower Kundan (Middle Ordovician) ‘Täljsten’ interval and its enclosing strata in Västergötland, Sweden. (15 hskp)
264. Rääf, Rebecka, 2010: Changes in beyrichiid ostracode faunas during the Late Silurian Lau Event on Gotland, Sweden. (30 hskp)
265. Petersson, Andreas, 2010: Zircon U-Pb, Hf and O isotope constraints on the growth versus recycling of continental crust in the Grenville orogen, Ohio, USA. (45 hskp)
266. Stenberg, Li, 2010: Geophysical and hydrogeological survey in a part of the Nhandugue River valley, Gorongosa National Park, Mozambique – Area 1 and 2. (45 hskp)
267. Andersen, Christine, 2010: Controls of seafloor depth on hydrothermal vent temperatures - prediction, observation & 2D finite element modeling. (45 hskp)
268. März, Nadine, 2010: When did the Kalahari craton form? Constraints from baddeleyite U-Pb geochronology and geo-chemistry

of mafic intrusions in the Kaapvaal and Zimbabwe cratons. (45 hp)

269. Dyck, Brendan, 2010: Metamorphic rocks in a section across a Svecnorwegian eclogite-bearing deformation zone in Halland: characteristics and regional context. (15 hp)
270. McGimpsey, Ian, 2010: Petrology and lithogeochemistry of the host rocks to the Nautanen Cu-Au deposit, Gällivare area, northern Sweden. (45 hp)
271. Ulmius, Jan, 2010: Microspherules from the lowermost Ordovician in Scania, Sweden – affinity and taphonomy. (15 hp)
272. Andersson, Josefin, Hybertsen, Frida, 2010: Geologi i Helsingborgs kommun – en geoturistkarta med beskrivning. (15 hp)
273. Barth, Kilian, 2011: Late Weichselian glacial and geomorphological reconstruction of South-Western Scania, Sweden. (45 hp)
274. Mashramah, Yaser, 2011: Maturity of kerogen, petroleum generation and the application of fossils and organic matter for paleotemperature measurements. (45 hp)
275. Vang, Ina, 2011: Amphibolites, structures and metamorphism on Flekkerøy, south Norway. (45 hp)
276. Lindvall, Hanna, 2011: A multi-proxy study of a peat sequence on Nightingale Island, South Atlantic. (45 hp)
277. Bjerg, Benjamin, 2011: Metodik för att förhindra metanemissioner från avfallsdeponier, tillämpad vid Albäcksdeponin, Trelleborg. (30 hp)
278. Pettersson, Hanna, 2011: El Hicha – en studie av saltstäppssediment. (15 hskp)
279. Dyck, Brendan, 2011: A key fold structure within a Sveconorwegian eclogite-bearing deformation zone in Halland, southwestern Sweden: geometry and tectonic implications. (45 hp)
280. Hansson, Anton, 2011: Torvstratigrafisk studie av en trädstamshorisont i Viss mosse, centrala Skåne kring 4 000 - 3 000 cal BP med avseende på klimat- och vattenståndsförändringar. (15 hp)
281. Åkesson, Christine, 2011: Vegetationsutvecklingen i nordvästra Europa under Eem och Weichsel, samt en fallstudie av en submorän, organisk avlagring i Bellinga stenbrott, Skåne. (15 hp)
282. Silveira, Eduardo M., 2011: First precise U-Pb ages of mafic dykes from the São Francisco Craton. (45 hp)
283. Holm, Johanna, 2011**:** Geofysisk utvärdering av grundvattenskydd mellan väg 11 och Vombs vattenverk. (15 hp)
284. Löfgren, Anneli, 2011: Undersökning av geofysiska metoders användbarhet vid kontroll av den omättade zonen i en infiltrationsdamm vid Vombverket. (15 hp)
285. Grenholm, Mikael, 2011: Petrology of Birimian granitoids in southern Ghana - petrography and petrogenesis. (15 hp)
286. Thorbergsson, Gunnlaugur, 2011: A sedimentological study on the formation of a hummocky moraine at Törnåkra in Småland, southern Sweden. (45 hp)
287. Lindskog, Anders, 2011: A Russian record of a Middle Ordovician meteorite shower: Extraterrestrial chromite in Volkhovian-Kundan (lower Darriwilian) strata at Lynna River, St. Petersburg region. (45 hp)
288. Gren, Johan, 2011: Dental histology of Cretaceous mosasaurs (Reptilia, Squamata): incremental growth lines in dentine and implications for tooth replacement. (45 hp)
289. Cederberg, Julia, 2011: U-Pb baddelyit dateringar av basiska gångar längs Romeleåsen i Skåne och deras påverkan av plastisk deformation i Protoginzonen (15 hp)
290. Wenxing Ning, 2011: Testing the hypothesis of a link between Earth's magnetic field and climate change: a case study from southern Sweden focusing on the 1st millennium BC. (45 hp)
291. Holm Östergaard, Sören, 2011: Hydrogeology and groundwater regime of the Stanford Aquifer, South Africa. (45 hp)

LUNDS UNIVERSITET

Geologiska enheten
Institutionen för geo- och ekosystemvetenskaper
Sölvegatan 12, 223 62 Lund